SASTA OLIPHANT SCIENCE AWARDS

SOUTH AUSTRALIAN SCIENCE TEACHERS ASSOCIATION

Prize Winner

Science Investigation

Year 11 - 12

Chloe Yew

University Senior College

ROWE SCIENTIFIC PTY. LTD. www.rowe.com.au

Government of South Australia
Department for Education

SASTA South Australian Science Teachers Association

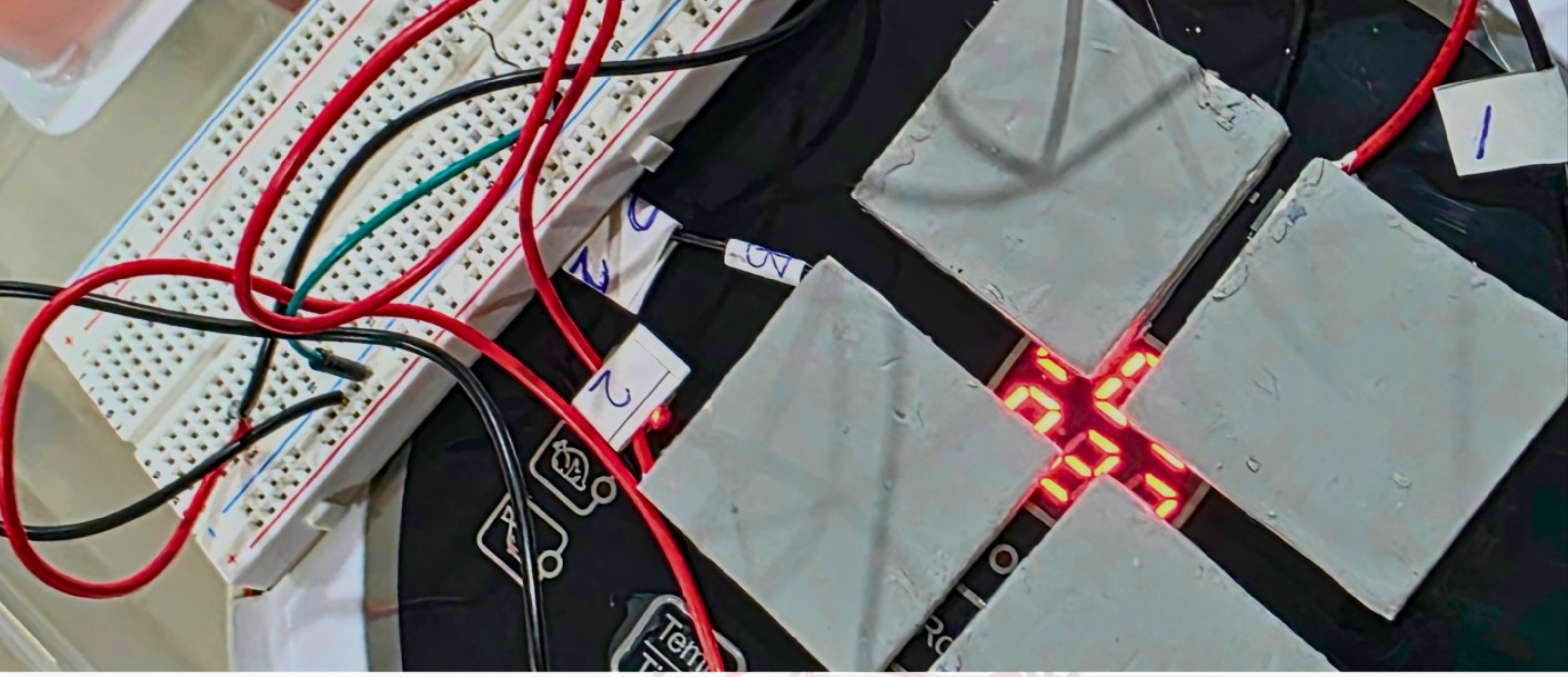

From Heat to Electricity: Investigating Energy Harvesting Using Thermoelectric Generators

To what extent do electrical configurations and heat sources influence the power output of a thermoelectric generator system composed of four SP1848-27145 modules?

Chloe Yaan Yuit Yew

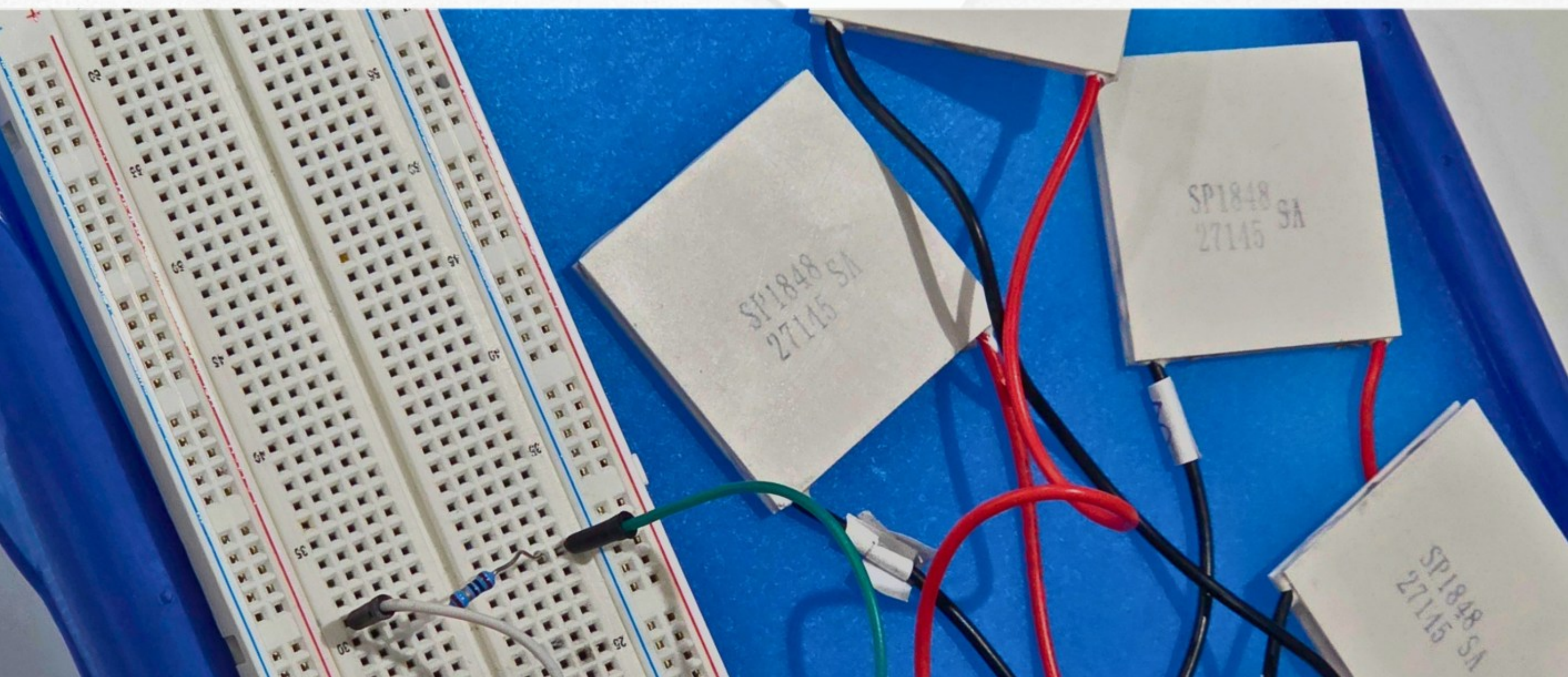

Scientific Report

Title

From Heat to Electricity: Investigating Energy Harvesting Using Thermoelectric Generators

Research Question

To what extent do electrical configurations and heat sources influence the power output of a thermoelectric generator system composed of four SP1848-27145 modules?

Background information

Rising global energy demand, driven by population growth and the proliferation of portable electronics, is intensifying reliance on finite resources while amplifying environmental and emissions constraints (Wang et al., 2018; Ochieng et al., 2022). This has accelerated the development of clean, decentralised, low-carbon energy technologies capable of harvesting otherwise wasted energy (Ochieng et al., 2022). Thermoelectric generators (TEGs) are solid-state devices that convert thermal energy directly into electrical energy through a temperature gradient, allowing recovery of low-grade waste heat such as the human body, household appliances, and industrial processes (Gámez-Avilez et al., 2026). As compact, lightweight systems with no moving parts, TEGs provide continuous, low-maintenance, emission-free operation without reliance on chemical fuels, supporting more sustainable energy utilisation (Jouhara et al., 2021). Consequently, TEGs are increasingly deployed in wearable and biomedical technologies, autonomous monitoring systems, industrial and automotive waste heat recovery, as well as remote and space-based power applications (Champier, 2017; Zhu, Yu & Li, 2019).

A typical TEG comprises thermocouples composed of alternating p-type and n-type semiconductor legs, sandwiched between electrically insulating, thermally conductive ceramic substrates (*Figure 1*) (Misra et al., 2015). The semiconductors are electrically connected in series to increase voltage output and thermally in parallel to ensure each junction experiences the same temperature gradient (Ridwan, Gasulla & Reverter, 2025). The ceramic plates provide mechanical stability, facilitate efficient thermal contact with external heat sources and sinks, and serve as dielectric barriers to prevent electrical short circuits (Ridwan, Gasulla & Reverter, 2025).

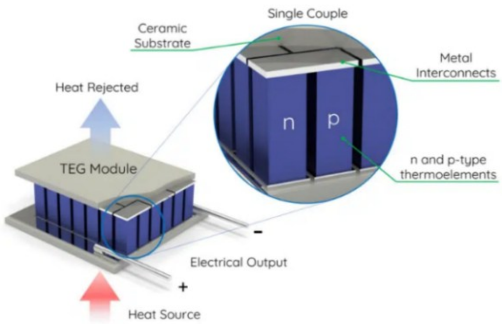

Figure 1. Internal Structure of a TEG module (Dhass et al., 2023).

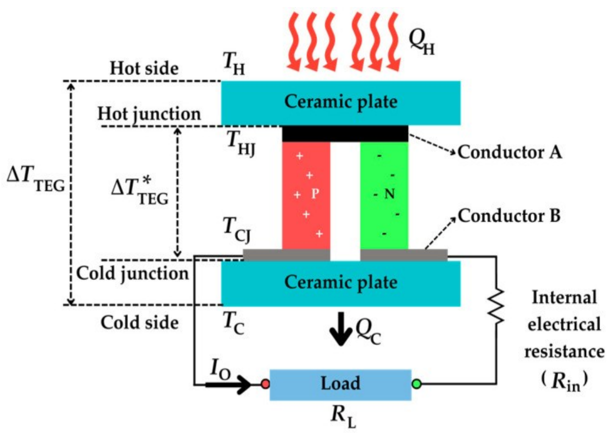

Figure 2. Schematic diagram of the Seebeck effect (Ridwan, Gasulla & Reverter, 2025).

TEGs operate via the Seebeck effect, where a temperature gradient drives the diffusion of charge carriers from the hot side to the cold side, generating an electric potential (Jouhara et al., 2021). In n-type semiconductors, electrons act as the negative charge carriers, whereas in p-type semiconductors, holes act as positive charge carriers (He & Tritt, 2017). The resulting charge separation establishes an internal electric field, producing a measurable voltage (*Figure 2*) (Zhu, Yu & Li, 2019). The Seebeck coefficient (α) quantifies this relationship:

$$a = -\frac{\Delta V}{\Delta T} = \frac{V_{hot} - V_{cold}}{T_{hot} - T_{cold}}$$

TEG performance is measured by the dimensionless figure of merit (**ZT**):

$$ZT = \frac{\alpha^2 \sigma T}{k}$$

where α = Seebeck coefficient,
σ = electrical conductivity,
k = thermal conductivity,
T = absolute temperature (Ryu et al., 2023; Zhu, Yu & Li, 2019).

High ZT requires maximising α and σ, while minimising k to preserve the temperature gradient (Zhu, Yu & Li, 2019). However, these properties are interdependent, meaning improvements in one often compromise another, constraining overall efficiency (Zhu, Yu & Li, 2019).

At the system level, power output depends on both temperature difference (ΔT) and the electrical configuration of the circuit (Manghwar et al., 2026). Since voltage scales with ΔT through the Seebeck effect, larger ΔT produce greater potential differences (Jouhara et al., 2021). However, power output also relies on current, which is influenced by the circuit resistance. Series configurations increase total voltage but increase internal resistance, whereas parallel configurations reduce effective resistance and increase current (Terashima, Sorimachi & Iwase, 2024). Hybrid series–parallel configurations balance these effects to optimise power output (Terashima, Sorimachi & Iwase, 2024) (*Figure 3*). Therefore, both thermal conditions and circuit configuration fundamentally govern the magnitude of power output. Investigating these variables provides a basis for evaluating strategies to enhance energy harvesting from low-grade heat sources.

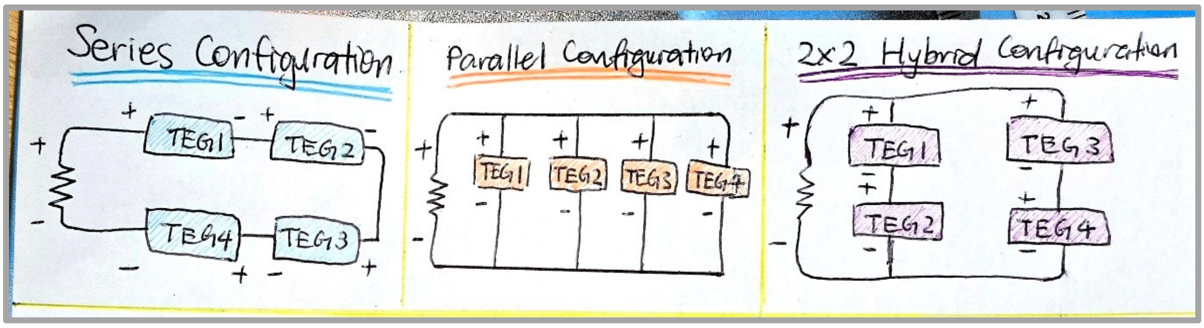

Figure 3. Schematic diagram of series, parallel, and 2×2 hybrid configurations.

Aim

This investigation examined how electrical configuration (parallel, series, and 2×2 hybrid) and heat source condition (static body heat, dynamic body heat, and appliance heat) influence the power output of a TEG system composed of four SP1848-27145 modules. Voltage and ΔT were measured directly, while current and power output were calculated to quantify energy-harvesting performance under varying thermal and electrical conditions.

Stage 1 served as a pilot study investigating the effect of load resistance on power output to identify an appropriate load resistor in the main experiment. Using this selected load resistance, Stage 2 systematically evaluated the electrical performance of a single-module baseline and three four-module configurations under the three heat source conditions. This allows analysis on the effects of electrical configurations and heat source conditions influencing thermoelectric energy conversion efficiency.

Hypotheses

Hypothesis 1	The 2×2 hybrid configuration will produce the highest power output under the tested thermal conditions, as it is expected to optimise the trade-off between voltage generation (enhanced in series connections) and current delivery (enhanced in parallel connections).
Hypothesis 2	Appliance heat will produce a greater power output than both static and dynamic body heat, as it is expected to create a larger and more stable temperature difference between the hot and cold sides of the TEG system.

Variables

Independent and Dependent Variables

Independent Variables	• Electrical configurations of the TEG system (Parallel, Series, 2×2 hybrid) • Heat source conditions (static body heat, dynamic body heat, appliance heat)
Dependent Variables	• Mean power output (P) of the TEG system (calculated from measured voltage and calculated current using P = VI)

Controlled Variables

Controlled variables were maintained to ensure a fair test:

Controlled variables	Method of Control	Effect on the Experiment
Type and number of TEGs	Four identical SP1848-27145 TEG modules were used in all configurations.	This ensured that any differences in power output were due to electrical configuration and heat source rather than variations in TEG characteristics including Seebeck coefficient, thermal conductivity and electric resistivity.
Load resistance	A fixed 10 Ω resistor was used throughout Stage 2.	This maintained a constant electrical load, ensuring that changes in dependent variables resulted from independent variables rather than differences in external circuit resistance.
Thermal pad material and thickness	The same 12.8 W/m·K thermal pads were used throughout Stage 1, and the same 21 W/m·K thermal pads were used throughout Stage 2.	This ensured consistent thermal conductivity between heat source and TEGs, reducing variation in heat transfer and ΔT caused by differing thermal interface properties.
Heat source placement for TEGs	TEGs were positioned at the same location on the air fryer top surface and at the same anatomical location (mid-portion of the quadriceps) on the same participant.	This maintained consistent heat exposure and contact conditions, maintaining comparable ΔT across trials.
Ambient conditions (environment)	All experiments were conducted under similar environmental conditions (12–16°C).	This minimised variation in heat loss to the surroundings and maintained relatively consistent cold-side cooling conditions.
Human body movement during	The same participant performed repeated knee	The mid-portion of the quadriceps was chosen because it has a relatively large and

dynamic body heat trials	flexion and extension of the same leg using the same resistance band at a standardised rate of 60 bpm guided by a metronome.	flat surface area allowing better thermal contact for TEG. The same anatomical area was marked for TEG placement to reduce variation in local metabolic heat production and TEG-skin contact conditions.
Measurement interval and trial duration	Measurements were recorded every 30 seconds for 3 minutes using the same procedure across all trials.	TEG output changes over time as thermal equilibrium develops. Standardising measurement intervals and trial duration ensured comparable sampling of thermal behaviour across trials. Repeated trials also reduced the influence of random error.
Measuring equipment	The same digital multimeter and infrared thermometer were used throughout the investigation.	This minimised systematic error arising from differences in calibration, measurement precision, or instrument characteristics, improving the reliability and consistency of collected data.

Uncontrolled Variables

Uncontrolled variables	Reason why it cannot be controlled and its effect on data
Fluctuations in heat source output (appliance and body heat)	Appliance heat varied due to thermostat cycling, while human metabolic heat production naturally fluctuated over time. These variations altered the heat flux supplied to the TEGs, affecting ΔT across the modules and consequently dependent variables.
Variations in human body movements during dynamic body heat condition	Although a metronome and the same resistance band were used to standardise movement, inter- and intra-individual variability in muscle activation and fatigue could not be completely eliminated. These factors affected the consistency of contact between the TEGs and the skin, resulting in variations in heat transfer and ΔT.
Instability in cold-side heat dissipation	The ice pack had to be briefly lifted during temperature measurements, and condensation formed on the cooling surface over time. These factors could not be completely controlled and may have altered the effectiveness of heat removal from the cold side of the TEGs, causing fluctuations in ΔT and power output.
Minor ambient temperature variation	Small changes in room temperature occurred throughout the investigation despite conducting all trials indoors. These variations may have influenced heat loss from the system and the rate of ice-pack warming, leading to slight changes in ΔT between trials.

Materials and Equipment

Materials	▪ Thermoelectric components:
	  ○ Four SP1848-27145 thermoelectric generator (TEG) modules, size: 40 mm x 40 mm x 4 mm
	  ○ Thermal pads
	    ▪ 12.8W/m·K thermal pads (Stage 1)
	    ▪ 21 W/m·K thermal pads (Stage 2)
	▪ Load resistors
	  ○ Stage 1: 10 Ω, 100 Ω, 220 Ω, 330 Ω, 1 kΩ, 2 kΩ, 5 kΩ, and 10 kΩ
	  ○ Stage 2: 10 Ω
	▪ Electric components
	  ○ Breadboard

	◦ Jumper wires, connecting Wires (22-26 AWG) ◦ Solder and soldering iron ▪ Cooling system ◦ Human body heat ◦ 400 mL rectangular ice pack wrapped in aluminium Foil ▪ Heat Sources: ◦ Human body heat ◦ Air fryer top surface (set to 200°C)
Equipment	▪ Measurement equipment ◦ Digital multimeter ◦ Infrared thermometer ◦ Stopwatch ▪ Dynamic body heat condition equipment ◦ Metronome ◦ Resistance band ◦ Chair ▪ General equipment ◦ Wire cutter ◦ Ruler ◦ Measuring tape ◦ Marker pen ◦ Labels
Personal Protective Equipment	▪ Safety glasses ▪ Heat-resistance gloves ▪ Surgical mask ▪ Lab coat ▪ Enclosed footwear

Risk Assessment

Safety Precautions Appropriate laboratory safety procedures were followed throughout the investigation. Personal protective equipment, including a lab coat, heat-resistant gloves, and safety glasses, was used when handling the soldering iron and heated equipment to mitigate burn and eye injury risks. Wire cutters, scissors, and exposed wire ends were handled carefully to prevent cuts and puncture injuries. Soldering was conducted in a well-ventilated area while wearing a mask to minimise inhalation of solder fumes. Electrical components were kept isolated from melted ice and condensation to prevent short circuits and equipment damage. All equipment was operated in accordance with manufacturer guidelines to ensure safe and controlled operation.
Environmental Consideration The experiment posed negligible environmental risk as it involved no hazardous chemicals or toxic materials. Waste generation was minimal, and components such as thermoelectric modules and wiring were reused where possible to reduce material consumption.
Ethical Consideration Informed consent was obtained from the participant involved in body heat trials. The procedures were non-invasive and involved only routine physical activity, presenting negligible risk. No personal or sensitive data were collected, and the investigation adhered to standard ethical guidelines for human participation. The study posed no foreseeable harm to individuals or society.

Procedure

Stage 1: Pilot Study – Determination of Load Resistance and Optimisation of Stage 2

Step	Procedure
1	Four SP1848-27145 TEG modules were assembled into three electrical configurations: parallel, series, and 2×2 hybrid.
2	A 0.5 mm-thick, 12.8 W/m·K thermal pad was applied to the hot side of each TEG module, while a 1.0 mm-thick, 12.8 W/m·K thermal pad was applied to the cold side to minimise thermal contact resistance at the interfaces with the heat source and the ice pack.
3	The hot side of the TEG system was exposed to one of three heat source conditions: static body heat, dynamic body heat, or appliance heat.
4	A rectangular ice pack wrapped in aluminium foil was attached to the cold-side thermal pad to act as a heat sink.
5	For appliance heat trials, the TEG system was placed at a fixed position on the top surface of an air fryer. For static and dynamic body heat trials, the system was positioned on the mid-region of the participant's right quadriceps. For dynamic trials, repeated knee flexion and extension were performed using a resistance band.
6	The system was connected to load resistors of 10 Ω, 100 Ω, 220 Ω, 330 Ω, 1 kΩ, 2 kΩ, 5 kΩ, and 10 kΩ.
7	Voltage across each load resistor was recorded using a digital multimeter at 30-second intervals for 2 minutes (0, 30, 60, 90, and 120 s).
8	The temperature of the heat source surface and the cold-side surface of the TEG system were measured using an infrared thermometer at the same intervals. The cold side of the TEG system was cooled using an ice pack. These measurements were used to estimate the ΔT across the TEG system, including the thermal pad, rather than directly measuring the ΔT across the internal thermoelectric junctions: $\Delta T = T\ (heat\ source\ surface) - T\ (TEG\ cold\ side\ surface)$
9	Current was calculated using Ohm's Law: $I = V/R$.
10	Power output was calculated using $P = VI$.
11	The procedure was repeated for each TEG configuration-heat source combination.

Improvements Implemented in Stage 2

Pilot results informed the following methodological refinements for Stage 2:

- A fixed load resistance of 10 Ω was selected due to consistently higher power output under most TEG configuration-heat source combination.
- Thermal pads were upgraded from 12.8 W/m·K to 21 W/m·K to reduce thermal resistance between the heat source and the hot side of the TEG modules, and between the cold side of the TEG modules and the ice pack.
- A metronome was introduced to standardise knee movement frequency during dynamic trials.
- Data collection duration was extended from 2 to 3 minutes, increasing resolution from 5 to 7 time points per trial (0–180 s at 30-second intervals). These changes provided a more detailed analysis of power output over time.

Stage 2: Experimental Investigation

Preparation	
Step	**Procedure**
1	Four SP1848-27145 TEG modules were assembled into three electrical configurations: parallel, series, and 2×2 hybrid (*Figure 4a*).
2	0.5 mm-thick, 21 W/m·K thermal pads were applied to both the hot and cold sides of each TEG module to minimise thermal contact resistance at the interfaces with the heat source and the ice pack.

3	A fixed 10 Ω load resistor was connected to all configurations.
4	A 400 mL rectangular ice pack wrapped in aluminium foil was positioned on the cold-side thermal pad to function as a heat sink.
Heat Source Conditions	
Condition	**Procedure**
Static Body Heat	The TEG system was placed on the mid-region of the participant's left quadriceps while seated at rest (*Figure 4b*).
Dynamic Body Heat	1. The TEG system was placed on the same anatomical location (*Figure 4b*). 2. The participant performed repeated knee flexion and extension using a resistance band. 3. Movement speed was standardised at 60 bpm using a metronome.
Appliance Heat	The TEG system was positioned at a fixed position on the top surface of an air fryer operating at 200°C (*Figure 4b*).
Data Collection	
Step	**Procedure**
1	Voltage across the load resistor was measured using a digital multimeter at 30-second intervals for 3 minutes (0, 30, 60, 90, 120, 150, and 180 s).
2	The temperature of the heat source surface and the cold-side surface of the TEG system were measured using an infrared thermometer at the same intervals. The cold side of the TEG system was cooled using an ice pack. These measurements were used to estimate the ΔT across the TEG system, including the thermal pad, rather than directly measuring the ΔT across the internal thermoelectric junctions: $\Delta T = T\,(heat\ source\ surface) - T\,(TEG\ top\ surface)$
3	Three repeated trials were conducted for the single TEG module (baseline condition) and each TEG configuration-heat source combination. The system remained fixed in position throughout each trial to maintain thermal stability. Between trials, a 2-minute stabilisation period was allowed to reduce transient thermal effects and ensure comparable testing conditions.

Parallel Setup **Series Setup** **2×2 Hybrid Setup**

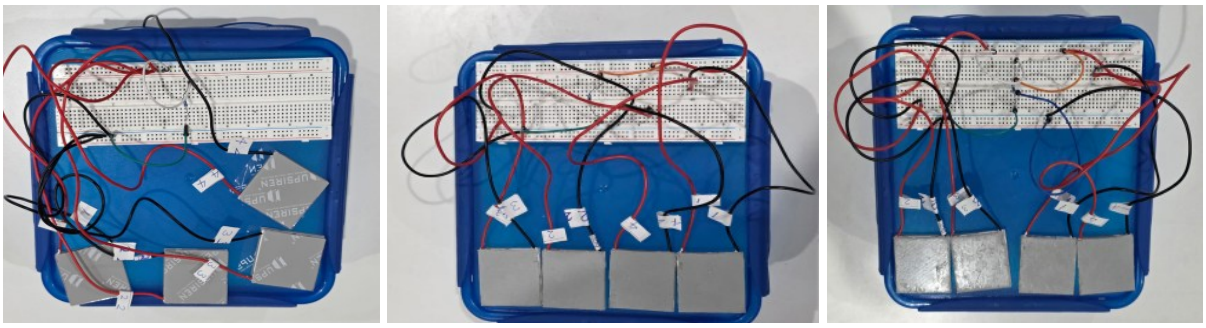

Figure 4a. TEG configurations (parallel, series, 2×2 hybrid).

Body Heat **Appliance Heat**

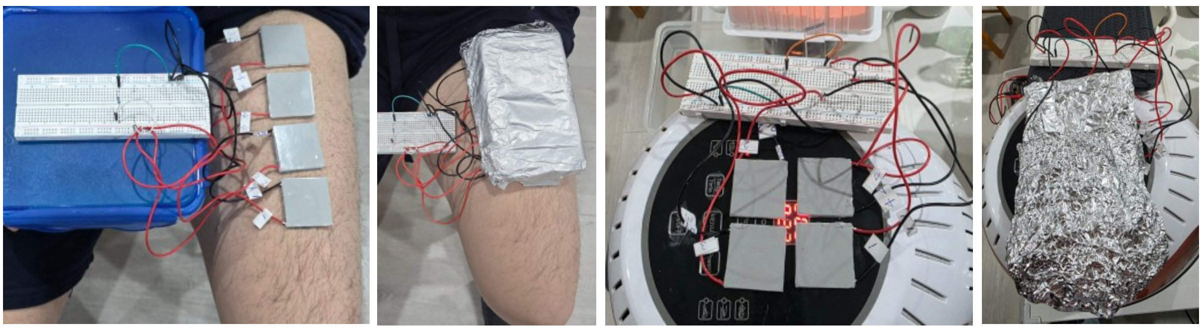

Figure 4b. Body heat and appliance heat conditions.

Processing and Analysing Data and Information

Data analysis for Stage 1

Step	Stage 1 Data Analysis
1	Temperature difference (ΔT) was calculated from measured hot-side and cold-side temperatures: ΔT = T (heat source surface) – T (TEG cold side surface).
2	Current was calculated using Ohm's Law: $I = V/R$.
3	Power output was calculated using $P = VI$.
4	Mean voltage and temperature difference for each condition were calculated by averaging the five repeated measurements. Mean current and power output were then calculated from the mean voltage.
5	Graphs of mean power output against load resistance were produced to evaluate the effect of load resistance on power output of different TEG configurations under various heat source conditions.

Data analysis for Stage 2

Step	Stage 2 Data Analysis
1	Temperature difference (ΔT) was calculated from measured hot-side and cold-side temperatures: ΔT = T (heat source surface) – T (TEG cold side surface)
2	Current was calculated using Ohm's Law: $I = V/R$.
3	Power output was calculated using $P = VI$.
4	Mean voltage and temperature difference for each condition were calculated by first averaging the seven measurements recorded during each trial, followed by averaging the three-trial means. Mean current and power output were then calculated from the mean voltage for each trial and averaged across the three repeated trials.
5	Relative voltage and power outputs of four-module configurations were calculated by normalising values to a single TEG module under identical heat source conditions.
6	Time-series graphs of voltage and ΔT were produced to compare the performance of different TEG configurations under each heat source condition.
7	A two-way ANOVA with replication was conducted on mean power output values to assess the effects of TEG configuration and heat source condition on power output, and to evaluate potential interaction effects between the independent variables. Assumptions of normality and homogeneity of variance were considered.
8	Pairwise t-tests (Two-Sample Assuming Unequal Variances) were conducted using mean power output values. To account for multiple comparisons, a Bonferroni-adjusted significance threshold of 0.0167 was applied. The tests were used to identify statistically significant differences between pairs of TEG configurations and between pairs of heat source conditions.

STAGE 1 RESULTS

Table 1a. Mean voltage (mV) under different electrical configurations and heat sources at various load resistance.

Static body heat				Dynamic body heat				Appliance heat			
Resistor (Ω)	Parallel	Series	2×2 Hybrid	Resistor (Ω)	Parallel	Series	2×2 Hybrid	Resistor (Ω)	Parallel	Series	2×2 Hybrid
10	69.1	59.4	46.3	10	60.5	64.9	69.9	10	55.0	101.9	83.9
100	107.8	250.4	54.7	100	70.1	177.7	99.0	100	69.8	301.0	141.0
220	112.6	267.0	65.2	220	70.6	253.8	105.6	220	78.4	294.0	153.0
330	125.6	259.0	57.5	330	74.3	287.6	133.2	330	63.0	295.2	156.0
1k	121.8	324.0	74.8	1k	77.9	309.0	150.6	1k	60.7	286.0	160.0
2k	115.2	320.4	61.1	2k	57.2	308.0	108.5	2k	61.8	282.2	162.0
5k	139.2	357.6	76.3	5k	84.0	355.2	110.0	5k	63.7	289.4	170.0

Table 1b. Mean current (mA) under different electrical configurations and heat sources at various load resistance.

Static body heat				Dynamic body heat				Appliance heat			
Resistor (Ω)	Parallel	Series	2×2 Hybrid	Resistor (Ω)	Parallel	Series	2×2 Hybrid	Resistor (Ω)	Parallel	Series	2×2 Hybrid
10	6.91	5.94	4.63	10	6.05	6.49	6.99	10	5.50	10.19	8.39
100	10.78	25.04	5.47	100	7.01	17.77	9.90	100	6.98	30.10	14.10
220	11.26	26.70	6.52	220	7.06	25.38	10.56	220	7.84	29.40	15.30
330	12.56	25.90	5.75	330	7.43	28.76	13.32	330	6.30	29.52	15.60
1k	12.18	32.40	7.48	1k	7.79	30.90	15.06	1k	6.07	28.60	16.00
2k	11.52	32.04	6.11	2k	5.72	30.80	10.85	2k	6.18	28.22	16.20
5k	13.92	35.76	7.63	5k	8.40	35.52	11.00	5k	6.37	28.94	17.00

Table 1c. Mean power output (µW) under different electrical configurations and heat sources at various load resistance.

Static body heat				Dynamic body heat				Appliance heat			
Resistor (Ω)	Parallel	Series	2×2 Hybrid	Resistor (Ω)	Parallel	Series	2×2 Hybrid	Resistor (Ω)	Parallel	Series	2×2 Hybrid
10	214.2	353.3	477.8	10	365.5	421.5	488.9	10	302.7	1037.5	703.6
100	29.9	627.0	116.2	100	49.1	315.7	98.0	100	48.7	906.0	198.8
220	19.3	324.0	57.6	220	22.6	292.8	50.7	220	28.0	392.9	106.4
330	10.0	203.3	47.8	330	16.7	250.6	53.8	330	12.0	264.1	73.7
1k	5.6	105.0	14.8	1k	6.1	95.5	22.7	1k	3.7	81.8	25.6
2k	1.9	51.3	6.6	2k	1.6	47.4	5.9	2k	1.9	39.8	13.1
5k	1.2	25.6	3.9	5k	1.4	25.2	2.4	5k	0.8	16.8	5.8

Table 1d. Mean temperature difference (ΔT, °C) under different electrical configurations and heat sources at various load resistance.

Static body heat				Dynamic body heat				Appliance heat			
Resistor (Ω)	Parallel	Series	2×2 Hybrid	Resistor (Ω)	Parallel	Series	2×2 Hybrid	Resistor (Ω)	Parallel	Series	2×2 Hybrid
10	9.8	10.7	10.3	10	8.3	9.9	10.7	10	15.9	8.5	15.1
100	10.5	10.7	10.2	100	8.7	10.8	10.7	100	17.2	15.3	17.8
220	9.0	11.1	10.4	220	9.3	10.7	10.2	220	14.9	15.9	18.7
330	10.6	11.1	10.2	330	9.3	10.8	9.7	330	15.0	11.1	13.4
1k	9.9	9.9	9.8	1k	8.3	11.1	10.4	1k	16.7	11.3	15.7
2k	10.7	12.5	10.4	2k	8.8	10.7	10.2	2k	16.3	11.8	13.2
5k	9.0	10.8	11.6	5k	9.7	11.7	9.3	5k	10.5	11.0	13.8

Table 2a. Mean voltage (mV) under different electrical configurations and heat sources at a load resistance of 10 Ω.

TEG configuration	Static body heat (mV)	Dynamic body heat (mV)	Appliance heat (mV)
2×2 Hybrid	69.12 ± 0.6	69.92 ± 0.2	83.88 ± 1.0
Series	59.44 ± 0.3	64.92 ± 0.7	101.86 ± 2.6
Parallel	46.28 ± 0.3	60.46 ± 0.1	55.02 ± 0.5

Table 2b. Mean current (mA) under different electrical configurations and heat sources at a load resistance of 10 Ω.

TEG configuration	Static body heat (mA)	Dynamic body heat (mA)	Appliance heat (mA)
2×2 Hybrid	6.91	6.99	8.39
Series	5.94	6.49	10.19
Parallel	4.63	6.05	5.50

Table 2c. Mean power output (μW) under different electrical configurations and heat sources at a load resistance of 10 Ω.

TEG configuration	Static body heat (μW)	Dynamic body heat (μW)	Appliance heat (μW)
2×2 Hybrid	477.8	488.9	703.6
Series	353.3	421.5	1037.5
Parallel	214.2	365.5	302.7

Table 2d. Mean temperature difference (ΔT, °C) across heat sources.

Heat Source	Mean Temperature Difference (°C)
Static Body Heat	10.6
Dynamic Body Heat	10.4
Appliance Heat	14.2

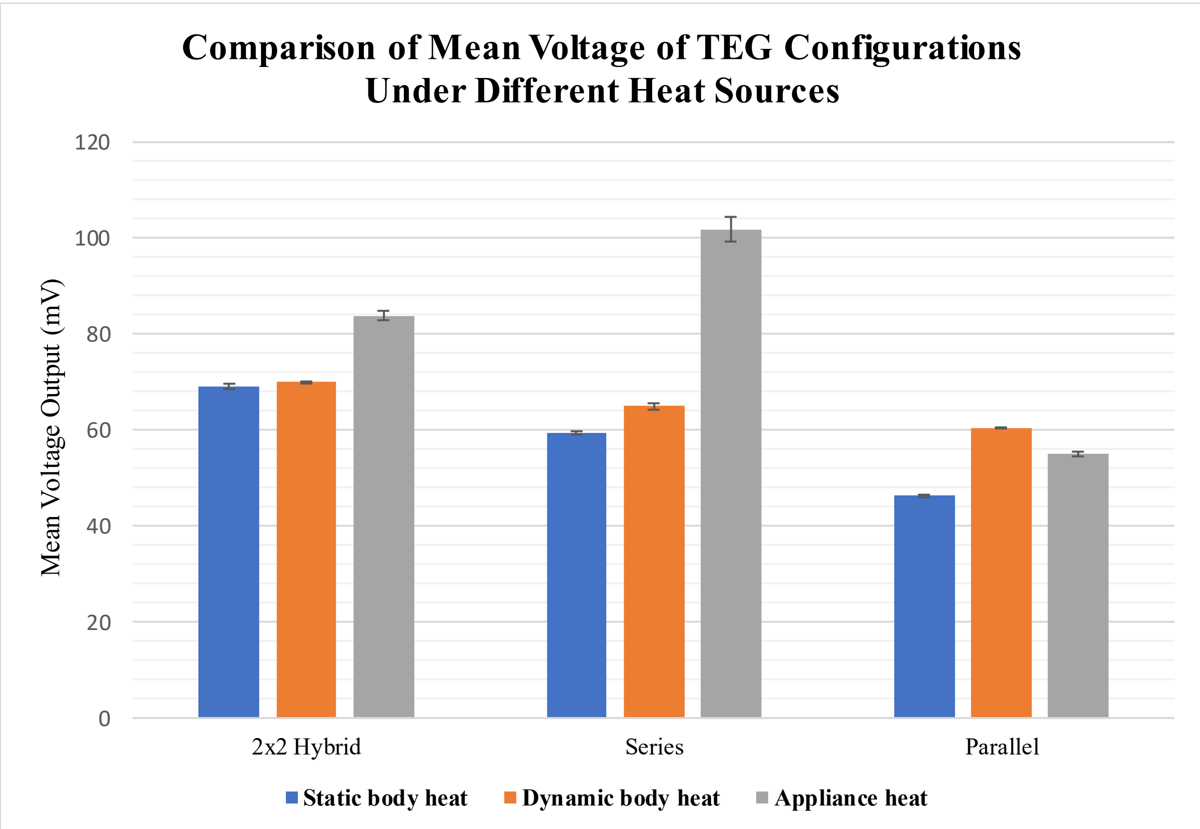

Figure 5a. Comparison of mean voltage (mV ± SD) of different TEG configurations under different heat source conditions.

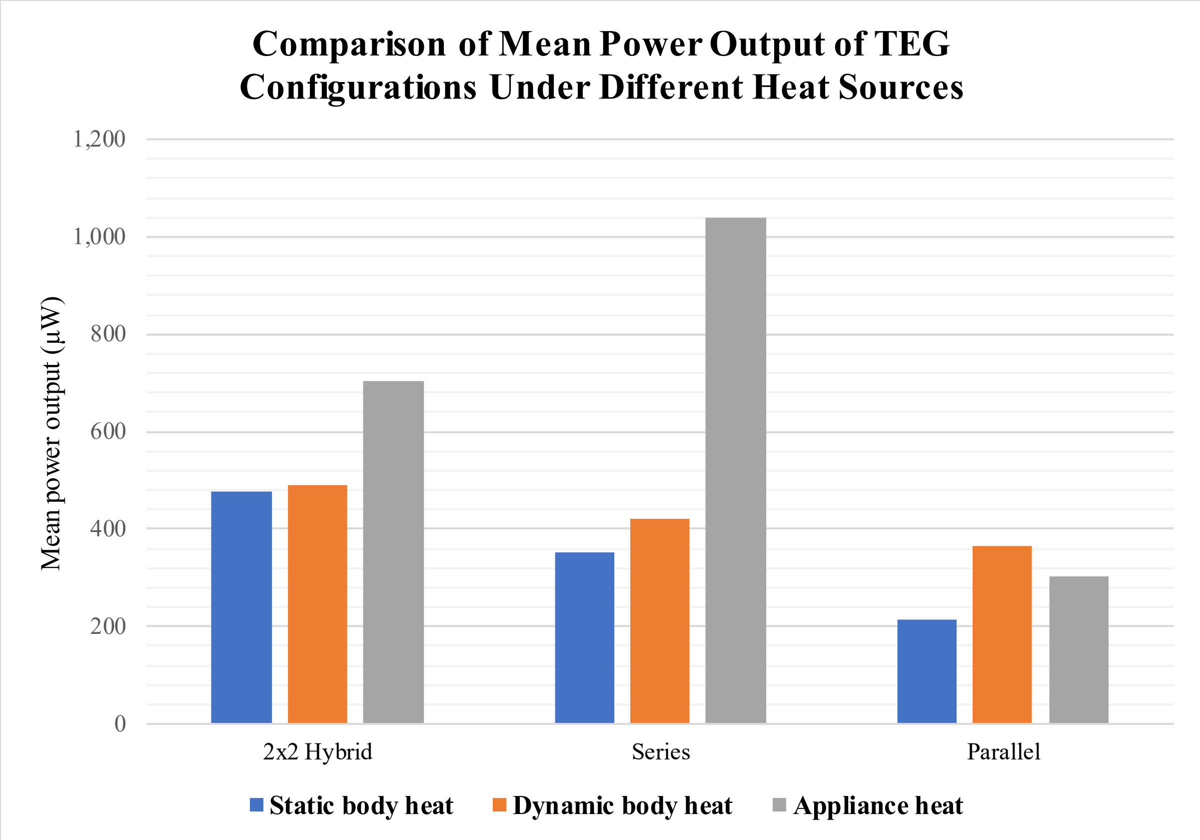

Figure 5b. Comparison of mean power output (µW) of different TEG configurations under different heat source conditions.

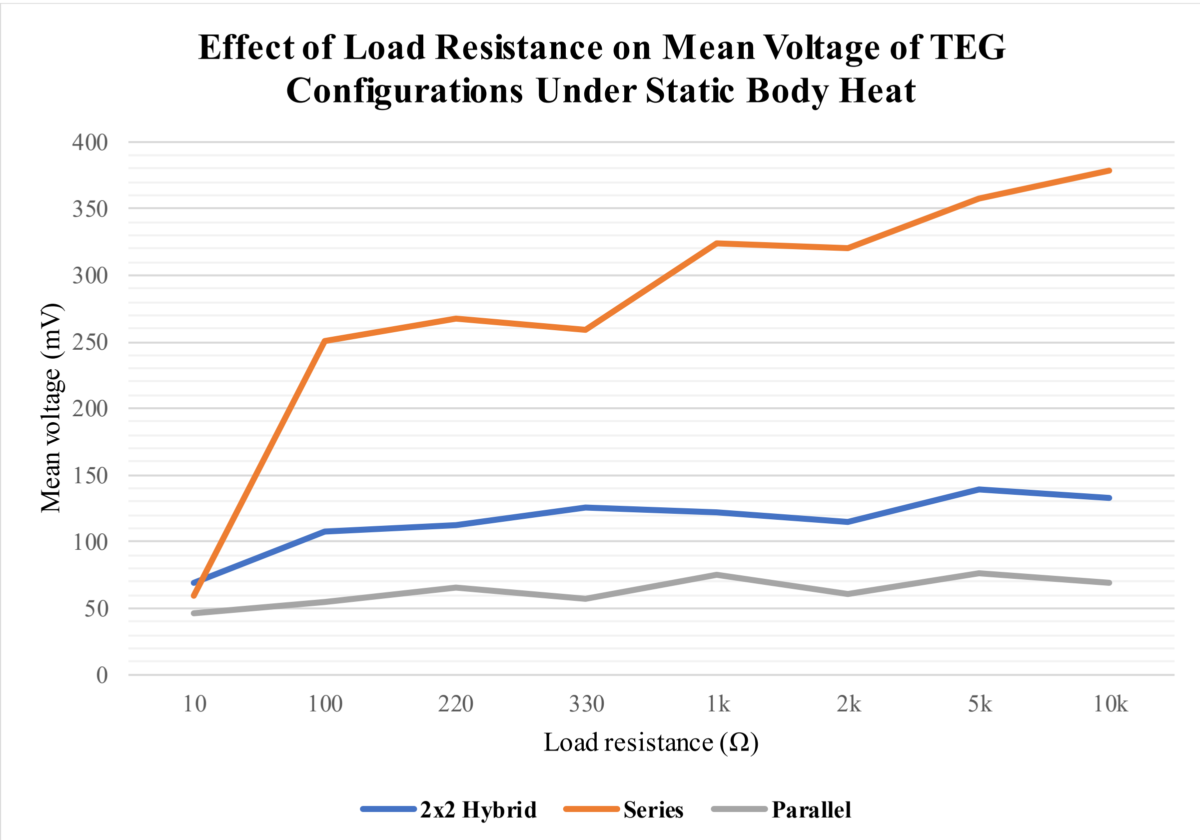

Figure 6a. Effect of load resistance on mean voltage (mV) of different TEG configurations under static body heat condition.

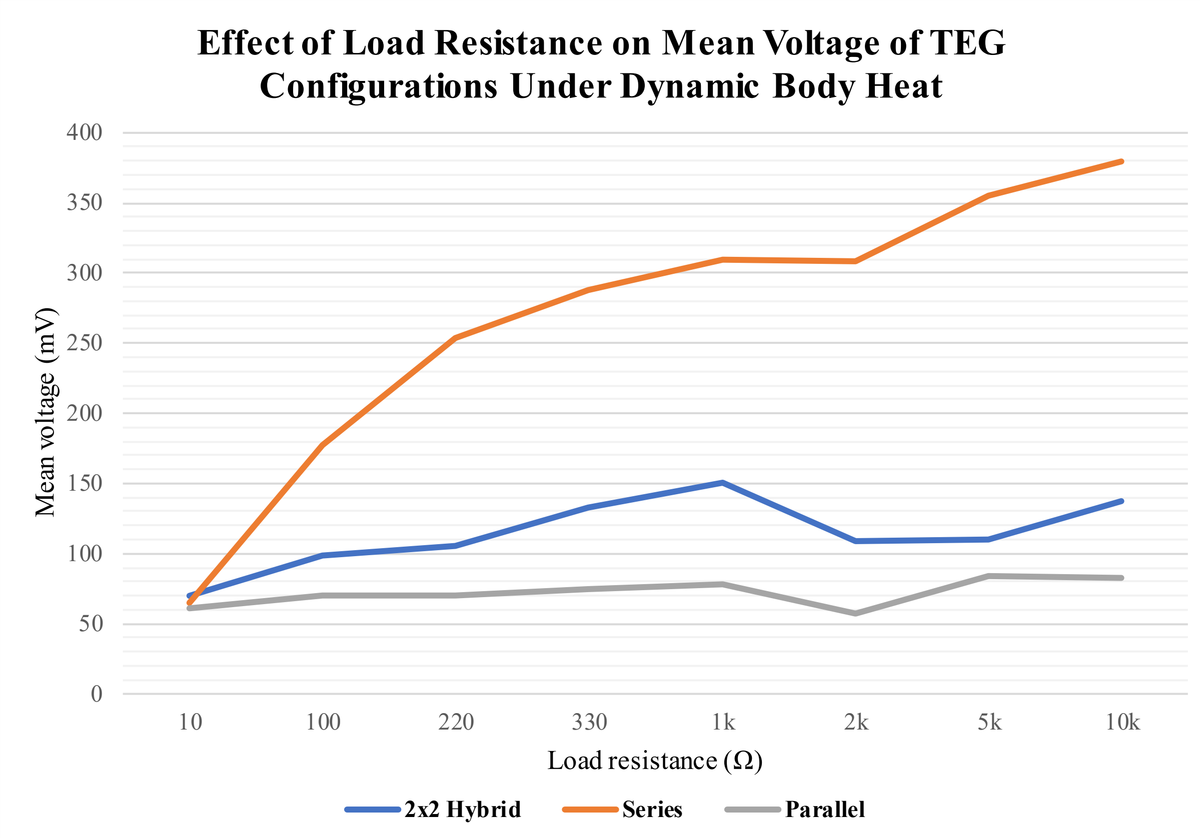

Figure 6b. Effect of load resistance on mean voltage (mV) of different TEG configurations under dynamic body heat condition.

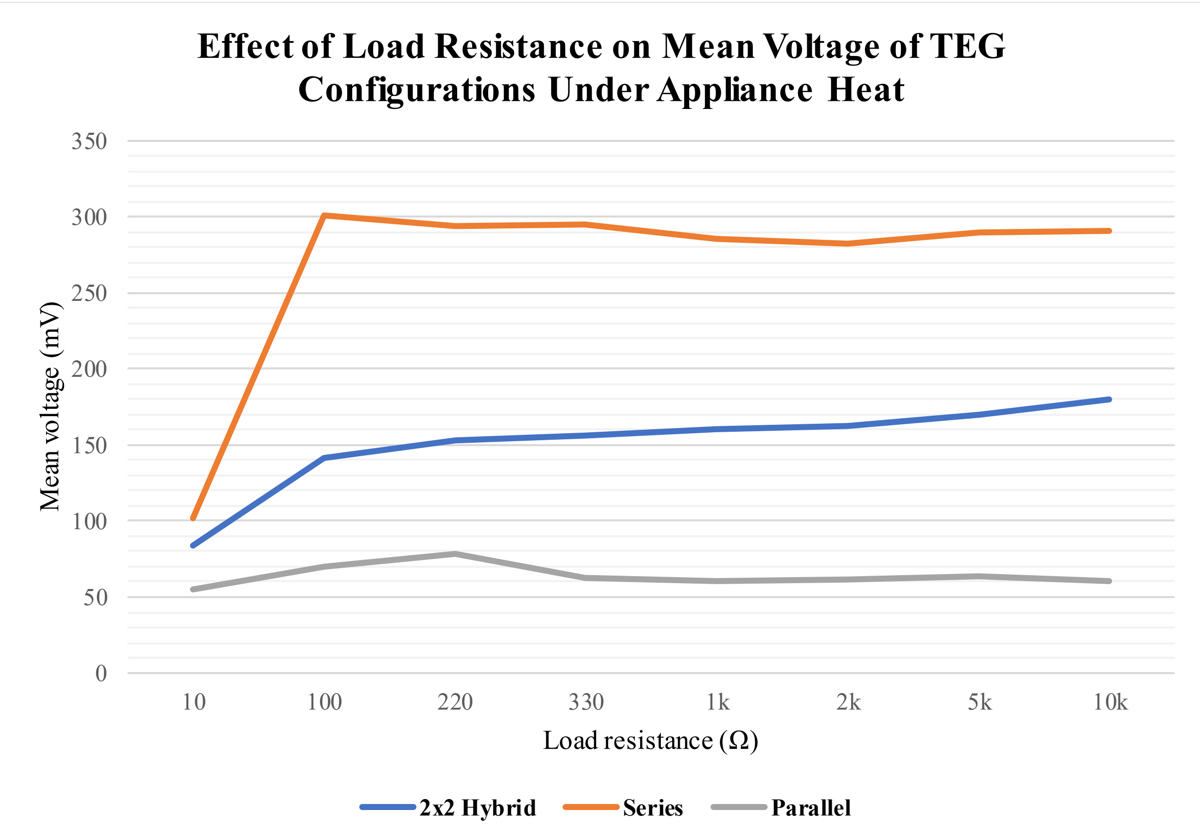

Figure 6c. Effect of load resistance on mean voltage (mV) of different TEG configurations under appliance heat condition.

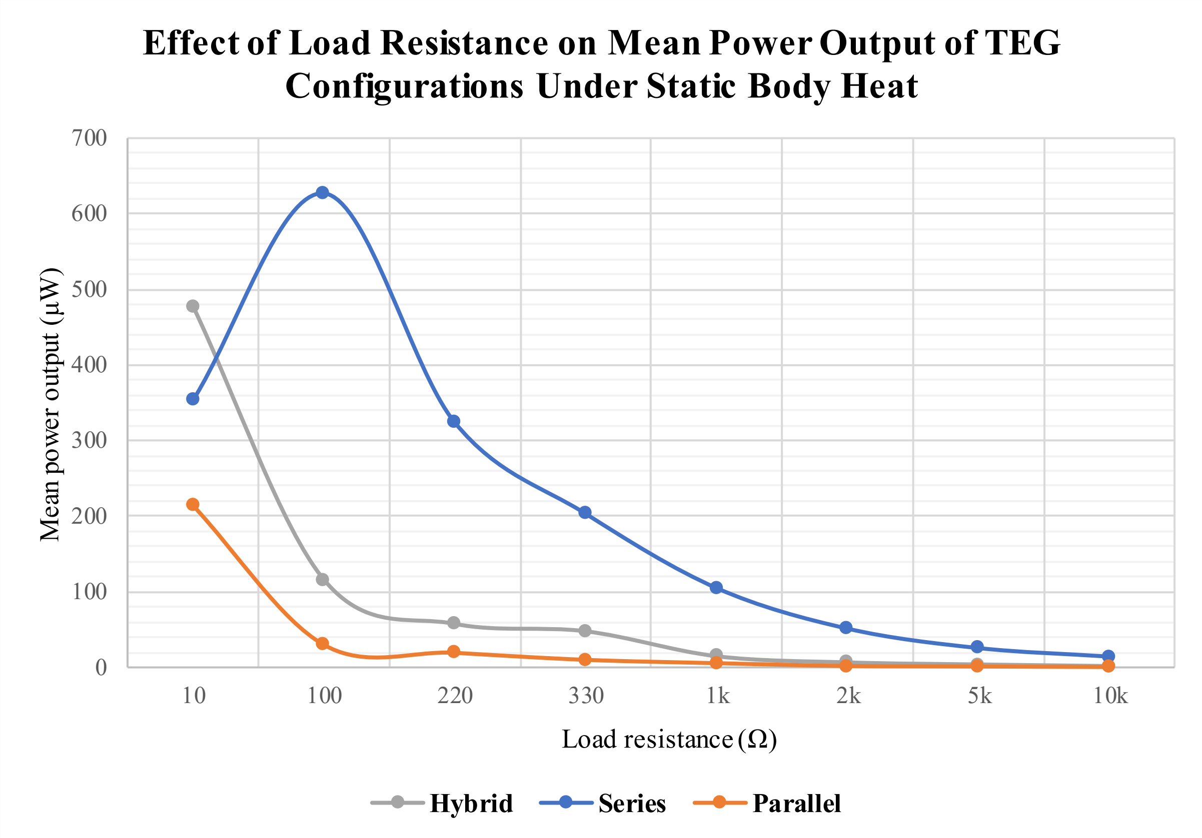

Figure 7a. Effect of load resistance on mean power output (µW) of different TEG configurations under static body heat condition.

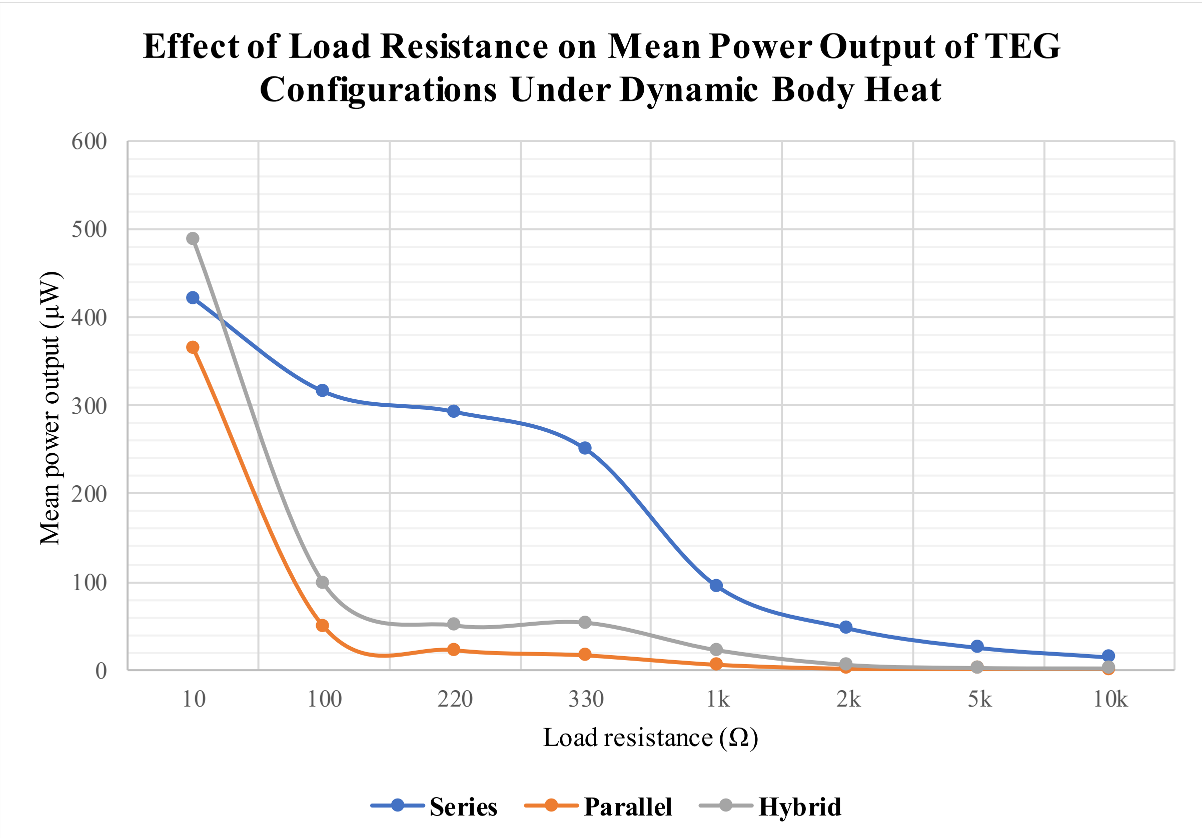

Figure 7b. Effect of load resistance on mean power output (µW) of different TEG configurations under dynamic body heat condition.

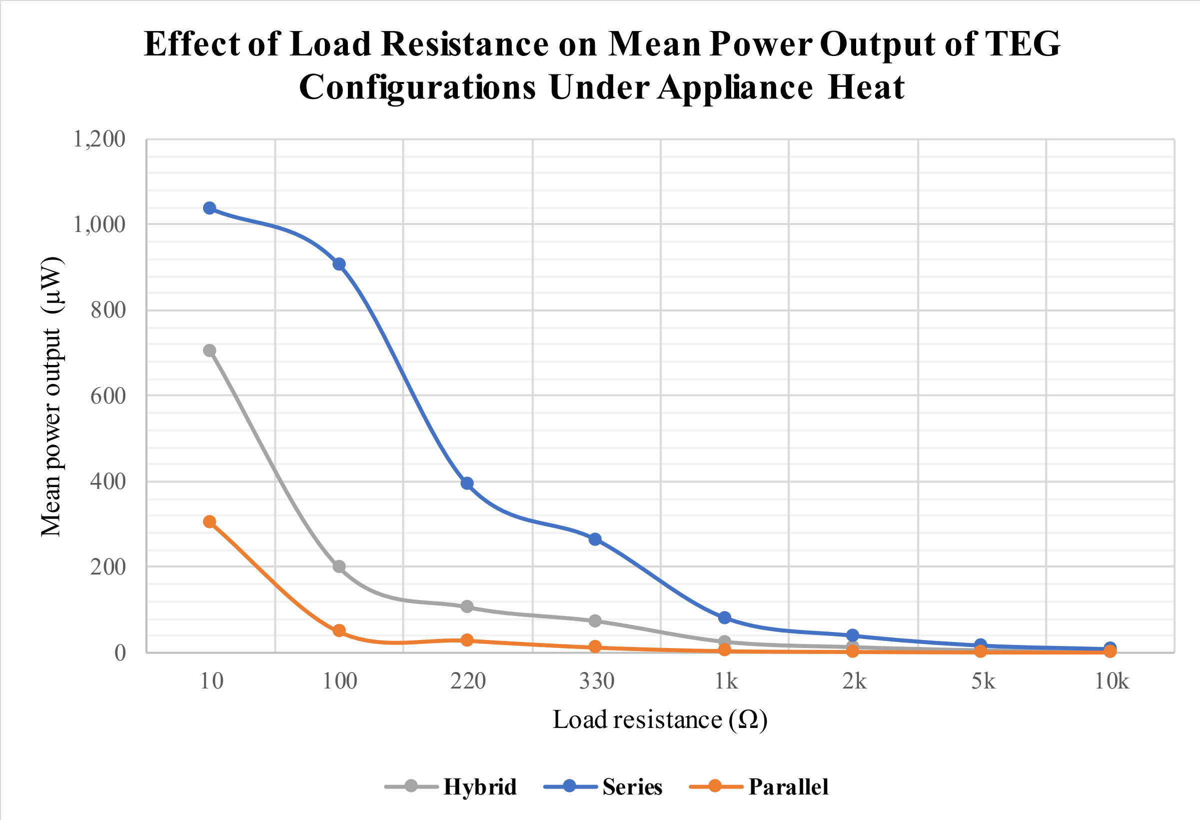

Figure 7c. Effect of load resistance on mean power output (µW) of different TEG configurations under appliance heat condition.

The results indicate that the 10 Ω load resistor produced the highest power output across the configurations and heat source conditions. Power output decreased non-linearly as load resistance increased from 10 Ω to 10 kΩ (*Figure 7*). Consequently, 10 Ω was selected as the fixed load resistance for Stage 2.

The series and 2×2 hybrid configurations consistently produced higher power output than the parallel configuration, indicating more effective voltage accumulation (*Figures 5, 6 and 7*). Appliance heat generated the highest power output for series (1037.5 µW) and hybrid (703.6 µW), corresponding to its greater temperature difference (14.2 °C compared to ~10.5 °C) (*Tables 2c and 2d*). This supports a positive relationship between ΔT and power output, although overall efficiency is dependent on electrical configuration.

STAGE 2 RESULTS

Raw Data:

Table 3a. Raw voltage output (mV) of TEG configurations under different heat source conditions at a fixed load resistance of 10 Ω across three trials.

Static body heat					Dynamic body heat					Appliance heat				
Trial 1 Time (s)	Paralle**l**	Series	2×2 Hybrid	Single TEG	Trial 1 Time (s)	Parallel	Series	2×2 Hybrid	Single TEG	Trial 1 Time (s)	Parallel	Series	2×2 Hybrid	Single TEG
0	171.0	251.0	410.0	149.4	0	153.0	144.0	323.0	119.2	0	111.5	98.4	153.0	77.5
30	143.9	241.0	378.0	145.8	30	126.8	169.0	256.0	94.7	30	67.3	102.9	140.2	82.8
60	148.0	198.0	390.0	160.4	60	122.2	148.0	261.0	91.2	60	89.8	102.8	144.8	86.4
90	150.5	238.0	316.0	167.8	90	106.6	185.0	277.0	105.8	90	63.8	105.9	138.7	76.8
120	162.9	228.0	307.0	170.9	120	117.2	175.0	238.0	89.8	120	119.2	107.2	136.9	78.8
150	126.6	256.0	286.0	178.2	150	121.8	203.0	*225.0*	81.8	150	112.8	107.1	136.1	76.0
180	134.3	298.0	264.0	164.8	180	130.0	139.0	187.0	92.4	180	111.8	124.9	132.1	83.3

Trial 2 Time (s)	Parallel	Series	2×2 Hybrid	Single TEG	Trial 2 Time (s)	Parallel	Series	2×2 Hybrid	Single TEG	Trial 2 Time (s)	Parallel	Series	2×2 Hybrid	Single TEG
0	132.8	232.0	226.0	159.4	0	134.8	198.0	226.0	104.9	0	83.8	122.4	144.5	82.2
30	107.8	248.0	232.0	144.5	30	98.6	201.0	211.0	109.8	30	90.9	125.2	136.4	84.5
60	76.2	265.0	230.0	136.5	60	114.8	210.0	201.0	116.9	60	93.3	125.8	137.8	95.8
90	117.5	257.0	205.0	126.7	90	99.7	196.0	201.0	103.5	90	89.1	121.4	128.8	80.7
120	104.8	270.0	235.0	124.8	120	101.8	196.0	210.0	111.8	120	90.9	118.2	127.9	79.0
150	61.8	198.0	228.0	106.9	150	95.6	199.0	200.0	106.3	150	95.9	120.3	148.8	82.4
180	100.2	228.0	222.0	105.8	180	118.1	149.0	198.0	107.9	180	129.9	121.2	139.6	73.4
Trial 3 Time (s)	**Parallel**	**Series**	**2×2 Hybrid**	**Single TEG**	**Trial 3 Time (s)**	**Parallel**	**Series**	**2×2 Hybrid**	**Single TEG**	**Trial 3 Time (s)**	**Parallel**	**Series**	**2×2 Hybrid**	**Single TEG**
0	144.5	228.0	200.0	91.8	0	110.5	153.0	194.0	126.9	0	101.6	118.8	145.4	79.9
30	77.1	213.0	195.0	96.5	30	107.8	150.0	172.0	106.6	30	104.5	116.0	134.4	82.3
60	98.2	173.0	166.0	118.6	60	94.7	170.0	179.0	96.6	60	97.4	126.0	140.2	79.7
90	114.8	232.0	239.0	114.8	90	95.8	158.0	166.0	99.6	90	113.2	122.9	137.4	81.2
120	106.9	207.0	263.0	109.9	120	103.3	201.0	203.0	97.5	120	97.6	122.1	142.5	74.8
150	101.5	217.0	205.0	100.4	150	102.6	198.0	186.0	96.8	150	107.9	125.5	139.2	83.8
180	94.7	221.0	216.0	94.8	180	101.8	144.0	189.0	90.8	180	129.9	121.2	139.6	73.4

Table 3b. Raw temperature difference (ΔT, °C) across TEG configurations under different heat source conditions at a fixed load resistance of 10 Ω across three trials.

Static body heat					Dynamic body heat					Appliance heat				
Trial 1 Time (s)	**Parallel**	**Series**	**2×2 Hybrid**	**Single TEG**	**Trial 1 Time (s)**	**Parallel**	**Series**	**2×2 Hybrid**	**Single TEG**	**Trial 1 Time (s)**	**Parallel**	**Series**	**2×2 Hybrid**	**Single TEG**
0	9.4	21.6	20.5	14.2	0	16.7	18.5	20.7	17.7	0	17.6	20.4	35.5	21.4
30	20.2	14.6	20.2	13.8	30	21.8	12.4	17.4	19.7	30	22.1	22.4	35.1	12.5
60	21.4	11.8	22.8	12.0	60	19.8	14.0	17.1	11.6	60	16.0	23.0	34.7	27.7
90	21.9	14.7	17.5	9.7	90	18.8	19.8	20.7	11.9	90	10.9	19.0	30.6	21.6
120	22.0	11.3	19.2	12.9	120	20.6	12.0	18.1	13.1	120	35.9	19.8	32.3	11.9
150	21.9	12.9	15.0	14.8	150	17.6	18.0	16.7	17.6	150	27.2	22.7	31.8	13.6
180	22.0	15.1	16.0	18.8	180	20.8	20.8	17.9	13.3	180	38.4	24.8	36.7	12.9
Trial 2 Time (s)	**Parallel**	**Series**	**2×2 Hybrid**	**Single TEG**	**Trial 2 Time (s)**	**Parallel**	**Series**	**2×2 Hybrid**	**Single TEG**	**Trial 2 Time (s)**	**Parallel**	**Series**	**2×2 Hybrid**	**Single TEG**
0	20.8	12.9	21.9	18.0	0	21.0	17.1	19.9	19.4	0	31.1	25.6	38.0	13.9
30	21.9	14.7	19.4	14.8	30	12.6	18.4	20.3	15.0	30	33.2	22.2	32.2	12.5
60	22.5	14.4	17.4	12.4	60	21.7	17.8	19.5	20.2	60	19.1	26.9	34.7	16.6
90	21.3	14.3	17.2	16.7	90	21.2	18.8	19.3	16.8	90	32.6	25.9	34.2	15.7
120	20.8	19.3	16.6	14.1	120	15.8	16.4	20.2	14.1	120	27.7	29.5	27.3	24.0
150	22.0	18.5	16.7	10.9	150	20.2	17.4	20.4	19.1	150	39.6	27.1	29.6	16.9
180	21.6	21.7	16.3	17.4	180	20.2	20.4	19.8	12.7	180	32.5	26.7	28.7	14.3
Trial 3 Time (s)	**Parallel**	**Series**	**2×2 Hybrid**	**Single TEG**	**Trial 3 Time (s)**	**Parallel**	**Series**	**2×2 Hybrid**	**Single TEG**	**Trial 3 Time (s)**	**Parallel**	**Series**	**2×2 Hybrid**	**Single TEG**
0	21.8	20.1	21.2	15.6	0	19.9	16.0	19.3	20.9	0	36.6	22.1	28.0	14.7
30	20.3	18.1	16.0	18.0	30	18.7	19.2	21.0	16.2	30	31.7	26.3	31.6	14.3
60	22.0	18.7	12.4	19.6	60	19.3	20.6	19.8	20.6	60	33.5	27.9	31.2	14.3
90	21.0	19.7	17.6	11.4	90	13.8	16.2	20.1	20.0	90	32.2	27.4	31.4	12.1
120	22.2	19.9	16.8	10.2	120	21.7	16.2	19.8	17.3	120	36.4	21.2	28.6	15.7
150	20.4	22.0	15.6	24.0	150	16.9	17.0	16.6	20.6	150	20.4	27.6	38.2	24.4
180	18.4	20.0	21.8	18.4	180	21.6	18.5	19.9	21.3	180	24.4	21.3	37.1	23.3

Processed Data and Graphical Representations:

Table 4a. Mean voltage (mV ± SD) of TEG configurations under different heat source conditions, calculated from three trials.

Electrical configuration	Single TEG (mV)	Parallel (mV)	Series (mV)	2×2 Hybrid (mV)
Static body heat	131.8 ± 29.4	117.9 ± 26.3	233.3 ± 17.6	257.8 ± 68.0
Dynamic body	102.4 ± 6.2	112.3 ±11.8	175.5 ± 14.9	214.4 ± 34.8
Appliance heat	81.0 ± 1.4	98.5 ± 3.7	117.1 ± 8.7	139.2 ± 1.3

Table 4b. Mean calculated current (mA ± SD) of TEG configurations under different heat source conditions, calculated from three trials.

Electrical configuration	Single TEG (mA)	Parallel (mA)	Series (mA)	2×2 Hybrid (mA)
Static body heat	13.18 ± 2.9	11.79 ± 2.6	23.33 ± 1.8	25.78 ± 6.8
Dynamic body	10.24 ± 0.6	11.23 ± 1.2	17.55 ± 1.5	21.44 ± 3.5
Appliance heat	8.10 ± 0.1	9.85 ± 0.4	11.71 ± 0.9	13.92 ± 0.1

Table 4c. Mean calculated power output (µW ± SD) of TEG configurations under different heat source conditions, calculated from three trials.

Electrical configuration	Single TEG (µW)	Parallel (µW)	Series (µW)	2×2 Hybrid (µW)
Static body heat	1795.9 ± 788.4	1436.4 ± 659.6	5462.8 ± 803.0	6952.1 ± 3759.6
Dynamic body	1051.5 ± 126.6	1269.6 ± 271.1	3095.7 ± 536.0	4678.7 ± 1531.4
Appliance heat	656.4 ± 22.0	972.0 ± 73.0	1376.4 ± 200.0	1937.5 ± 37.2

Table 4d. Mean temperature difference (ΔT, °C ± SD) across TEG configurations under different heat source conditions, calculated from three trials.

Electrical configuration	Single TEG (°C)	Parallel (°C)	Series (°C)	2×2 Hybrid (°C)
Static body heat	15.1 ± 1.5	20.8 ± 0.9	17.0 ± 2.6	18.0 ± 0.7
Dynamic body	17.9 ± 2.3	19.1 ± 0.3	17.4 ± 0.8	19.3 ± 0.8
Appliance heat	16.9 ± 0.6	28.5 ± 3.9	24.3 ± 2.3	32.7 ± 0.9

Table 5a. Relative voltage of four-module TEG configurations normalised to a single TEG under each heat source condition, based on mean values from three trials.

Electrical configuration	Single TEG	Parallel	Series	2×2 Hybrid
Static body heat	1.0	0.9	1.8	2.0
Dynamic body	1.0	1.1	1.7	2.1
Appliance heat	1.0	1.2	1.4	1.7

Table 5b. Relative power output of four-module TEG configurations normalised to a single TEG under each heat source condition, based on mean values from three trials.

Electrical configuration	Single TEG	Parallel	Series	2×2 Hybrid
Static body heat	1.0	0.8	3.0	3.9
Dynamic body	1.0	1.2	2.9	4.4
Appliance heat	1.0	1.5	2.1	3.0

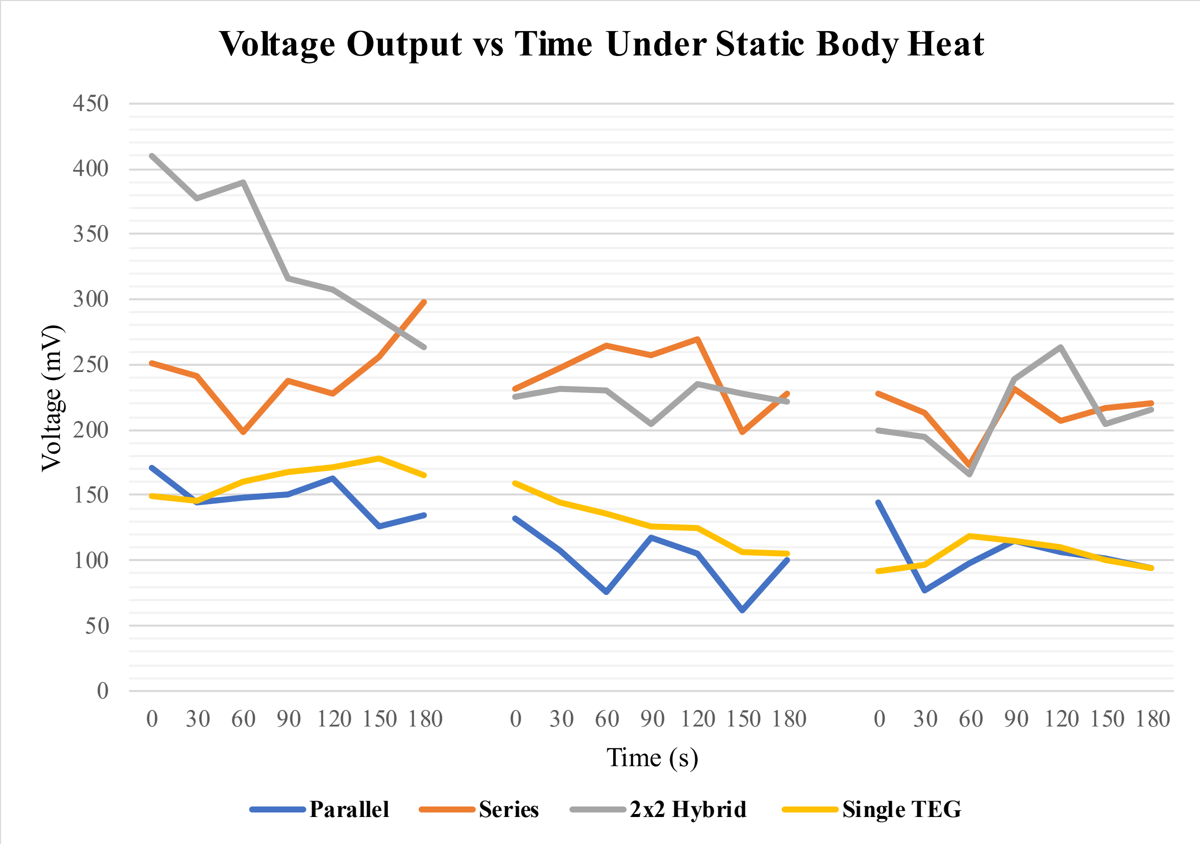

Figure 8a. Voltage output (mV) of TEG configurations over time under static body heat, shown across three repeated trials (each 180 s).

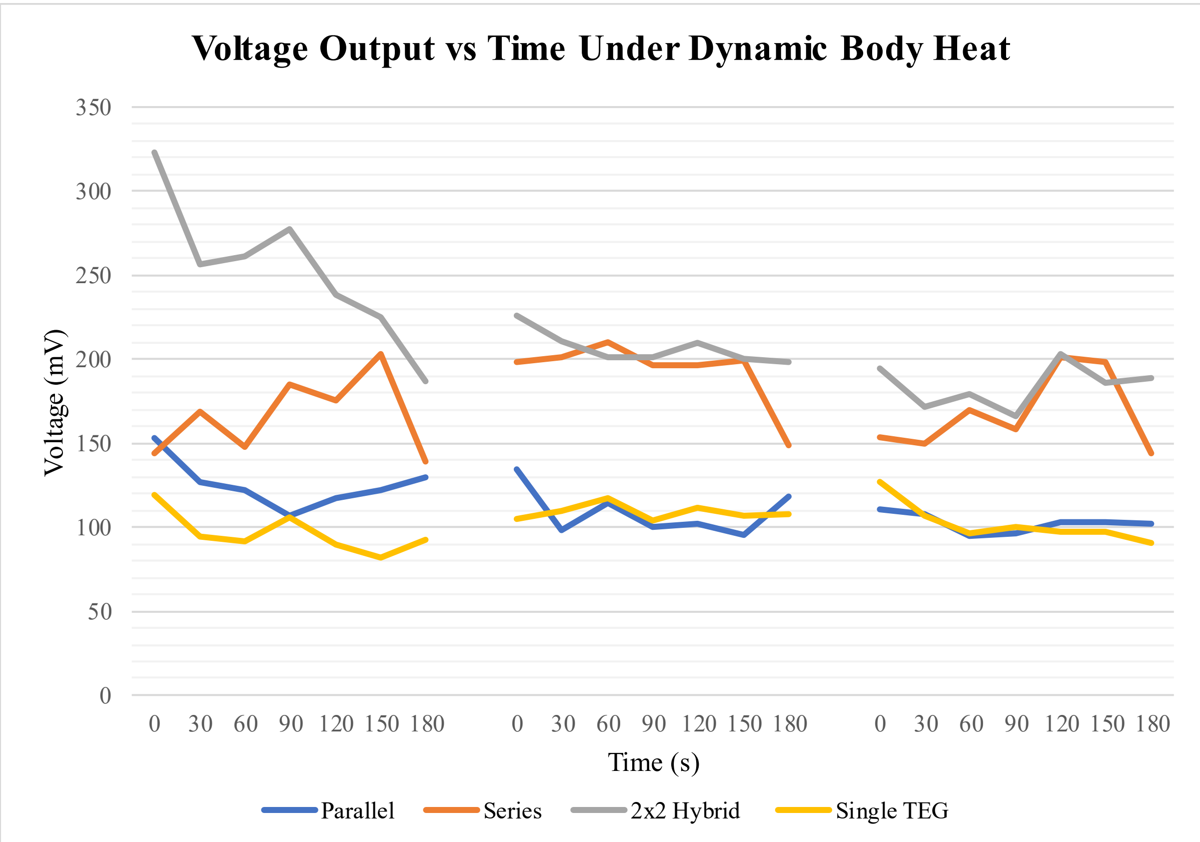

Figure 8b. Voltage output (mV) of TEG configurations over time under dynamic body heat, shown across three repeated trials (each 180 s).

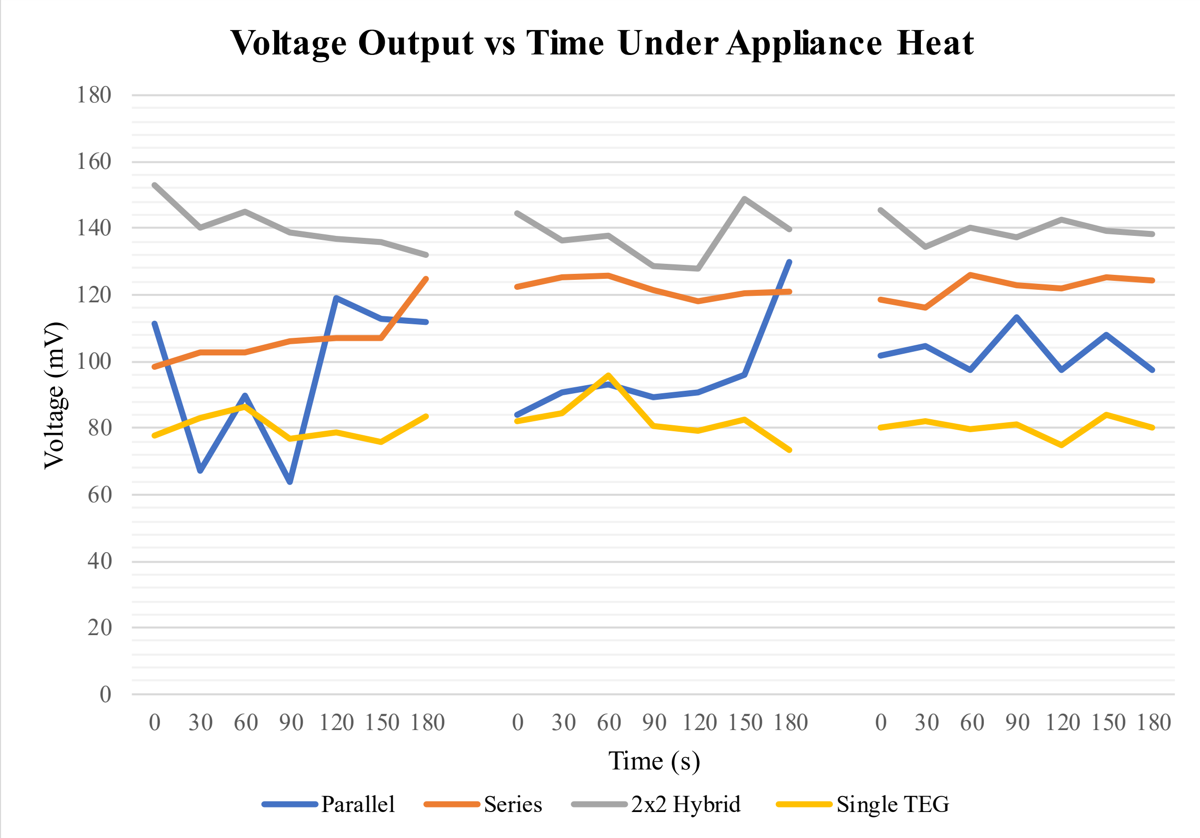

Figure 8c. Voltage output of different TEG configurations over time under appliance heat condition, shown across three repeated trials (each 180 s).

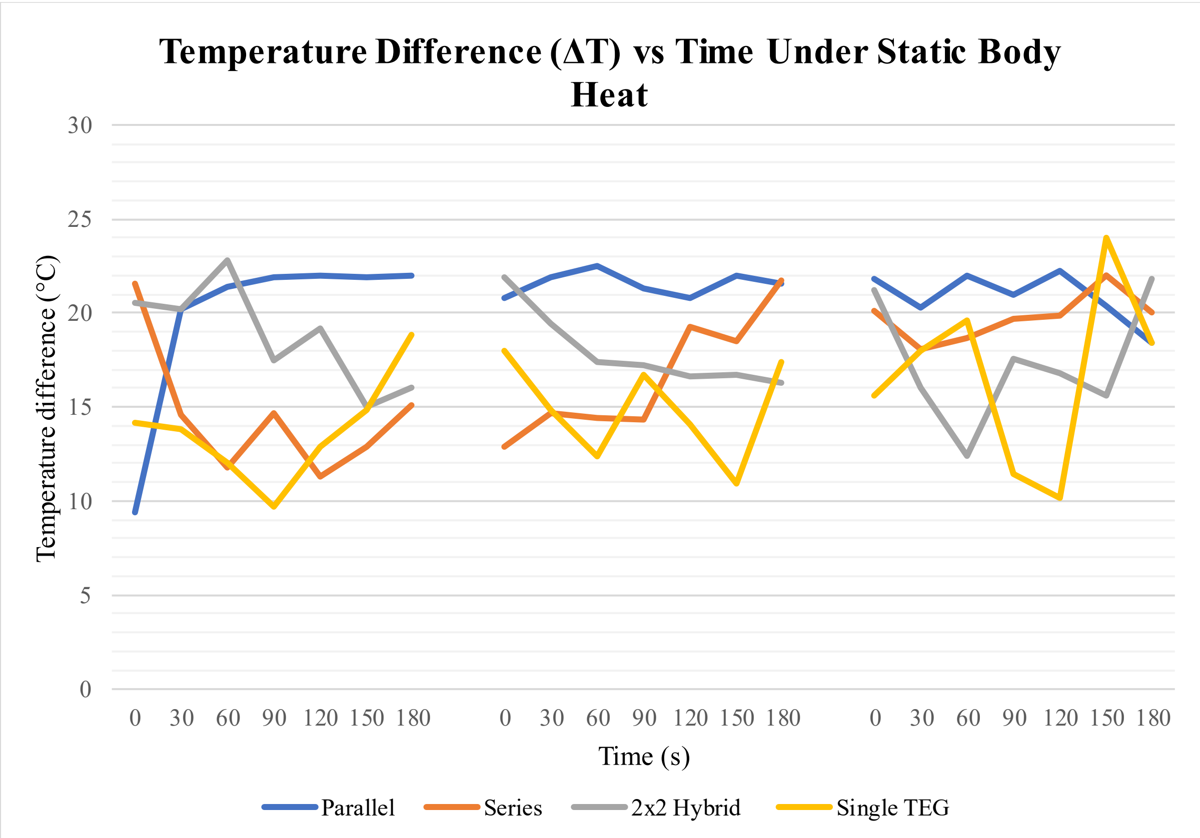

Figure 9a. Temperature difference (ΔT, °C) across TEG configurations over time under static body heat, shown across three repeated trials (each 180 s).

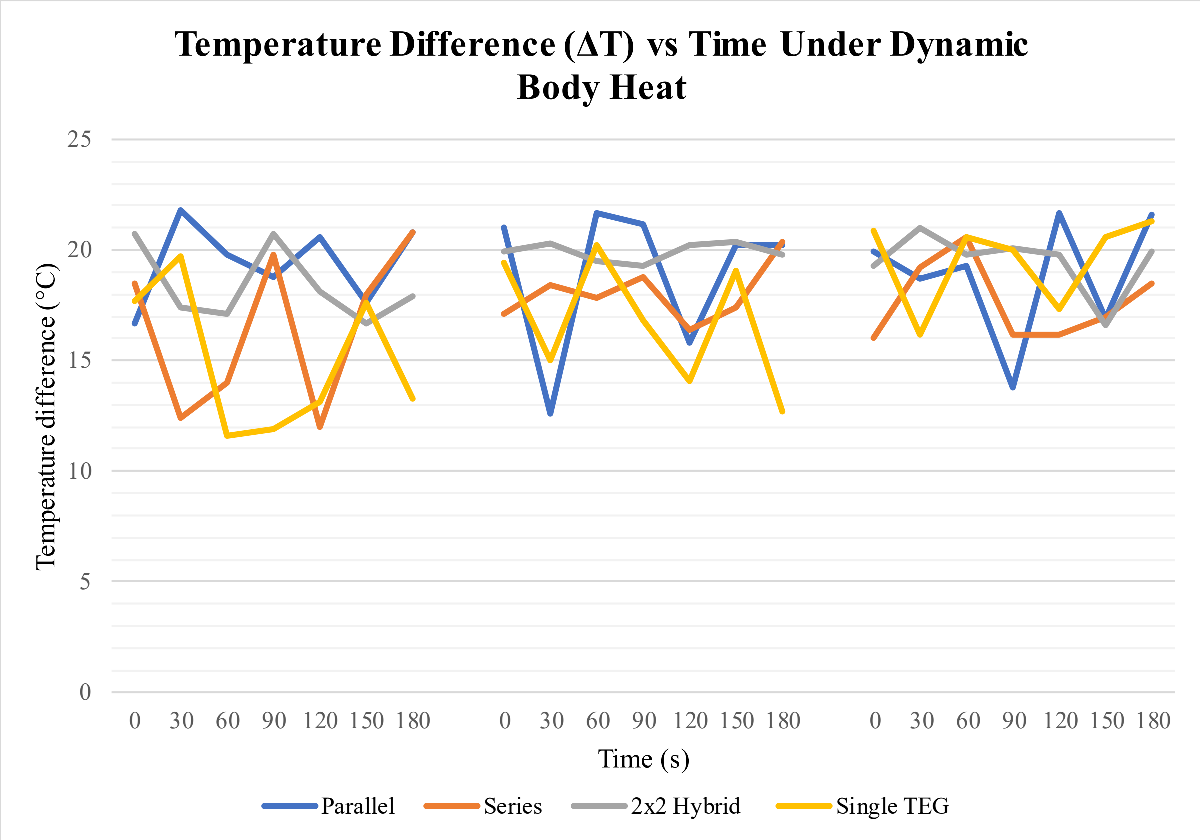

Figure 9b. Temperature difference (ΔT, °C) across TEG configurations over time under dynamic body heat, shown across three repeated trials (each 180 s).

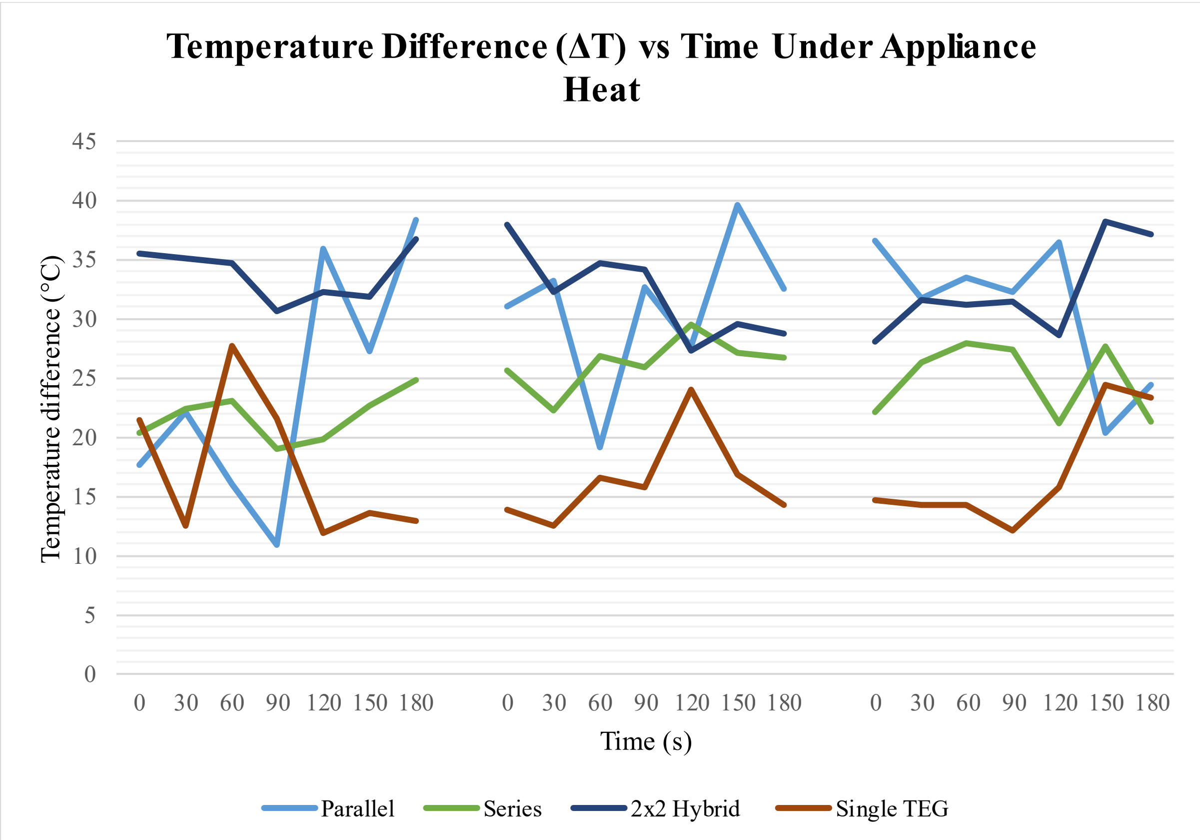

Figure 9c. Temperature difference (ΔT, °C) across TEG configurations over time under appliance heat, shown across three repeated trials (each 180 s).

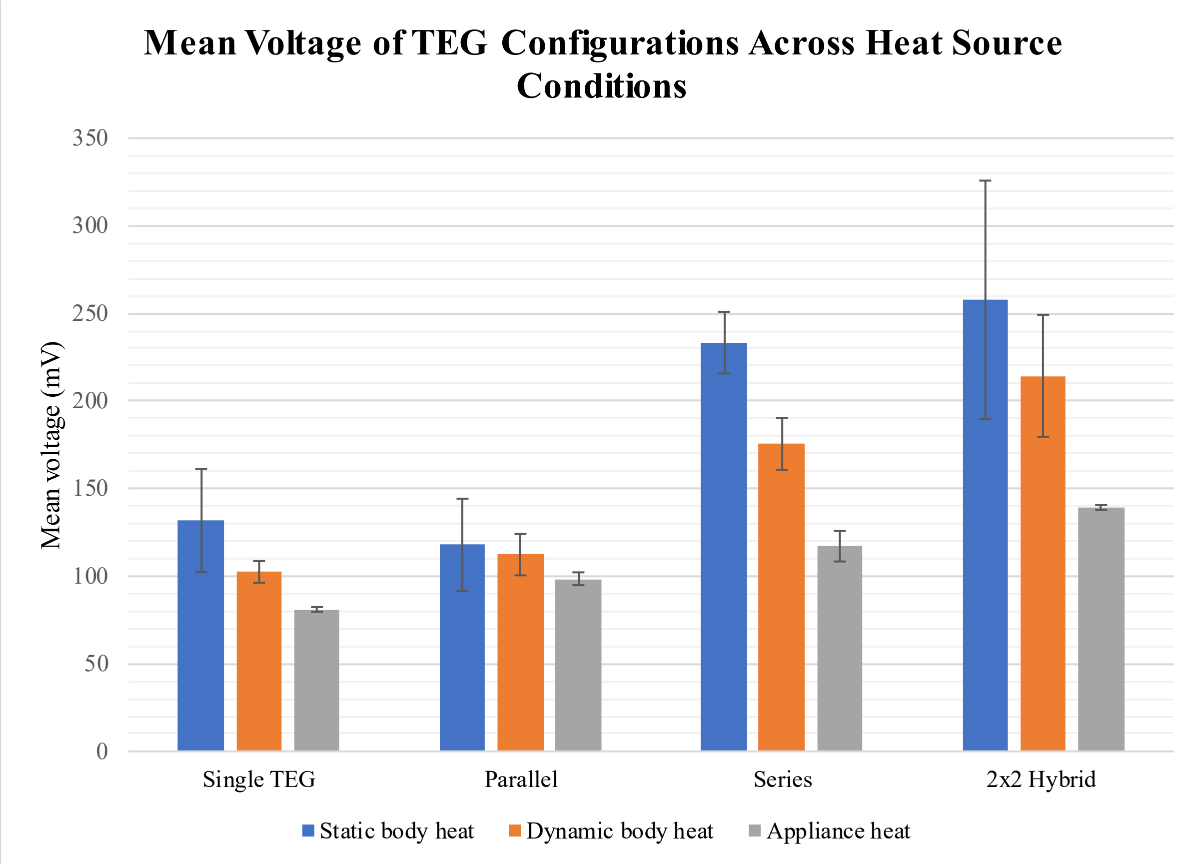

Figure 10a. Mean voltage (mV ± SD) of TEG configurations under different heat source conditions.

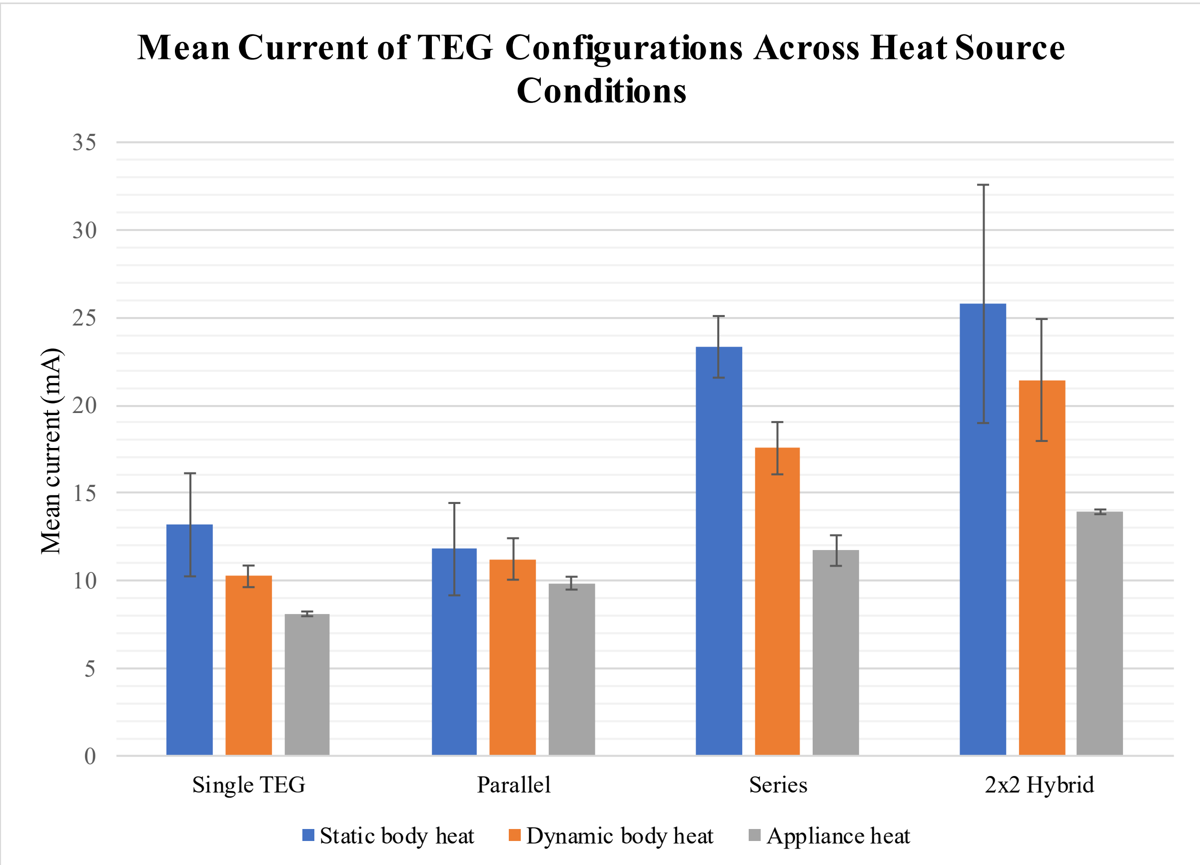

Figure 10b. Mean current (mA ± SD) of TEG configurations under different heat source conditions.

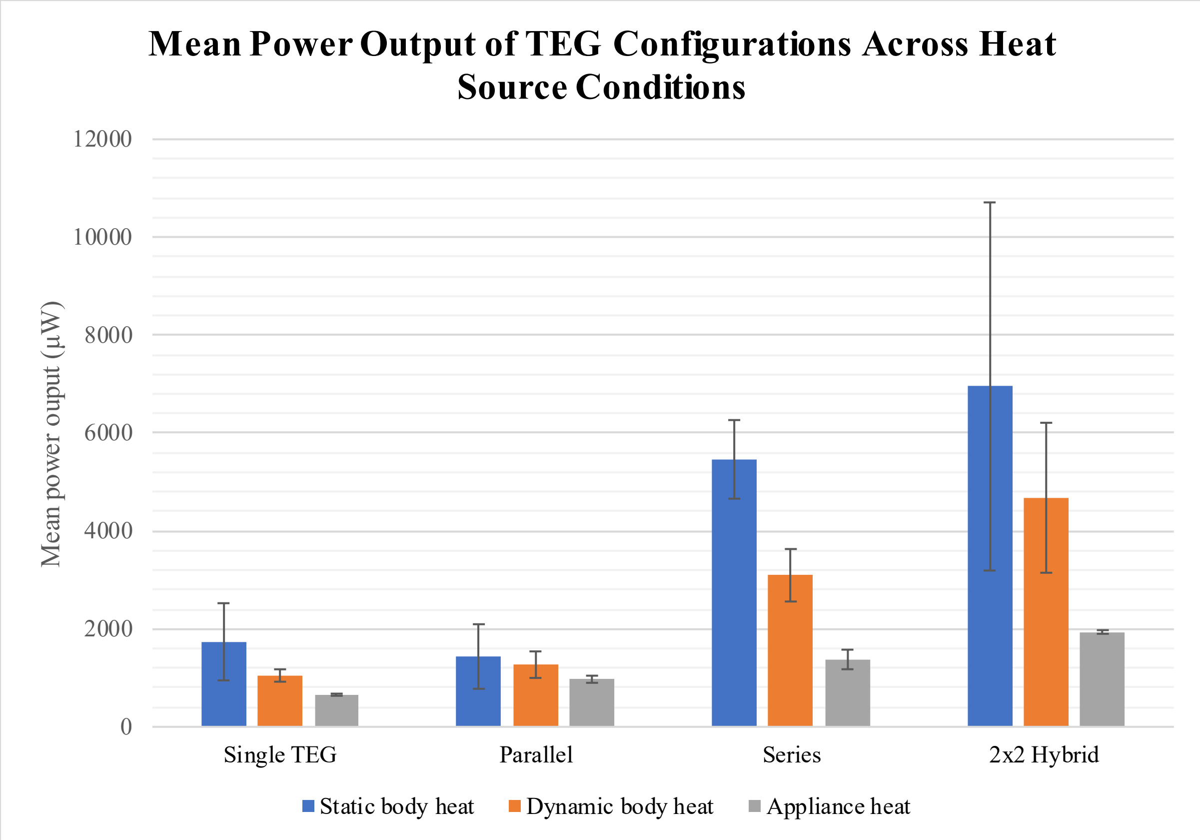

Figure 10c. Mean power output (µW ± SD) of TEG configurations under different heat source conditions.

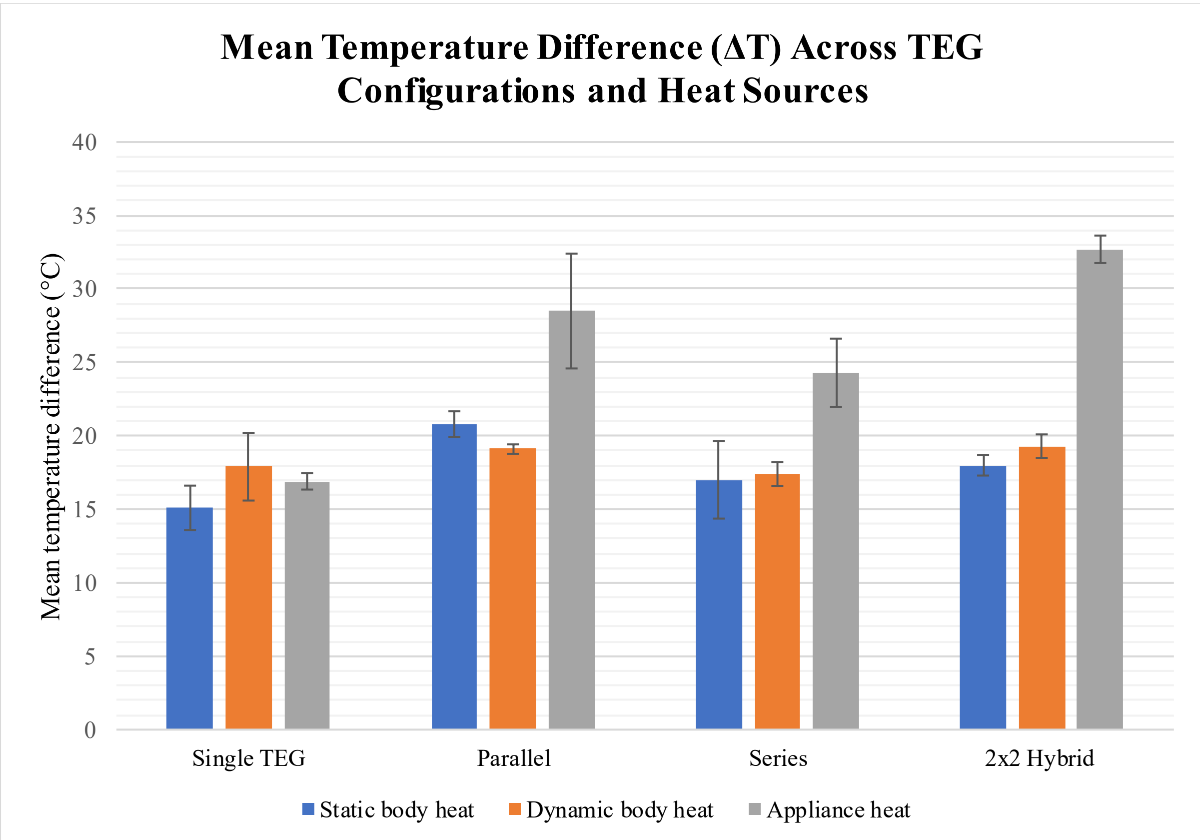

Figure 10d. Mean temperature difference (ΔT, °C ± SD) across TEG configurations under different heat source conditions.

Two-Way Anova and Post-Hoc Unequal Variances t-Tests

Table 6a. Two-way ANOVA results assessing the effects of heat source and TEG configuration on power output.

Source of Variation	df	F	p-value	Interpretation
Heat source	2	12.54	0.00039	Statistically significant effect
TEG configuration	2	11.46	0.00062	Statistically significant effect
Heat source × Configuration	4	2.21	0.108	No statistically significant interaction

Table 6b. Post-hoc pairwise comparisons using two-sample t-tests assuming unequal variances with Bonferroni-adjusted significance threshold ($\alpha = 0.0167$).

Comparison	p-value	p < 0.0167	Significant Difference
Dynamic body heat vs Appliance heat	0.0234	No	Not significant
Static body heat vs Appliance heat	0.0168	No	Not significant
Static body heat vs Dynamic body heat	0.2034	No	Not significant
Parallel vs Series	0.0091	Yes	Significant
2×2 Hybrid vs Series	0.3181	No	Not significant
2×2 Hybrid vs Parallel	0.011	Yes	Significant

Stage 2 evaluated the performance of a single TEG module and three four-module TEG configurations (parallel, series, and 2×2 hybrid) under three heat source conditions (static body heat, dynamic body heat, and appliance heat) using a fixed load resistance of 10 Ω. Across all heat source conditions, the hybrid configuration consistently exhibited the highest mean voltage, and derived current and power output, followed by the series configuration, with the parallel configuration producing the lowest values (*Table 4; Figures 8 and 10*). Voltage and ΔT exhibited temporal variation across all configurations and heat source conditions, indicating non-steady-state behaviour (*Figures 8 and 9*).

A two-way ANOVA with replication was performed using trial mean power output values. Both TEG configuration ($p = 0.00062$) and heat source condition ($p = 0.00039$) had statistically significant effects on power output. No statistically significant interaction was detected between TEG configuration and heat source condition ($p = 0.108$), indicating independent main effects on power output (*Table 6a*).

To further investigate pairwise differences, post-hoc unequal variances t-tests with a Bonferroni-adjusted threshold ($\alpha = 0.0167$) identified no statistically significant differences between individual heat source conditions. In contrast, the parallel configuration produced significantly lower power output than both the series ($p = 0.0091$) and hybrid ($p = 0.011$) configurations, while no significant difference was observed between the series and hybrid configurations ($p = 0.3181$) (*Table 6b*).

Discussion and Evaluation

Load Resistance Optimisation and Power Transfer (Stage 1)

Power output decreased non-linearly as load resistance increased from 10 Ω to 10 kΩ, indicating that the system operated beyond its maximum power point (*Figure 7*). According to the maximum power transfer theorem, maximum power occurs when external load resistance (R_{load}) equals internal resistance ($R_{internal}$) (*Figure 11)* (Attar, Lee & Snyder, 2020). The absence of a peak within the tested range indicates that $R_{internal}$ is less than 10 Ω for all configurations, and thus the dataset captures only the descending region of the expected power–resistance curve. Consequently, the true maximum power point lies below 10 Ω.

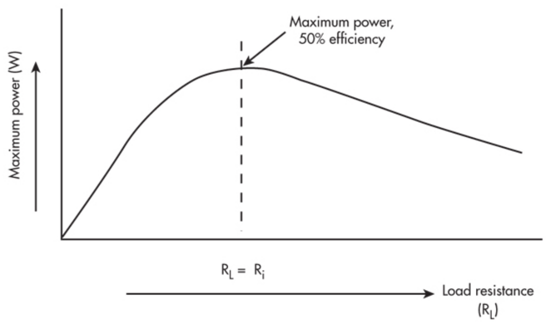

Figure 11. Maximum power transfer theorem graph (Barbour, 2014).

The selection of 10 Ω for Stage 2 therefore represents the closest approximation to load matching within the tested range, but not an optimal condition. This introduces a systematic limitation, as configurations with lower internal resistance including hybrid and parallel were forced to operate further from their maximum power point than the series configuration. Future investigations should implement finer load sweeping, particularly in the 0.1–10 Ω range, or use maximum power point tracking (MPPT) to dynamically identify optimal operating conditions (Priya & Stonier, 2025).

These findings highlight a limitation in real-world applicability. Practical thermoelectric systems do not operate under fixed resistive loads but instead utilise DC–DC converters and MPPT circuits to dynamically adjust load conditions and optimise energy extraction (Liu et al., 2025). Hence, the experimentally determined "optimal" resistances represents a constrained approximation rather than a realistic operating model.

Electrical Configuration and Load-Dependent Power Transfer (Stage 2)

Electrical configuration significantly influenced power output ($p = 0.00062$), with mean values following the consistent trend: 2×2 hybrid > series > parallel (*Tables 4, 5, and 6a; Figures 8 and 10*). This supports Hypothesis 1. Under the fixed 10 Ω load, power is determined by $P = V^2/R$, such that voltage differences are amplified quadratically. Consequently, the hybrid configuration that maximise voltage dominates power output.

This behaviour reflects underlying circuit characteristics. In series configurations, Seebeck voltage scales linearly with module number ($V_{total} \approx nV$), while internal resistance also increases ($R_{total} \approx nR$) (Northwestern Materials Science and Engineering, 2024; Montecucco, Siviter & Knox, 2014). In parallel configurations, internal resistance decreases ($R_{total} \approx R/n$), but voltage remains unchanged (Montecucco, Siviter & Knox, 2014). The hybrid configuration combines these effects, enabling partial voltage accumulation while reducing resistive losses, resulting in superior power transfer under fixed load conditions.

Despite higher mean power output, the hybrid configuration was not significantly different from the series configuration ($p = 0.3181$) (*Table 6b*). This likely reflects load-matching effects. Estimated internal resistances (~12 Ω series, ~3 Ω hybrid, ~0.75 Ω parallel) indicate that the 10 Ω load most closely matches the series configuration, allowing it to operate nearer its maximum power point (*Table 7*). In contrast, hybrid and parallel were substantially mismatched, leading to underestimation of their true performance (Kramer et al., 2019).

Table 7. Estimation of internal resistance of different electrical configurations.

For four-module TEG electrical configurations
Assumption: 3 Ω per TEG module
Values assume ideal ohmic behaviour and negligible contact resistance.

Series configuration: $R_{series} = R_1 + R_2 + R_3 + R_4 = 3\,\Omega \times 4 = 12\,\Omega$

Parallel configuration: $R_{parallel} = \frac{R}{n} = \frac{3\Omega}{4} = 0.75\,\Omega$

2×2 Hybrid configuration:
Each series string: $R_{branch} = R_1 + R_2 = 3\,\Omega + 3\,\Omega = 6\,\Omega$
Two identical branches in parallel: $R_{total} = \frac{R}{n} = \frac{6\Omega}{2} = 3\,\Omega$

The parallel configuration produced the lowest power output (*Table 4; Figures 8 and 10*). Although parallel circuits theoretically increase current capacity, this advantage could not be independently assessed because current was derived rather than directly measured. This constrains interpretation to resistance-related effects and limits evaluation of current-dependent performance differences between configurations.

Overall, under low ΔT and fixed-load conditions, voltage generation is the dominant factor of power output. Given that $P = V^2/R$, small increases in voltage yield disproportionately large increases in power. Hence, configurations that maximise voltage (series and hybrid) are inherently more effective for low-grade thermoelectric energy harvesting than those optimised for current.

Heat Source Condition and Effective Thermal Gradient (Stage 2)

Heat source condition showed a statistically significant main effect ($p = 0.00039$); however, post-hoc comparisons were not significant after Bonferroni correction, indicating small effect sizes relative to within-group variability (*Table 6*). This suggests that thermal input differences were less influential than electrical configuration.

Observed trends from mean values (static > dynamic > appliance) contradicted the expectation that higher ΔT yields higher power output (*Table 4 and 6a; Figure 10*). Although appliance heat produced the largest measured surface ΔT, it resulted in the lowest power output, indicating that measured ΔT did not reflect the effective temperature gradient across thermoelectric junctions. These findings demonstrate that effective ΔT, rather than measured surface ΔT, governs thermoelectric performance, explaining the rejection of Hypothesis 2.

This discrepancy is attributable primarily to thermal interface effects. The use of higher-conductivity thermal pads increased heat transfer but reduced the ability to sustain a temperature gradient by accelerating thermal equilibration between hot and cold sides (Jung et al., 2023). Thermoelectric performance depends on maintaining a sustained ΔT rather than maximising instantaneous heat flow, and thus increased thermal conductance reduced effective Seebeck voltage generation (Jouhara et al., 2021).

Measurement limitations contributed additional uncertainty. Infrared thermometer captures surface temperatures rather than internal junction temperatures, and periodic lifting of the cooling system further disrupted steady-state conditions. These factors introduced measurement error but were secondary to the underlying thermal dynamics.

Scaling Behaviour of Multi-Module Configurations (Stage 2)

To evaluate scaling efficiency, voltage and power outputs of four-module configurations were normalised to a single TEG module under identical thermal conditions. Under ideal scaling, a four-module system would produce a four-fold increase in output (Chen et al., 2012); however, this was not consistently observed.

Voltage scaling was configuration-dependent. The hybrid configuration produced the greatest increase (1.7–2.1×), followed by the series configuration (1.4–1.8×), while the parallel configuration showed minimal gain (0.9–1.2×) (*Table 5a*). Power scaling exhibited greater divergence, with hybrid (3.0–4.4×) approaching the theoretical four-fold scaling. Series showed moderate scaling (2.1–3.0×), whereas parallel exhibited limited scaling (0.8–1.5×), occasionally underperforming relative to a single module (*Table 5b*). No consistent trend was observed across heat source conditions for either voltage or power scaling, suggesting that relative performance was primarily determined by electrical configuration instead of heat source condition within the tested range.

Non-linear scaling arises from internal resistance effects and load mismatch. As module number increases, total internal resistance changes according to circuit configuration, altering the degree of matching with the fixed 10 Ω load. Configurations operating closer to their maximum power point (e.g., series) exhibit more efficient scaling, while highly mismatched configurations (e.g., parallel) show suppressed or even negative scaling effects (Apertet et al., 2012).

These results demonstrate that performance gains in multi-module thermoelectric systems are not inherently proportional to module number. Instead, system-level optimisation of electrical configuration and load matching is required to achieve efficient energy conversion. Consequently, in low-grade thermoelectric applications, circuit design exerts a greater influence on performance than simply increasing device quantity.

Evaluation

A major source of variability was transient thermal behaviour immediately after contact with the heat source. Voltage peaked initially before declining to a fluctuating steady state, as ΔT decreased toward equilibrium. Variations in contact pressure, skin temperature, positioning, and cooling efficiency altered the transient response, contributing to random error and elevated standard deviations, particularly under body heat conditions. Implementing a controlled equilibration period and mechanical clamping to standardise contact pressure and positioning would reduce this variability.

Limitation / Error Source	Type & Impact	Improvement
The use of an infrared thermometer to estimate surface temperature likely produced inaccurate ΔT values due to emissivity variation and indirect measurement.	Systematic error; introduces measurement bias, weakening the validity of the relationship between ΔT and electrical output.	Use calibrated thermocouples positioned at both hot and cold junctions with continuous data logging for accurate, real-time ΔT measurements.
Cold-side cooling was inconsistent due to periodic ice pack removal and condensation formation.	Both systematic error (underestimation of cooling efficiency) and random error (fluctuating heat extraction), reducing validity and reliability.	Implement a fixed heat sink with circulating coolant or phase-change material and continuous temperature monitoring to stabilise thermal conditions.
Variations in appliance heating and muscle activity caused fluctuations in thermal input.	Random error; increases variability and reduces measurement precision.	Replace human heat sources with a controlled thermal source (e.g. regulated hot plate or water bath) to ensure consistent and reproducible heat input.
Current was not measured directly but calculated using Ohm's law.	Systematic methodological limitation; restricts independent evaluation of electrical performance and reduces analytical validity.	Incorporate simultaneous voltage–current measurement using a multichannel data acquisition system for direct power characterisation.
A fixed 10 Ω load resistor prevented operation at maximum power point.	Systematic design limitation; reduces validity of performance comparison between configurations.	Determine optimal load resistance for each configuration via load sweeping or maximum power point tracking prior to comparison.

Despite these limitations, consistent trends across repeated trials indicate that reliability was maintained, supporting the validity of the conclusions within experimental constraints.

Conclusion

Electrical configuration was the primary determinant of power output in the four-module thermoelectric generator under the tested conditions. The 2×2 hybrid configuration yielded the highest power output, reflecting an optimal balance between voltage generation and internal resistance, hence supporting Hypothesis 1. Hypothesis 2 was not supported. Despite producing the largest measured surface temperature differences, appliance heat generated the lowest mean power output. This indicates that performance is governed by the effective temperature gradient across thermoelectric junctions rather than measured surface ΔT, highlighting the role of thermal coupling efficiency and internal heat transfer limitations. Within the investigated range, optimisation of electrical configuration exerted a greater influence on power generation than variation in heat source conditions. These findings inform the design of compact, self-powered systems, where efficient energy extraction from body heat or ambient waste heat is critical for applications such as wearable sensors, biomedical monitoring devices, and distributed environmental monitoring technologies. Future investigations should incorporate dynamic load matching, direct current measurement, and enhanced thermal control to reduce systematic error and better approximate operational conditions. Such refinements would allow more accurate characterisation and optimisation of thermoelectric systems, strengthening their practical viability as sustainable, low-power energy solutions.

Word Count

2059 words (excluding headings, titles, figure captions, tables, and references).

Bibliography

Apertet, Y, Ouerdane, H, Glavatskaya, O, Goupil, C & Lecoeur, P 2012, ‘Optimal working conditions for thermoelectric generators with realistic thermal coupling’, *Europhysics Letters*, vol. 97, no. 2, p. 28001, accessed June 2026, <https://doi.org/10.1209/0295-5075/97/28001>.

Attar, A, Lee, H & Snyder, GJ 2020, ‘Optimum load resistance for a thermoelectric generator system’, *Energy Conversion and Management*, vol. 226, p. 113490, accessed June 2026, <https://www.sciencedirect.com/science/article/abs/pii/S0196890420310220>.

Barbour, A 2014, *Help compare my results to the maximum power transfer theorem and explain using algorithms*, Electrical Engineering Stack Exchange, accessed June 2026, <https://electronics.stackexchange.com/questions/125836/help-compare-my-results-to-the-maximum-power-transfer-theorem-and-explain-using>.

Champier, D 2017, ‘Thermoelectric generators: A review of applications’, *Energy Conversion and Management*, vol. 140, pp. 167–181, accessed June 2026, <https://www.sciencedirect.com/science/article/pii/S0196890417301851?casa_token=a_2hKQ-uEVcAAAAA:6ftqZf43CWJKq5kqzRtwhwSAbTmPznsZVWVRpzEpwWTlHiMwMnLSSFOFpFCpUS9wol8CPkt4Qk53#s0020>.

Chen, W-H, Liao, C-Y, Hung, C-I & Huang, W-L 2012, ‘Experimental study on thermoelectric modules for power generation at various operating conditions’, *Energy*, vol. 45, no. 1, pp. 874–881, accessed June 2026, <https://doi.org/10.1016/j.energy.2012.06.076>.

Dhass, AD, Babu L., G, Pradhan, R, Murthy, GVK & Sreenivasan, M 2023, ‘Energy Harvesting Through Thermoelectric Generators’, *Materials and Technologies for a Green Environment*, Bentham Science Publishers, pp. 32–66, accessed June 2026, <https://doi.org/10.2174/9789815051216123010004>.

Gámez-Avilez, JD, Islas-Pereda, S, Velázquez-Limón, N, Aguilar-Jiménez, JA & López-Martínez, LA 2026, ‘Advances in Thermoelectric Generators Modules (TEGs): Applications, Performance, and Global Trends in Renewable Energy Systems’, *Processes*, vol. 14, MDPI AG, no. 6, p. 901, accessed June 2026, <https://www.mdpi.com/2227-9717/14/6/901>.

He, J & Tritt, T 2017, ‘Advances in thermoelectric materials research: Looking back and moving forward’, *Science*, vol. 357, no. 6358, accessed June 2026, <https://science.sciencemag.org/content/sci/357/6358/eaak9997.full.pdf>.

Jouhara, H, Żabnieńska-Góra, A, Khordehgah, N, Doraghi, Q, Ahmad, L, Norman, L, Axcell, B, Wrobel, L & Dai, S 2021, 'Thermoelectric generator (TEG) technologies and applications', *International Journal of Thermofluids*, vol. 9, p. 100063, accessed June 2026, <https://www.sciencedirect.com/science/article/pii/S266620272100001X>.

Jung, Y, Kim, M, Kim, T, Ahn, J, Jun Hyeok Lee & Seung Hwan Ko 2023, 'Functional Materials and Innovative Strategies for Wearable Thermal Management Applications', *Nano-micro Letters*, vol. 15, Springer Science+Business Media, no. 1, accessed June 2026, <https://pmc.ncbi.nlm.nih.gov/articles/PMC10310690/>.

Kramer, LR, Maran, ALO, de Souza, SS & Ando Junior, OH 2019, 'Analytical and Numerical Study for the Determination of a Thermoelectric Generator's Internal Resistance', *Energies*, vol. 12, no. 16, p. 3053, accessed June 2026, <https://doi.org/10.3390/en12163053>.

Kunika 2025, *The Role of Thermoelectric Generators in Sustainable Power Generation*, UnitBirwelco, accessed June 2026, <https://www.unitbirwelco.com/post/the-role-of-thermoelectric-generators-in-sustainable-power-generation>.

Liang, G, Zhou, J & Huang, X 2011, 'Analytical model of parallel thermoelectric generator', *Applied Energy*, vol. 88, no. 12, pp. 5193–5199, accessed June 2026, <https://doi.org/10.1016/j.apenergy.2011.07.041>.

Liu, W, Lu, M, Bai, H, Liu, Z & Lv, S 2025, 'All-day autonomous MPPT energy storage PV-TEG hybrid system based on dual axis solar tracker', *Renewable Energy*, vol. 256, Pergamon, p. 124094, accessed June 2026, <https://www.sciencedirect.com/science/article/abs/pii/S0960148125017586>.

Manghwar, R, Selvaraj, J, Khoharo, H, Kumar, L & Ahmad, MS 2026, 'Computational and experimental investigation of thermoelectric generators in series-parallel configurations under variable resistive loads and temperature gradients', *Case Studies in Thermal Engineering*, vol. 80, Elsevier BV, p. 107913, accessed June 2026, <https://doi.org/10.1016/j.csite.2026.107913>.

Misra, V, Bozkurt, A, Calhoun, B, Jackson, T, Jur, J, Lach, J, Lee, B, Muth, J, Oralkan, O, Ozturk, M, Trolier-McKinstry, S, Vashaee, D, Wentzloff, D & Zhu, Y 2015, 'Flexible Technologies for Self-Powered Wearable Health and Environmental Sensing', *Proceedings of the IEEE*, vol. 103, no. 4, pp. 665–681, accessed June 2026, <10.1109/JPROC.2015.2412493>.

Montecucco, A, Siviter, J & Knox, AR 2014, 'The effect of temperature mismatch on thermoelectric generators electrically connected in series and parallel', *Applied Energy*, vol. 123, pp. 47–54, accessed June 2026, <http://eprints.gla.ac.uk/92098/1/92098.pdf>.

Northwestern Materials Science and Engineering 2024, *Thermoelectrics at NU-MSE*, Northwestern.edu, accessed June 2026, <https://thermoelectrics.matsci.northwestern.edu/thermoelectrics/engineering.html>.

Ochieng, AO, Megahed, TF, Ookawara, S & Hassan, H 2022, 'Comprehensive review in waste heat recovery in different thermal energy-consuming processes using thermoelectric generators for electrical power generation', *Process Safety and Environmental Protection*, vol. 162, pp. 134–154, accessed June 2026, <https://doi.org/10.1016/j.psep.2022.03.070>.

Priya, P & Stonier, AA 2025, 'Advancements in maximum power point tracking (MPPT) techniques for solar photovoltaic (PV) applications: A comprehensive review', *Energy Conversion and Management: X*, vol. 29, Elsevier, no. 101438, p. 101438, accessed June 2026, <https://www.sciencedirect.com/science/article/pii/S2590174525005707>.

Ridwan, M, Gasulla, M & Reverter, F 2025, 'Principle and Applications of Thermoelectric Generators: A Review', *Sensors*, vol. 25, no. 8, p. 2484, accessed June 2026, <https://pmc.ncbi.nlm.nih.gov/articles/PMC12031398/>.

Ryu, B, Chung, J, Kumagai, M, Mato, T, Ando, Y, Gunji, S, Tanaka, A, Yana, D, Fujimoto, M, Imai, Y, Katsura, Y & Park, S 2023, 'Best thermoelectric efficiency of ever-explored materials', *iScience*, vol. 26, no. 4, p. 106494, accessed June 2026, <https://www.sciencedirect.com/science/article/pii/S2589004223005710>.

Terashima, S, Sorimachi, R & Iwase, E 2024, 'Series/Parallel Switching for Increasing Power Extraction from Thermoelectric Power Generators', *Micromachines*, vol. 15, MDPI AG, no. 8, p. 1015, accessed June 2026, <https://pmc.ncbi.nlm.nih.gov/articles/PMC11356095/>.

Wang, Y, Shi, Y, Mei, D & Chen, Z 2018, 'Wearable thermoelectric generator to harvest body heat for powering a miniaturized accelerometer', *Applied Energy*, vol. 215, pp. 690–698, accessed June 2026, <https://www.sciencedirect.com/science/article/pii/S0306261918301880>.

Zhu, S, Fan, Z, Feng, B, Shi, R, Jiang, Z, Peng, Y, Gao, J, Miao, L & Koumoto, K 2022, 'Review on Wearable Thermoelectric Generators: From Devices to Applications', *Energies*, vol. 15, no. 9, p. 3375, accessed June 2026, <https://www.mdpi.com/1996-1073/15/9/3375>.

Zhu, X, Yu, Y & Li, F 2019, 'A review on thermoelectric energy harvesting from asphalt pavement: Configuration, performance and future', *Construction and Building Materials*, vol. 228, p. 116818, accessed June 2026, <https://doi.org/10.1016/j.conbuildmat.2019.116818

Scientific Journal

15.01.2026 – 15.02.2026

Generating topic of interest/ Exploring potential topics:

Topic: From Heat to Electricity: Investigating Energy Harvesting Using Thermoelectric Generators

Research question: How do different electrical configuration and heat source conditions affect the power generation of thermoelectric generators?

Discussion of ideas/ brainstorming:

Main interest: Investigating to what extent different TEG configuration (electrical conditions) and heat source conditions (thermal conditions) affect the power generation?

Investigating the effect of Seebeck effect: Investigating the power output of thermoelectric generators (TEGs) under different heat sources and electrical configurations.

Future work of interest:
Exploring thermoelectric C\clothing/wearables: Harvesting body heat to charge wearable devices. For example, embedding TEG modules into fabric to capture body heat, measure how much power can be produced, and how it can generate usable power to charge small wearable electronics in static and dynamic conditions and at different ambient temperatures.

Key concept:
Thermoelectric generators use the Seebeck effect to convert temperature differences between heat source and environment directly into electricity.

Investigation:
Under a pre-determined experimental design, I will investigate how TEG configuration influence generation of usable power. How much temperature difference is needed to achieve this? Would different heat source conditions achieve this?

- Focus on low grade energy - body heat and waste heat.

Previous research – conducting literature search and reading:

Impact of the investigation: Could the investigation outcome provide values to understand the effect of TEG configuration and low-grade heat sources on TEG performance and how to generate the highest power output?

Steps to do:

1. Research & Planning: To design 3 TEG electric configurations and 3 heat source conditions representing typical usability (2 independent variable)
2. Gather materials & components: Their availability also impact to how I could conduct the experiment
3. Conduct experiments, e.g. investigating the effect of different TEG electric configuration
4. Data collection and analysis – what data to collect and what analysis tools I would use
5. Effect on society: future potentials
6. Complete report

Notes:

Literature search and review:

Ali, A, Shaukat, H, Bibi, S, Altabey, WA, Noori, M & Kouritem, SA 2023, 'Recent progress in energy harvesting systems for wearable technology', Energy Strategy Reviews, vol. 49, p. 101124, <https://www.sciencedirect.com/science/article/pii/S2211467X23000743>.

Champier, D 2017, 'Thermoelectric generators: A review of applications', Energy Conversion and Management, vol. 140, pp. 167–181, <https://www.sciencedirect.com/science/article/pii/S0196890417301851?casa_token=a_2hKQ-uEVcAAAAA:6ftqZf43CWJKq5kqzRtwhwSAbTmPznsZVWVRpzEpwWTlHiMwMnLSSFOFpFCpUS9wol8CPkt4Qk53#s0020>.

Devanathan, V 2021, 'The Wiedemann-Franz Law for Electrical and Thermal Conduction in Metals', vol. 4, pp. 1–26, <https://www.researchgate.net/publication/355196811_The_Wiedemann-Franz_Law_for_Electrical_and_Thermal_Conduction_in_Metals>.

He, W, Zhang, G, Zhang, X, Ji, J, Li, G & Zhao, X 2015, 'Recent development and application of thermoelectric generator and cooler', Applied Energy, vol. 143, pp. 1–25, <https://www.sciencedirect.com/science/article/abs/pii/S0306261914013324>.

Jaafar Ali.Mahdi, Hasanain J. A. Juaifer, Kurji, HJ & Imran, MS 2025, 'Conversion of Waste Energy from CI Engines to Electrical Power with TEG', Journal of Fluid Flow Heat and Mass Transfer, vol. 12, <https://www.researchgate.net/publication/390701800_Conversion_of_Waste_Energy_from_CI_Engines_to_Electrical_Power_with_TEG?_tp=eyJjb250ZXh0Ijp7ImZpcnN0UGFnZSI6Il9kaXJlY3QiLCJwYWdlIjoiX2RpcmVjdCJ9fQ>.

Jaziri, N, Boughamoura, A, Müller, J, Mezghani, B, Tounsi, F & Ismail, M 2019, 'A comprehensive review of Thermoelectric Generators: Technologies and common applications', Energy Reports, vol. 6, <https://www.sciencedirect.com/science/article/pii/S2352484719306997>.

Jia, Y, Jiang, Q, Sun, H, Liu, P, Hu, D, Pei, Y, Liu, W, Crispin, X, Fabiano, S, Ma, Y & Cao, Y 2021, 'Wearable Thermoelectric Materials and Devices for Self-Powered Electronic Systems', Advanced Materials, vol. 33, no. 42, p. 2102990,, <https://doi.org/10.1002/adma.202102990>.

Liu, J, Hyland, M, Hunter, H, Hall, MJ, Veety, E & Vashaee, D 2021, Wearable Thermoelectric Generators Powered by Body Heat - HDIAC, <https://hdiac.dtic.mil/articles/wearable-thermoelectric-generators-powered-by-body-heat/>.

Martin-Gonzalez, M, Lohani, K & Neophytou, N 2025, 'Phonon and electron transport engineering for enhanced thermoelectric performance and the challenges of device integration', Energy Materials, vol. 5, OAE Publishing Inc., no. 9, <https://www.oaepublish.com/articles/energymater.2025.32>.

Ochieng, AO, Megahed, TF, Ookawara, S & Hassan, H 2022, 'Comprehensive review in waste heat recovery in different thermal energy-consuming processes using thermoelectric generators for electrical power generation', Process Safety and Environmental Protection, vol. 162, pp. 134–154, <https://doi.org/10.1016/j.psep.2022.03.070>.

Proto, A, Schmidt, M, Vondrak, J, Kubicek, J, Paternò, G, Jargus, J & Penhaker, M 2024, 'Wearable device for body heat energy harvesting in real-life scenarios', Sensors and Actuators A: Physical, vol. 379, Elsevier, p. 115999, <https://www.sciencedirect.com/science/article/pii/S0924424724009932>.

Prunet, G, Pawula, F, Fleury, G, Cloutet, E, Robinson, AJ, Hadziioannou, G & Pakdel, A 2021, 'A review on conductive polymers and their hybrids for flexible and wearable thermoelectric applications', Materials Today Physics, vol. 18, p. 100402, <https://www.sciencedirect.com/science/article/pii/S2542529321000638>.

Rao, Y, Bechtold, T & Hohlfeld, D 2025, 'Design of packaged thermoelectric generators for implantable medical devices: A comprehensive parameter study', Energy, vol. 320, p. 134932, <https://doi.org/10.1016/j.energy.2025.134932>.

Ryu, B, Chung, J, Kumagai, M, Mato, T, Ando, Y, Gunji, S, Tanaka, A, Yana, D, Fujimoto, M, Imai, Y, Katsura, Y & Park, S 2023, 'Best thermoelectric efficiency of ever-explored materials', iScience, vol. 26, no. 4, p. 106494, <https://www.sciencedirect.com/science/article/pii/S2589004223005710>.

Sezer, N & Koç, M 2021, 'A comprehensive review on the state-of-the-art of piezoelectric energy harvesting', Nano Energy, vol. 80, no. 105567, p. 105567, <https://www.sciencedirect.com/science/article/pii/S2211285520311411>.

Shakouri, A 2011, 'Recent Developments in Semiconductor Thermoelectric Physics and Materials', Annual Review of Materials Research, vol. 41, no. 1, pp. 399–431, <https://doi.org/10.1146/annurev-matsci-062910-100445>.

Tabaie, Z & Omidvar, A 2023, 'Human body heat-driven thermoelectric generators as a sustainable power supply for wearable electronic devices: Recent advances, challenges, and future perspectives', Heliyon, vol. 9, no. 4, p. e14707, <https://www.sciencedirect.com/science/article/pii/S240584402301914X>.

Torfs, T, Leonov, V & Vullers, R 2007, Pulse oximeter fully powered by human body heat, Researchgate.net, <https://www.researchgate.net/publication/237338112_Pulse_Oximeter_Fully_Powered_by_Human_Body_Heat>.

Wang, Y, Shi, Y, Mei, D & Chen, Z 2018, 'Wearable thermoelectric generator to harvest body heat for powering a miniaturized accelerometer', Applied Energy, vol. 215, pp. 690–698, <https://www.sciencedirect.com/science/article/pii/S0306261918301880>.

Yang, J, Xi, L, Qiu, W, Wu, L, Shi, X, Chen, L, Yang, J, Zhang, W, Uher, C & Singh, DJ 2016, 'On the tuning of electrical and thermal transport in thermoelectrics: an integrated theory–experiment perspective', npj Computational Materials, vol. 2, no. 1, <https://www.researchgate.net/publication/303101324_On_the_tuning_of_electrical_and_thermal_transport_in_thermoelectrics_An_integrated_theory-experiment_perspective>.

Yu, R, Feng, S, Sun, Q, Xu, H, Jiang, Q, Guo, J, Dai, B, Cui, D & Wang, K 2024, 'Ambient energy harvesters in wearable electronics: fundamentals, methodologies, and applications', Journal of Nanobiotechnology, vol. 22, BioMed Central, no. 1, <https://jnanobiotechnology.biomedcentral.com/articles/10.1186/s12951-024-02774-0>.

Zhang, Q, Sun, Y, Xu, W & Zhu, D 2014, 'Organic Thermoelectric Materials: Emerging Green Energy Materials Converting Heat to Electricity Directly and Efficiently', Advanced Materials, vol. 26, no. 40, pp. 6829–6851, <https://doi.org/10.1002/adma.201305371>.

Zhu, S, Fan, Z, Feng, B, Shi, R, Jiang, Z, Peng, Y, Gao, J, Miao, L & Koumoto, K 2022, 'Review on Wearable Thermoelectric Generators: From Devices to Applications', Energies, vol. 15, no. 9, p. 3375, <https://www.mdpi.com/1996-1073/15/9/3375>.

Zhu, X, Yu, Y & Li, F 2019, 'A review on thermoelectric energy harvesting from asphalt pavement: Configuration, performance and future', Construction and Building Materials, vol. 228, p. 116818, <https://doi.org/10.1016/j.conbuildmat.2019.116818>.LED or buzzer), the voltage drops by at least half due to the TEG's internal resistance.

16.02.2026 – 01.03.2026

Research and planning:

Independent variables:
- 3 TEG electrical configurations
- 3 Heat source conditions

Dependent variables:
- Voltage (V) across a load
- Calculated current based on the load resistance used (A)
- Calculated power output P = VI (w)
- Temperature difference ΔT (°C)

Tests for the dependent variables:
1. Stage 1 - pilot study
    - To understand the TEG behaviours
    - To identify suitable resistance of resistor/load I can use for Stage 2.
    - To evaluate the plausibility of the experiment and what to improve.
2. Stage 2
    - To find out the best configuration if exists and analyse 3 heat source conditions

Notes:

Basic thermoelectric principle: Seebeck effect: a temperature gradient across the TEG module generates a voltage.

TEG materials (e.g., Bismuth Telluride) - semiconductor-based Peltier thermoelectric device that functions as a small electric generator.

- *Bismuth telluride-based alloys for low-temperature applications*
- *Skutterudites for mid-temperature ranges*

Types of TEGS: rigid vs. flexible - designed to generate power through the Seebeck effect

Small rigid TEGs:

- *SP1848-27145 – the TEG that I've chosen.*
  - *The hot side is against the heat source.*
  - *The cold side is exposed to ambient air or enhanced with heat sinks.*

Temperature Differential (°C)	*20*	*40*	*60*	*80*	*100*
Open Circuit Output Voltage (V)	*0.97*	*1.8*	*2.4*	*3.6*	*4.8*
Short Circuit Output Current (mA)	*225*	*368*	*469*	*558*	*669*

Specifications:
Model: SP1848-27145
Dimensions: 40mm x 40mm x 3.6mm
Max Temperature Difference (ΔT): 150°C
Operating Voltage (Generating Mode): 3V–5V (typical)
Open Circuit Voltage: Up to 5.8V
Output Power: ~2W (depending on ΔT and load)
Internal Resistance: ~2.9 Ohms
Sealing: Ceramic plates for heat resistance and insulation
Wire Leads: Pre-attached, ~15cm length

Features:
Small size
Light weight, long life
No moving parts, easy to move
High reliability and no pollution
Cold side with printed words
Hot side is blank
Red wire to positive, black wire to negative, it generates electricity when there occurs a temperature difference

Operating Tips:
Do not exceed the maximum operating temperature of the module.
Life expectancy: 200,000 hours.
Failure rate based on longtime testings: 0.2%.

Different TEGs has different Seebeck coefficients, internal resistances and heat transfer characteristics

Ref:
faranux.com; support.envistiamall.com+6envistiamall.com+6componentstree.com+6botnroll.com
https://mikroelectron.com/product/me-13348?srsltid=AfmBOoqUiuiDsrwIUmh3ZNfPVAufFMCdp38ckueAanIMVvKQ5W0WPfLN

TECs: operated for cooling purpose via the Peltier effect

- *TEC1-04903*
- *TEC1-12706 can deliver output 1–2V with a ΔT of 10–15°C and deliver a few mW to ~100 mW depending on configuration.*

Ref:
link.springer.com+4filotronix.com+4phippselectronics.com+4roseelectronics.pk+4synronic.com+4embeddinator.com+4

Seebeck coefficient (α) = a material's ability to convert thermal energy generated at a temperature gradient into electrical voltage.

$$\boldsymbol{a = -\frac{\Delta V}{\Delta T} = \frac{V_{hot} - V_{cold}}{T_{hot} - T_{cold}}}$$

where ΔV = voltage generated,
ΔT = temperature difference across the material (Prunet et al., 2021).
The negative sign represents the conventional direction of voltage relative to the temperature gradient, depending on the type of charge carriers (Prunet et al., 2021).

A dimensionless figure of merit (ZT) measures the efficiency of thermoelectric materials.

$$ZT = \frac{\alpha^2 \sigma T}{k}$$

where α = Seebeck coefficient,
σ = electrical conductivity,
k = thermal conductivity,
T = absolute temperature (Ryu et al., 2023; Zhu, Yu & Li, 2019).

Design a TEG layout to achieve:

- *Harvest small, fluctuating voltage from TEGs*
- *Store energy reliably*
- *Provide a regulated output (3.3V or 5V) to power wearables*

Que. What is open-circuit voltage?

Open-circuit voltage is the maximum possible voltage a TEG can produce when it is not connected to anything.

- *Zero Current Flows: In an open-circuit state, the TEG creates an electrical pressure (voltage) but no actual current (amperage) flows through a circuit.*

- *The 50% Drop Rule: The moment when connecting a load to power a LED or buzzer, the voltage will instantly drop by about half. This happens because the TEG has its own internal electrical resistance that consumes a large portion of the voltage as soon as current begins to flow.*

In wearable technologies, capturing body heat for low-power electronics offers a sustainable alternative to batteries. The human body maintains a constant internal temperature (~37°C), which can drive power generation when exposed to cooler ambient environments.

Body heat can be used to passively harvest a small amount of electrical energy to power small wearable devices.

Wearable device is ever evolving.

- *Medical sensor to monitor physiological changes, e.g. blood glucose level, respiratory rate, brain wave*
- *Medical implants, e.g. pacemaker*
- *Health device, e.g. hearing aids*
- *Fitness trackers, BLE devices, or low-power microcontrollers*
- *Smart watch, smart glasses, smart phones, LEDs*

Notes:

Research on materials & components:

- *Thermoelectric Generators SP1848-27145 × 4, size: 40mm x 40mm x 4mm, operating temperature: -30C to +120C –* to convert heat difference to voltage
- *Thermal pad – GEEK 12.8 W/mK Thermal Pads, 100 x 100 x 0.5mm/1mm/1.5mm High Temperature Heat Resistant Silicone Grease Thermal Pads for Heat Sinks – to facilitate heat transfer*
- *Supercapacitor (e.g. 1F, 5.5V or 5F, 2.7V or 2F 2.5VDC) –* to *store harvested energy*
- *Ultra Low Voltage Boost Converter Voltage Boost Converter LTC3108 – to step up ultra-low voltage*
- *Boost Converter Voltage Regulator Step Up MT3608 – to step up voltage to usage level (e.g. 3.3V/5V)*
- *Blocking diode - Schottky diode (1N5819) for low voltage drop –* to prevent *backflow into TEGs*
- *Connecting Wires (22-26 AWG) e.g. 24 Gauge silicone wire – for electrical connections*
- *Aluminium or copper heat sink – to dissipate heat*
- *Breadboard and jumper wires*
- *LEDs or microcontroller*

Tools needed:

- *Soldering iron + solder – to connect wiring*
- *Digital multimeter SZ304 - to test voltage, current, and general electrical properties of the TEG systems*
- *Infrared thermometer Inkbird INK-IFT01- to measure heat source hot and cold side temperatures*
- *Stop watch*
- *Metronome*
- *Exercise band*

Note:

1. *To achieve maximum voltage and current output, the cold side of the device must be attached to a heatsink, cold plate or chiller in order to remove the heat from it. Without adequate cooling, the device will heat up quickly, the output power will decrease, and the device will fail if allowed to overheat.*
2. *TEG SP1848-27145 manufacturer data corresponding to a ΔT of 20 °C:*

- *Open-circuit voltage: ~0.97 V*
- *Current: ~225 mA*
- *Power output: ~0.22 W*

Reflection:
However, real-world factors such as suboptimal thermal contact, heat losses, and the dynamic nature of human movement can further diminish the actual power output.

01.03.2026 – 15.03.2026

Research and planning:

Notes:

Que: What configuration can TEG systems be formulated?

Option A: Series connection
Connect red to black across modules.

- *Advantage: Increases total voltage.*
- *Disadvantage: Power mismatch between modules can reduce efficiency; voltage adds but current limited to weakest module.*

Option B: Parallel connection
Connect all reds together and all blacks together.

- *Advantage: Increases current; more tolerant to variation between modules.*
- *Disadvantage: Voltage remains that of the weakest module.*

Option C: Hybrid (Series-Parallel) connection

- *Advantage: Can optimise for both voltage and current.*
- *Disadvantage: More complex wiring.*

Consideration: The intrinsic characteristics of all TEGs may vary.

Ref: https://www.allaboutcircuits.com/textbook/direct-current/chpt-5/what-are-series-and-parallel-circuits/

Harvesting waste heat to charge wearable devices requires careful consideration of how TEG modules are integrated, connected, and regulated.

Prediction:
Since voltage is the bigger challenge in TEG systems, so series connection could be used for easier voltage boost with small ΔT (temp difference). However, hybrid connection could be the best since it can reduce the disadvantages of both parallel and series connections.

Que: How many TEG SP1848 modules are required?

Wearable devices require usable power:

- *Smartwatch (e.g. 3.7V x 2mA = 7.4 mW)*
- *BLE Tracker (e.g. 3.3V x 10mA = 33 mW)*
- *Blood Glucose Monitor (e.g. 3.0V x 20mA = 60 mW)*

Estimate each TEG produces ~20–40 mV at 5–10°C ΔT
For one TEG, 5% power output of ~220 mW at 20°C ΔT = 11mW
4 TEGS may produce 11mW x 4 = 44mW - in a series connection
Ultra-low voltage step-up converter) can be used to boost tiny voltage to usable voltage for charging devices.

Ref:
https://advanced.onlinelibrary.wiley.com/doi/10.1002/adfm.202404861
https://www.sciencedirect.com/science/article/abs/pii/S0196890416301121
https://sheetak.com/understanding-thermoelectric-generators-tegs-and-te-energy-harvesting-turning-waste-heat-into-electricity/

16.04.2026 – 26.04.2026

Notes:

Common Limitation:
Low ΔT (5–10°C): e.g. Human skin temp vs ambient air is small → limits power output.
Power Output: Generally ~10–50 µW per cm², often not enough for continuous operation.

Trouble shooting:
0V from TEG – Poor contact to heat source - not enough input voltage, disconnected due to poor soldering or wrong pins, poor dissipation from cold side, no temperature gradient
Solution: Use Aluminium foil and ice pack – to dissipate heat, hence achieving temperature gradient

Possible research design:
Power output vs. temperature difference (ΔT) between heat source and environment
Theoretically, the chosen TEG increases voltage output as temperature difference increases based on manufacturer data.
Of interest, I will investigate what heat source could perform better and why?
Also, compare the electrical configuration: series vs. parallel vs. hybrid connections for optimal power.

Applications:
Estimate if generated power can support small wearable devices (e.g. powering LEDs).
Design a small power management circuit to store generated energy in a capacitor or battery.

Setup: TEG output → LTC3108 → MT3608 → Supercapacitor → ESP32
Measure charging rate - ti*me to charge from 0 to 1.0V, 1.5V, 2.0V*

Notes:

Que: Is thermoelectric power valuable?

When exposed to a (ΔT), it can be beneficial for:

1. *Energy-autonomous sensors using body heat (e.g. health monitors)*
2. *Energy harvesting using waste heat*
3. *Proof-of-concept prototypes*
4. *Smart textiles research*

Choosing measuring instrument:
Data logger such as ESP32 for data logging and processing – will the reading of ultra-low voltage be unstable, or use a multimeter to measure voltage manually.

Que: why may real-world voltage drop?

Variables to be controlled.

- *Thermal interface losses: A huge amount of heat is lost at the boundaries. Without thermal paste or sufficient clamping pressure, the actual ΔT across the internal ceramic plates will only be a fraction of the target 5–10°C.*
- *Poor heat sinking: If the cold side cannot dissipate heat fast enough, the cold plate will quickly warm up. This may rapidly collapse the internal ΔT, resulting in voltage output drops.*
- *Open-circuit vs. load voltage: The 20–40 mV per °C estimate applies to open-circuit voltage (Voc). The moment a load (e.g. LED or buzzer) is connected, the voltage drops by at least half due to the TEG's internal resistance.*

Notes:

Thermal pad helps to transfer heat.

Que: What is thermal conductivity?

Thermal conductivity (k or λ) is an intrinsic material property that quantifies how efficiently a material conducts heat. Defined as the rate of heat transfer through a unit thickness of material per unit area per unit temperature difference. Expressed in W/(m·K) or W/(m·°C).

- *Thermal Conductivity is a bulk material property — it depends on the material's composition, microstructure, temperature, and phase, but is independent of sample geometry.*
- *High thermal conductivity materials (e.g. copper: 400 W/m·K, aluminium: 205 W/m·K, diamond: 2000 W/m·K) are used where efficient heat spreading is needed.*
- *Low thermal conductivity materials (e.g. polyurethane foam: 0.02–0.03 W/m·K, aerogel: 0.015 W/m·K) serve as thermal insulators.*

Que. What Is Thermal Impedance?

Thermal impedance (Rth or Zth) is a system-level property that quantifies the total resistance to heat flow between a heat source (e.g., a power semiconductor junction) and a defined reference point (e.g., the case, heatsink, or ambient). Expressed in °C/W or K/W.

Thermal impedance characterises a complete thermal pathway that may include material layers, interfaces, bond lines, thermal interface materials (TIMs), and convective boundaries. It depends on geometry, thickness, interface quality, and all material layers in the heat flow path.

Rth = ΔT / P
where ΔT = the temperature difference between the heat source and reference point
P = the power dissipated.

Thermal Resistance vs. Thermal Impedance
Thermal resistance (Rth) is the steady-state value.
Thermal impedance (Zth) is the transient or frequency-dependent version—important for pulsed-power applications where thermal mass (heat capacity) determines the temperature excursion during a power pulse.

Ref:
https://infinitalab.com/blog/thermal-impedance-vs-conductivity-guide/

Stage 1: Pilot study

Objectives:
To find out the best resistance of resistor/load I can use for this experiment.
To evaluate the plausibility of the experiment and what to improve.

Experimental design:

Experiments & Data Collection:

Independent variables:
- 3 TEG configurations: Parallel, Series, 2×2 Hybrid
- 3 Heat source conditions: Static body heat, Dynamic body heat, Appliance heat
- 8 resistors of known resistance (Ω): 10 Ω, 100 Ω, 220 Ω, 330 Ω, 1k Ω, 2k Ω, 5k Ω, 10k Ω

Dependent variables: Compare electrical power output of the TEG system across conditions
- Voltage (V) across a load (i.e. resistor)
- Calculated current based on the resistance (A) using Ohm's Law: I = V/R
- Calculated power output: P = V I (w)
- Temperature difference ΔT (°C)

Materials and equipment:
- TEGs (SP1848-27145) x4
- Thermal pad 12.8 W/mK, 0.5mm for hot side and 1mm for cold side - to facilitate heat transfer → to prevent thermal equilibrium
- Resistors x8: 10 Ω, 100 Ω, 220 Ω, 330 Ω, 1k Ω, 2k Ω, 5k Ω, 10k Ω
- Aluminium foil with enclosed ice pack – used as heat sink to dissipate heat
- 830-point breadboard and jumper wires
- Connecting wires. 24 AWG silicone wire, JST XH 2.54mm connector, heat shrink
- Diodes – to prevent reverse current flow, protecting the TEGs.
- Soldering iron + solder – to make reliable electrical connections
- Digital multimeter SZ304
- Infrared thermometer Inkbird INK-IFT01 - to measure heat source hot and cold side temperatures
- Stop watch
- Metronome, Exercise band – used for dynamic body heat condition

Possible Hypotheses:

- The effect of configuration on voltage, current, and power
  The 2×2 hybrid configuration is expected to provide the most effective balance between voltage and current output and may therefore produce the highest power output under the tested conditions.
- The effect of heat source on power
  Static body heat produces the higher voltage and generates higher power output than dynamic body heat. The power output of the TEG system will increase with greater body activity levels due to larger temperature gradients between the skin and environment as body heat production rises during physical exertion. – However, a bit harder to justify if the knee movements can produce body heat production significantly.
  Appliance heat source generates more electrical power output of the TEG system due to larger temperature gradients between the appliance and environment.

Notes:

Multiple testing on TEGs system set up with and without breadboard to design pilot study.

Que: Why was air fryer top surface used as appliance heat source?

A TEG was attached to an air flyer top surface, observed for 15 minutes. The hot side TEG temperature is 31.8C, the cold side TEG temperature was 15C. The voltage measured as 9-180mV.

Que: Why aluminium foil and ice pack was used for the experiment?

To achieve a larger temperature gradient
Hot side TEG was attached to body skin. Skin temperature was 27.4C.
The cold side is exposed to ambient air or enhanced with heat sinks.

Open circuit voltage
For one TEG with diode to test voltage values:

- *At room temperature, cold side TEG temperature was 24.5C, voltage measured as 20-100mV.*
- *When ice was applied on the cold side of TEG to reduce the temperature of cold side TEG to about 5C, voltage measured as 170-190mV.*

4 TEGs connected with diode in parallel to test voltage values:

- *At room temperature, cold side TEG temperature was 24.5C, voltage measured as 9 mV.*
- *With ice pack wrapped with Aluminium foil, cold side TEG temperature was 5C, voltage measured as 100-300 mV.*

Cold pack may not be the ideal heat sink, it is applied to all conditions to allow fair comparison.
Further extension:
A low-voltage LTC3108 converter captures TEG output, stores it in supercapacitors, and boosts it via MT3608 for use by an ESP32 microcontroller.

Procedure:

1. Inspect TEGs, all materials and equipment.
2. Cut 4 thermal pads to match the size of the TEGs which will interface with hot and cold sides of TEGs
3. Apply 12.8 W/mK thermal pads - 0.5mm thermal pad on the hot side and 1.0mm thermal pad on the cold side
4. Connect the components of TEG systems to complete the circuit for 3 configurations: Parallel, Series, 2×2 Hybrid.
5. Take 5 time-series measurements every 30 seconds for each resistance in 3 TEG configuration for 3 heat source conditions – measure voltage and temperature of hot and cold sides of TEGs

- Conduct data collection.
- Visually analyse results using tables and graphs.

Stage 1 pilot study results

The pilot study investigated the effect of load resistance on the power output of three TEG configurations (parallel, series, and 2×2 hybrid) under three heat source conditions (static body heat, dynamic body heat, and appliance heat). Load resistances of 10 Ω, 100 Ω, 220 Ω, 330 Ω, 1 kΩ, 2 kΩ, 5 kΩ, and 10 kΩ were tested.

The results showed that the 10 Ω load resistor generally produced the highest power output across the tested configuration-heat source combinations. Therefore, a fixed load resistance of 10 Ω was selected for Stage 2.

Notes:

Investigate power-resistance relationship

- *Hyperbola graph – bell shape*

Load resistance directly affects the voltage, current, and power delivered by a TEG system. As maximum power transfer occurs when the load resistance matches the internal resistance of the TEG configuration, varying the load resistance could influence power output independently of the experimental variables. Therefore, a fixed load resistance was used to ensure a fair comparison between configurations and heat sources.

Key findings:

- The 10 Ω resistor produced the highest power output under all tested conditions except for the series configuration under static body heat conditions.
- The series and 2×2 hybrid configurations generally produced greater power output than the parallel configuration.
- At a load resistance of 10 Ω, the series configuration produced the highest power output under appliance heat conditions, whereas the 2×2 hybrid configuration produced the highest power output under both static and dynamic body heat conditions.
- Appliance heat generated greater power output than both body heat conditions for the series and 2×2 hybrid configurations.
- For all heat source conditions and TEG configurations, power output decreased substantially as load resistance increased above 220 Ω. The power output vs. load resistance graphs exhibited a peak at low resistance values followed by a progressive decline towards 10 kΩ.

Data presentation:

Table 1. Voltage, current, mean voltage, mean power output and mean temperature difference of TEG configurations under different heat source conditions at various load resistances

Mean temperature difference (°C) for different heat source conditions

Thermal conditions	Ave Temp Diff (°C)
Static body heat	10.60
Dynamic body heat	10.43
Appliance heat	14.20

2×2 Hybrid configuration - Static body heat - Ave ΔT (°C) = 10.4

Resistor (Ω)	Hot side Temp (°C)	Cold side Temp (°C)	ΔT (°C)	V1	V2	V3	V4	V5	V ave (mV)	I ave (mA)	P = VI (uW)
10	21.8	11.5	10.3	69.8	69.6	68.9	68.8	68.5	69.1	6.91	477.8
100	22.6	12.4	10.2	103.0	109.0	109.0	109.0	109.0	107.8	1.08	116.2
220	25.0	14.6	10.4	112.0	112.0	113.0	113.0	113.0	112.6	0.51	57.6
330	21.2	11.0	10.2	121.0	125.0	126.0	126.0	130.0	125.6	0.38	47.8
1K	21.6	11.8	9.8	122.0	122.0	122.0	122.0	121.0	121.8	0.12	14.8
2K	22.8	12.4	10.4	115.0	115.0	115.0	115.0	116.0	115.2	0.06	6.6
5K	24.5	12.9	11.6	139.1	139.4	139.5	139.0	139.1	139.2	0.03	3.9
10K	25.0	13.9	10.4	132.2	132.0	132.3	133.0	134.0	132.7	0.01	1.8

2×2 Hybrid configuration - Dynamic body heat - Ave ΔT (°C) = 10.2

Resistor (Ω)	Hot side Temp (°C)	Cold side Temp (°C)	ΔT (°C)	V1	V2	V3	V4	V5	V ave (mV)	I ave (mA)	P = VI (uW)
10	24.8	14.1	10.7	70.0	70.2	69.9	69.9	69.6	69.9	6.99	488.9
100	24.0	13.8	10.7	98.5	98.6	99.1	99.2	99.7	99.0	0.99	98.0
220	23.4	13.7	10.2	102.9	104.8	105.9	106.8	107.6	105.6	0.48	50.7
330	23.5	13.1	9.7	132.0	133.0	133.0	134.0	134.0	133.2	0.40	53.8
1K	22.8	12.6	10.4	149.2	150.0	150.8	151.2	151.6	150.6	0.15	22.7
2K	21.2	11.9	10.2	107.9	107.7	108.0	109.2	109.8	108.5	0.05	5.9
5K	22.5	11.9	9.3	112.0	110.0	111.0	109.0	108.0	110.0	0.02	2.4
10K	22.0	11.5	10.6	36.8	137.8	137.5	137.0	137.0	137.2	0.01	1.9

2×2 Hybrid configuration - Appliance heat - Ave ΔT (°C) = 15.4

Resistor (Ω)	Hot side Temp (°C)	Cold side Temp (°C)	ΔT (°C)	V1	V2	V3	V4	V5	V ave (mV)	I ave (mA)	P = VI (uW)
10	29.4	14.3	15.1	83.5	83.4	84.8	85.0	82.7	83.9	8.39	703.6
100	29.4	11.6	17.8	141.0	141.0	141.0	141.0	141.0	141.0	1.41	198.8
220	30.0	11.3	18.7	153.0	153.0	153.0	153.0	153.0	153.0	0.70	106.4
330	26.5	13.1	13.4	156.0	156.0	156.0	156.0	156.0	156.0	0.47	73.7
1K	27.5	11.8	15.7	160.0	160.0	160.0	160.0	160.0	160.0	0.16	25.6
2K	26.3	13.1	13.2	162.0	162.0	162.0	162.0	162.0	162.0	0.08	13.1
5K	28.3	14.5	13.8	170.0	170.0	170.0	170.0	170.0	170.0	0.03	5.8
10K	22.0	11.5	10.6	36.8	137.8	137.5	137.0	137.0	137.2	0.01	1.9

Series configuration - Static body heat - Ave ΔT (°C) = 11.0

Resistor (Ω)	Hot side Temp (°C)	Cold side Temp (°C)	ΔT (°C)	V1	V2	V3	V4	V5	V ave (mV)	I ave (mA)	P = VI (uW)
10	22.8	12.1	10.7	59.9	59.5	59.5	59.3	59.0	59.4	5.94	353.3
100	22.3	11.6	10.7	254.0	249.0	249.0	250.0	250.0	250.4	2.50	627.0
220	23.6	12.5	11.1	266.0	266.0	267.0	268.0	268.0	267.0	1.21	324.0
330	22.3	11.2	11.1	259.0	259.0	259.0	259.0	259.0	259.0	0.78	203.3
1K	21.0	22.8	9.9	324.0	324.0	324.0	324.0	324.0	324.0	0.32	105.0
2K	22.8	10.3	12.5	320.0	320.0	320.0	321.0	321.0	320.4	0.16	51.3
5K	22.1	11.3	10.8	358.0	358.0	358.0	357.0	357.0	357.6	0.07	25.6
10K	23.8	12.7	11.1	383.0	378.0	378.0	377.0	377.0	378.6	0.04	14.3

Series configuration - Dynamic body heat - Ave ΔT (°C) = 10.9

Resistor (Ω)	Hot side Temp (°C)	Cold side Temp (°C)	ΔT (°C)	V1	V2	V3	V4	V5	V ave (mV)	I ave (mA)	P = VI (uW)
10	23.4	13.5	9.9	65.1	65.2	65.8	64.4	64.1	64.9	6.49	421.5
100	22.4	11.6	10.8	176.0	177.3	177.3	178.8	179.0	177.7	1.78	315.7
220	22.7	12.0	10.7	251.0	254.0	255.0	255.0	254.0	253.8	1.15	292.8
330	23.1	12.3	10.8	287.0	287.0	288.0	288.0	288.0	287.6	0.87	250.6
1K	23.0	11.9	11.1	304.0	308.0	312.0	311.0	310.0	309.0	0.31	95.5
2K	21.5	10.8	10.7	308.0	308.0	308.0	308.0	308.0	308.0	0.15	47.4
5K	22.7	11.0	11.7	352.0	353.0	356.0	358.0	357.0	355.2	0.07	25.2
10K	23.8	12.4	10.8	377.0	379.0	380.0	381.0	381.0	379.6	0.04	14.4

Series configuration - Appliance heat - Ave ΔT (°C) = 12.6

Resistor (Ω)	Hot side Temp (°C)	Cold side Temp (°C)	ΔT (°C)	V1	V2	V3	V4	V5	V ave (mV)	I ave (mA)	P = VI (uW)
10	25.3	16.8	8.5	105.6	103.3	100.6	99.1	100.7	101.9	10.19	1,037.5
100	31.9	16.6	15.3	299.0	296.0	300.0	304.0	306.0	301.0	3.01	906.0
220	30.8	14.9	15.9	294.0	294.0	294.0	294.0	294.0	294.0	1.34	392.9
330	26.0	14.9	11.1	294.0	295.0	295.0	296.0	296.0	295.2	0.89	264.1
1K	29.2	17.9	11.3	286.0	286.0	286.0	286.0	286.0	286.0	0.29	81.8
2K	26.8	15.0	11.8	281.0	282.0	282.0	283.0	283.0	282.2	0.14	39.8
5K	29.6	18.6	11.0	290.0	290.0	289.0	289.0	289.0	289.4	0.06	16.8
10K	23.0	11.5	11.5	291.0	291.0	291.0	291.0	291.0	291.0	0.03	8.5

Parallel configuration - Static body heat - Ave ΔT (°C) = 10.4

Resistor (Ω)	Hot side Temp (°C)	Cold side Temp (°C)	ΔT (°C)	V1	V2	V3	V4	V5	V ave (mV)	I ave (mA)	P = VI (uW)
10	21.8	11.5	10.3	69.8	69.6	68.9	68.8	68.5	69.1	6.91	477.8
100	22.6	12.4	10.2	103.0	109.0	109.0	109.0	109.0	107.8	1.08	116.2

220	25.0	14.6	10.4	112.0	112.0	113.0	113.0	113.0	112.6	0.51	57.6
330	21.2	11.0	10.2	121.0	125.0	126.0	126.0	130.0	125.6	0.38	47.8
1K	21.6	11.8	9.8	122.0	122.0	122.0	122.0	121.0	121.8	0.12	14.8
2K	22.8	12.4	10.4	115.0	115.0	115.0	115.0	116.0	115.2	0.06	6.6
5K	24.5	12.9	11.6	139.1	139.4	139.5	139.0	139.1	139.2	0.03	3.9
10K	25.0	13.9	10.4	132.2	132.0	132.3	133.0	134.0	132.7	0.01	1.8

Parallel configuration - Dynamic body heat - Ave ΔT (°C) = 10.2

Resistor (Ω)	Hot side Temp (°C)	Cold side Temp (°C)	ΔT (°C)	V1	V2	V3	V4	V5	V ave (mV)	I ave (mA)	P = VI (uW)
10	24.8	14.1	10.7	70.0	70.2	69.9	69.9	69.6	69.9	6.99	488.9
100	24.0	13.8	10.7	98.5	98.6	99.1	99.2	99.7	99.0	0.99	98.0
220	23.4	13.7	10.2	102.9	104.8	105.9	106.8	107.6	105.6	0.48	50.7
330	23.5	13.1	9.7	132.0	133.0	133.0	134.0	134.0	133.2	0.40	53.8
1K	22.8	12.6	10.4	149.2	150.0	150.8	151.2	151.6	150.6	0.15	22.7
2K	21.2	11.9	10.2	107.9	107.7	108.0	109.2	109.8	108.5	0.05	5.9
5K	22.5	11.9	9.3	112.0	110.0	111.0	109.0	108.0	110.0	0.02	2.4
10K	22.0	11.5	10.6	136.8	137.8	137.5	137.0	137.0	137.2	0.01	1.9

Parallel configuration - Appliance heat - Ave ΔT (°C) = 14.6

Resistor (Ω)	Hot side Temp (°C)	Cold side Temp (°C)	ΔT (°C)	V1	V2	V3	V4	V5	V ave (mV)	I ave (mA)	P = VI (uW)
10	34.3	18.4	15.9	54.4	54.6	55.2	55.4	55.5	55.0	5.50	302.7
100	36.4	19.2	17.2	70.1	69.9	69.8	69.7	69.5	69.8	0.70	48.7
220	33.2	18.3	14.9	78.7	78.2	78.3	78.4	78.5	78.4	0.36	28.0
330	35.1	20.1	15.0	62.7	62.9	63.0	63.2	63.4	63.0	0.19	12.0
1K	36.0	19.3	16.7	60.7	60.8	61.0	60.5	60.7	60.7	0.06	3.7
2K	34.3	18.0	16.3	60.4	61.2	61.8	62.5	63.2	61.8	0.03	1.9
5K	28.4	17.9	10.5	63.4	63.5	63.9	64.0	63.8	63.7	0.01	0.8
10K	28.0	16.7	11.3	59.9	60.2	60.5	60.6	60.7	60.4	0.01	0.4

Table 2. Mean voltage output of TEG configurations under different heat source conditions at various load resistances

2×2 Hybrid configuration: Mean voltage output (mV) under various load resistances

Resistor (Ω)	Static body heat voltage (mV)	Dynamic body heat voltage (mV)	Appliance heat voltage (mV)
10	69.1	69.9	83.9
100	107.8	99.0	141.0
220	112.6	105.6	153.0
330	125.6	133.2	156.0
1k	121.8	150.6	160.0
2k	115.2	108.5	162.0
5k	139.2	110.0	170.0
10k	132.7	137.2	180.0

Series configuration: Mean voltage output (mV) under various load resistances

Resistor (Ω)	Static body heat voltage (mV)	Dynamic body heat voltage (mV)	Appliance heat voltage (mV)
10	59.4	64.9	101.9
100	250.4	177.7	301.0
220	267.0	253.8	294.0
330	259.0	287.6	295.2
1k	324.0	309.0	286.0
2k	320.4	308.0	282.2
5k	357.6	355.2	289.4
10k	378.6	379.6	291.0

Parallel configuration: Mean voltage output (mV) under various load resistances

Resistor (Ω)	Static body heat voltage (mV)	Dynamic body heat voltage (mV)	Appliance heat voltage (mV)
10	46.3	60.5	55.0
100	54.7	70.1	69.8
220	65.2	70.6	78.4
330	57.5	74.3	63.0
1k	74.8	77.9	60.7
2k	61.1	57.2	61.8
5k	76.3	84.0	63.7
10k	69.7	82.2	60.4

Table 3. Mean power output of TEG configurations under different heat source conditions at various load resistances

2×2 Hybrid configuration: Mean power output (μW) under various load resistances

Resistor (Ω)	Static body heat Power (μW)	Dynamic body heat Power (μW)	Appliance heat Power (μW)
10	477.8	488.9	703.6
100	116.2	98.0	198.8
220	57.6	50.7	106.4
330	47.8	53.8	73.7
1k	14.8	22.7	25.6
2k	6.6	5.9	13.1
5k	3.9	2.4	5.8
10k	1.8	1.9	3.2

Series configuration: Mean power output (μW) under various load resistances

Resistor (Ω)	Static body heat Power (μW)	Dynamic body heat Power (μW)	Appliance heat Power (μW)
10	353.3	421.5	1,037.5
100	627.0	315.7	906.0
220	324.0	292.8	392.9
330	203.3	250.6	264.1
1k	105.0	95.5	81.8
2k	51.3	47.4	39.8
5k	25.6	25.2	16.8
10k	14.3	14.4	8.5

Parallel configuration: Mean power output (μW) under various load resistances

Resistor (Ω)	Static body heat Power (μW)	Dynamic body heat Power (μW)	Appliance heat Power (μW)
10	214.2	365.5	302.7
100	29.9	49.1	48.7
220	19.3	22.6	28.0
330	10.0	16.7	12.0
1k	5.6	6.1	3.7
2k	1.9	1.6	1.9
5k	1.2	1.4	0.8
10k	0.5	0.7	0.4

Figure 1. Effect of load resistance on mean voltage output of different electrical configuration under different heat source conditions

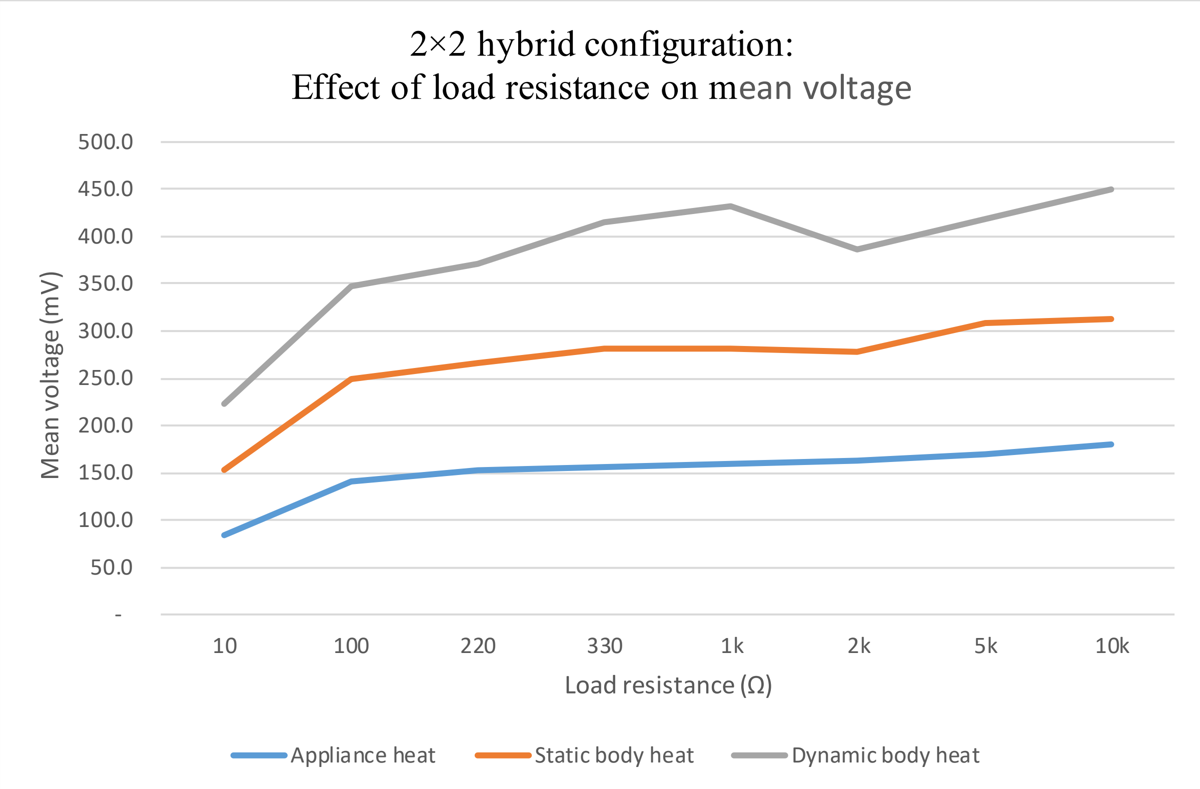

Figure 1(a). Effect of load resistance on mean voltage output of the 2×2 hybrid configuration under different heat source conditions

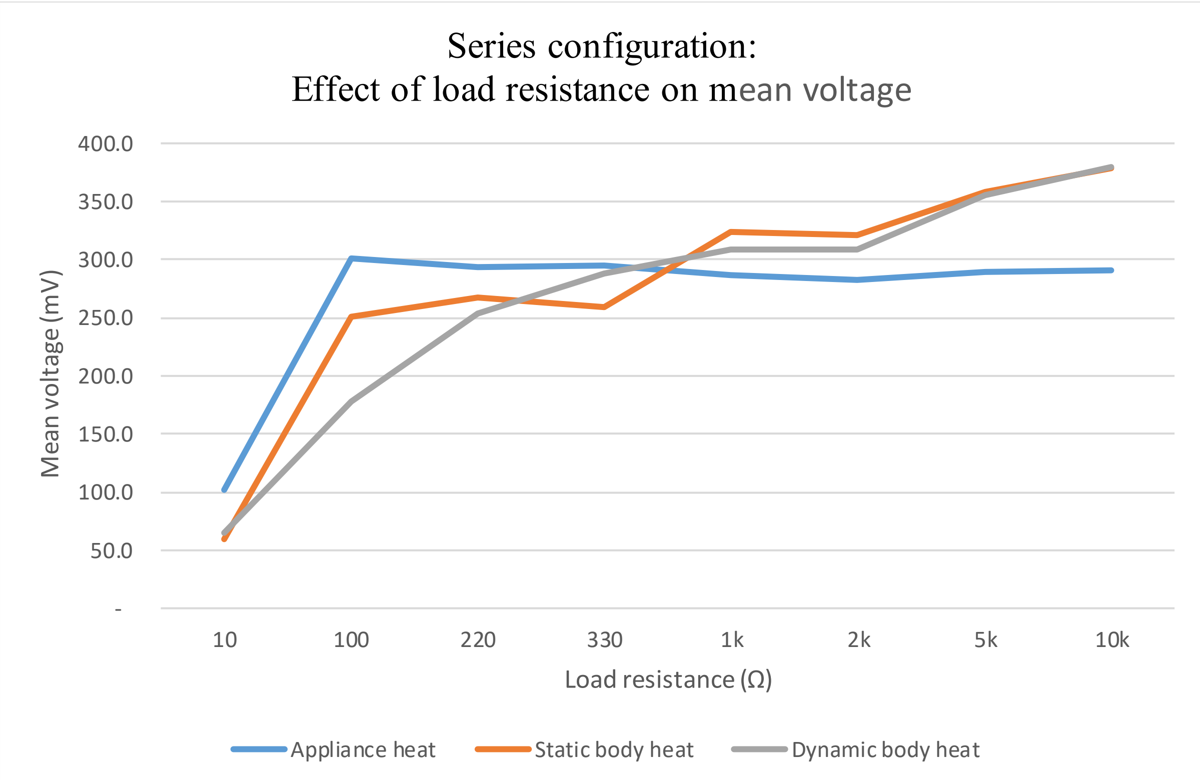

Figure 1(b). Effect of load resistance on mean voltage output of the series configuration under different heat source conditions

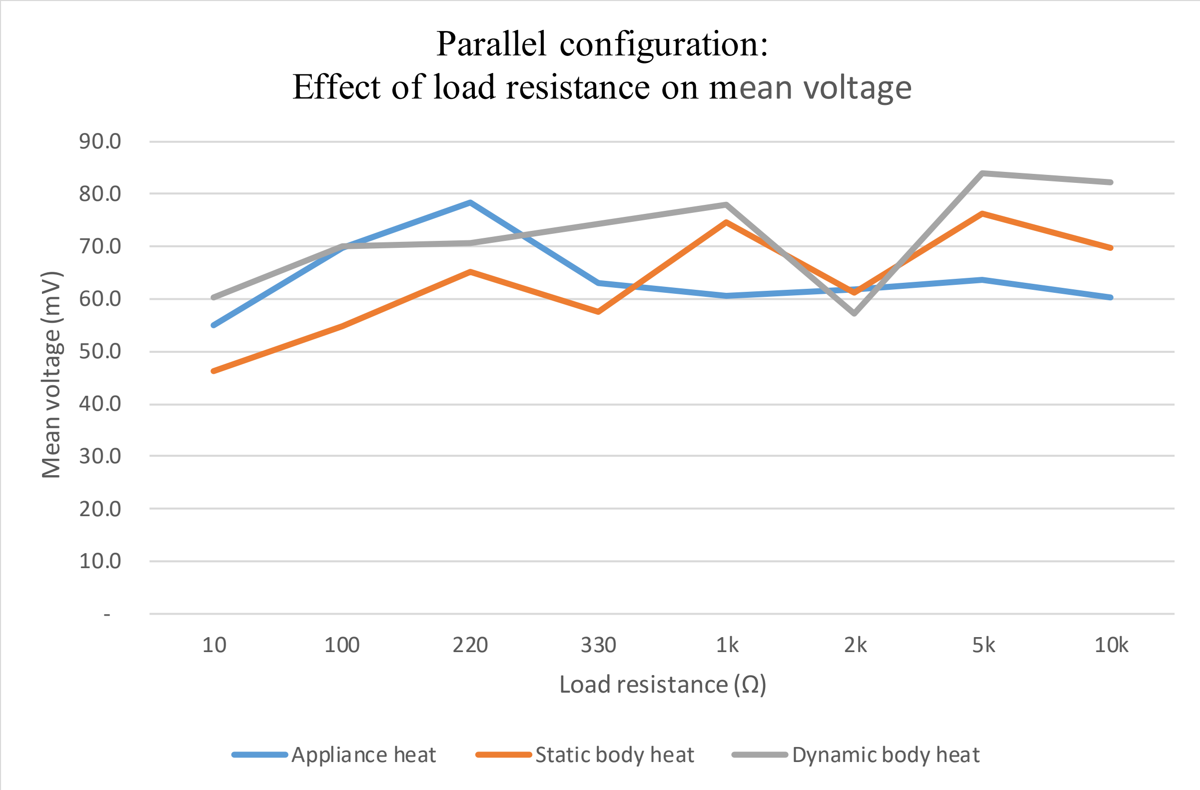

Figure 1(c). Effect of load resistance on mean voltage output of the parallel configuration under different heat source conditions

Figure 2. Effect of load resistance on mean power output of different electrical configuration under different heat source conditions

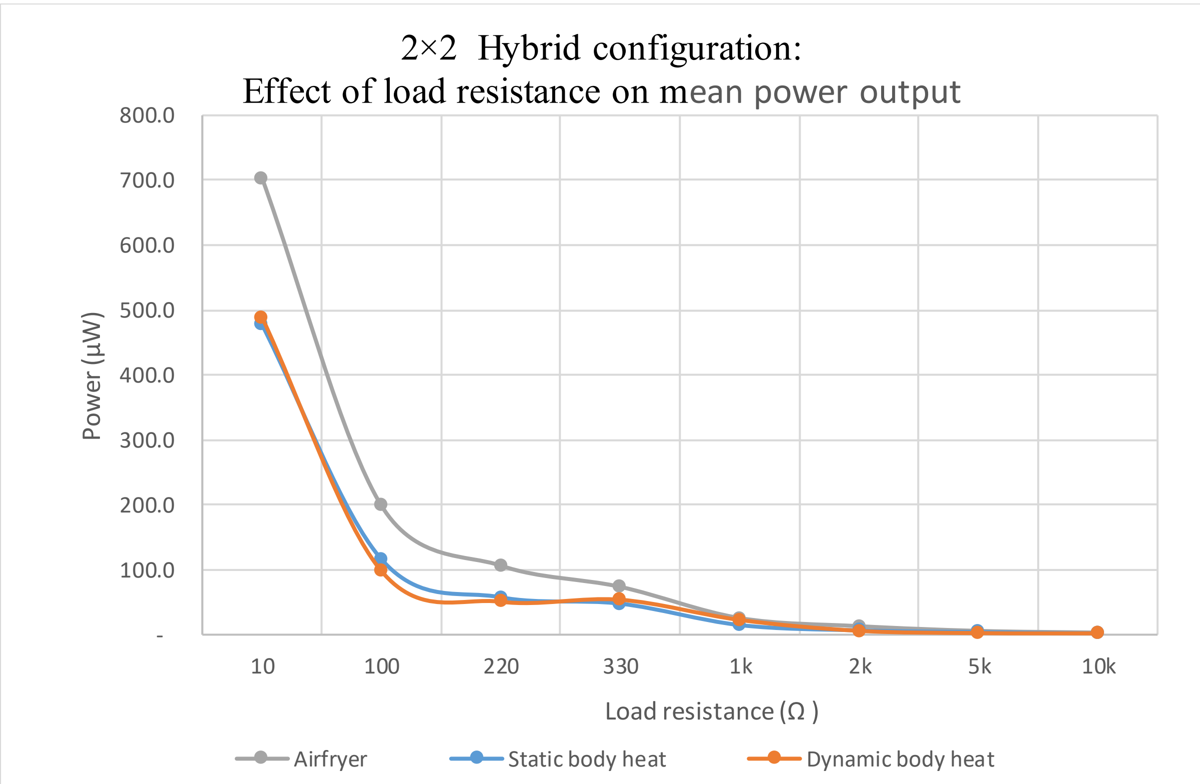

Figure 2(a). Effect of load resistance on mean power output of the 2×2 hybrid configuration under different heat source conditions

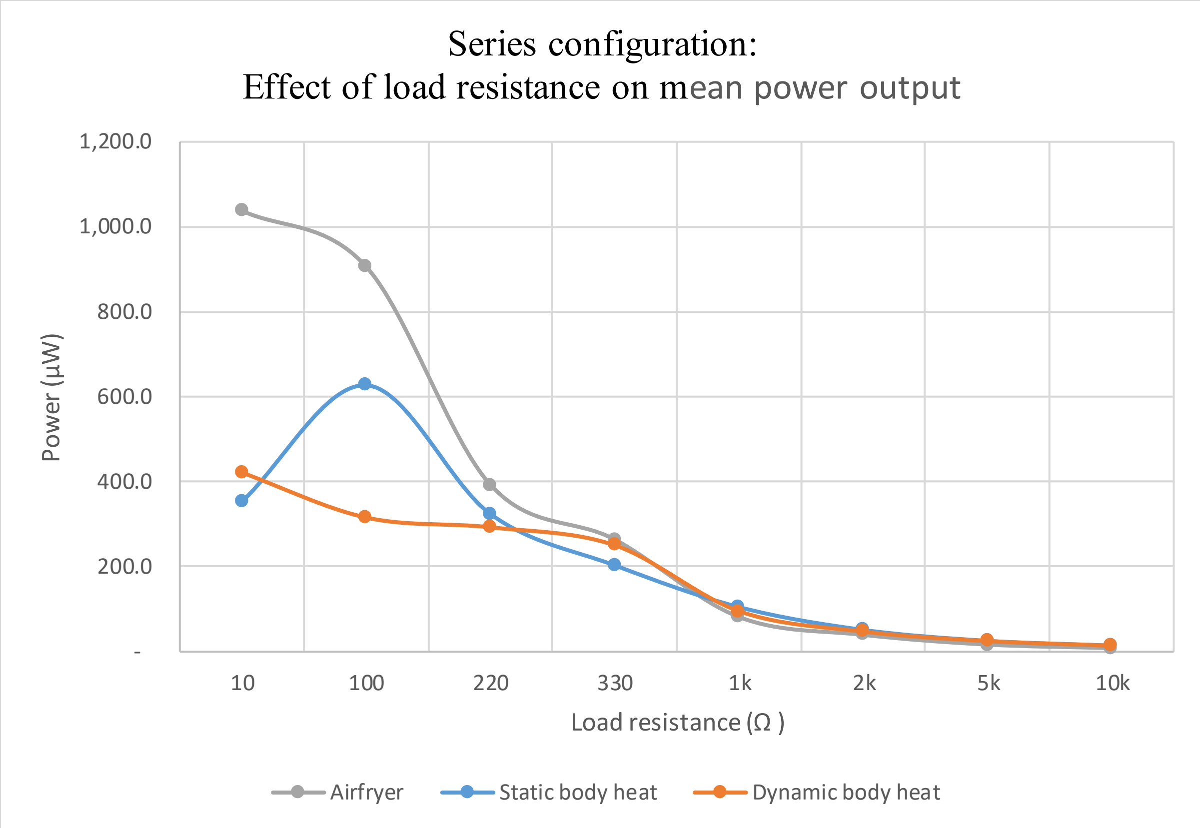

Figure 2(b). Effect of load resistance on mean power output of the series TEG configuration under different heat source conditions

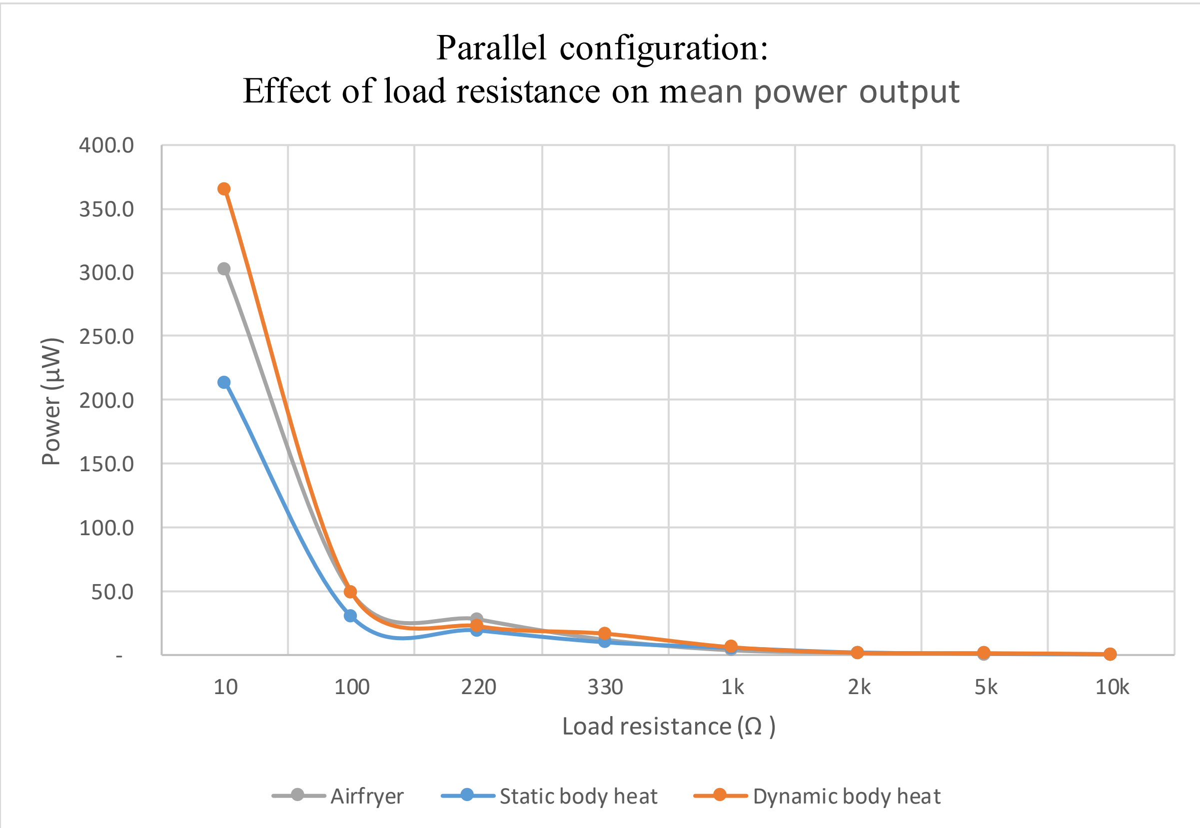

Figure 2(c). Effect of load resistance on mean power output of the parallel TEG configuration under different heat source conditions

Notes:

New learning:

Que. What is the internal resistance of a TEG module?

The internal resistance of a TEG is 2–4 Ω per TEG at room temperature.
A commonly cited nominal value is approximately 3 Ω.
The exact value changes with:

- *Temperature difference (ΔT)*
- *Mean operating temperature*
- *Manufacturing variation*

Maximum Power Transfer Theorem:
Maximum power is delivered to the load when R load = R int.

There exists an optimal load resistance that matches the internal resistance of the TEG system, at which maximum power output occurs (Maximum Power Point).

Que. What is the internal resistance of each TEG configuration?
How to estimate internal resistance?

Estimation of internal resistance of different four-module TEG electrical configuration:
Assumption: 3 Ω per TEG.
Internal resistances add:

Series configuration:
R series = R1 + R2 + R3 + R4 = 3 Ω x 4 = 12 Ω
Parallel configuration:
For n identical resistors in parallel = 1/R parallel
R parallel = R/n = 1/R1 + 1/R2 + 1/R3 + 1/R4 = 4/3
1/R parallel = 3/4 Ω = 0.75 Ω

2×2 hybrid configuration:
Each series string: R1 + R2 or R3 + R4 = 3 Ω x 2 = 6 Ω
R parallel = 1/6 + 1/6 = 1/3 Ω
1/R parallel = 3 Ω

*** Interestingly, the 2×2 hybrid configuration has approximately the same internal resistance as a single TEG, while producing roughly twice the voltage and twice the current capability. This will make hybrid arrangements more attractive in thermoelectric energy-harvesting systems.*

Next Que:
A 10 Ω load is indeed much closer to the estimated internal resistance of the 4-series configuration (~12 Ω) (compared to 4-parallel: ~0.75 Ω and 2×2 hybrid: ~3 Ω), it is not an unreasonable load choice for a pilot study transitioning into the main investigation. Wil this reason favours the result of series configuration?

The series configuration was the closest match to the 10 Ω load resistance and may therefore have operated closer to its maximum power point than the hybrid or parallel configurations. Stage 1 finding supports this hypothesis. This represents a potential source of systematic bias.

*** To control this variable, I used the same 10 Ω resistor load for all three configurations and measure the voltage across the resistor with a multimeter.*

Reflection:
If I had access to a wider range of low-resistance resistors, I would repeat this pilot study to determine the load resistance that best matches the internal resistance of the TEG configuration and maximises power output in the Stage 2 experiments.

I controlled the load resistance at 10 Ω to ensure fair comparison between configurations, while recognising that further investigation could identify the maximum power point.

Future work: A limitation of this investigation was the availability of only a 10 Ω load resistor. Future work could investigate a wider range of low-resistance loads to determine the maximum power point for each TEG configuration and compare the optimal load resistance with the estimated internal resistance of the TEG configuration.

My investigation is not primarily about finding the maximum power point but comparing the performance of different TEG configurations under a controlled load.

For stage 2 experiments, however, using the same 10 Ω load for every configuration controls an important variable – load resistance. This allows me to attribute differences in voltage, current, and power to the TEG configuration rather than to changing load resistance.

Que: How does a graph of power output vs. load resistance look like?

For a TEG, the power output vs load resistance curve is typically a single-peaked curve (an inverted U-shape)

Shape of the curve
At very low load resistance (near a short circuit), the voltage across the load is very small, so power is low.
As load resistance increases, power increases.
Power reaches a maximum when: R (load) = R (internal). This is known as the maximum power transfer point.
Beyond this point, current decreases faster than voltage increases, so power falls.
At very high load resistance (approaching open circuit), current approaches zero, so power again approaches zero.

For 4-SP1848 TEG system:
Power should rise from 1 Ω to around the optimum resistance.
Peak power should occur at a resistance close to the total internal resistance of the configuration.
Power should then decrease as resistance increases further (e.g., 50 Ω, 100 Ω, 220 Ω).

The resulting graph is a non-linear bell-shaped curve with a single maximum corresponding to the maximum power transfer point.

In summary, the power–load resistance relationship exhibited a non-linear, single-peaked curve. Power output increased with load resistance until a maximum value was reached, after which it decreased. This behaviour is consistent with the maximum power transfer theorem, which predicts that maximum power is delivered when the external load resistance is approximately equal to the internal resistance of the TEG system.

Ref:
https://www.electronics-tutorials.ws/dccircuits/dcp_9.html
https://electricalacademia.com/basic-electrical/maximum-power-transfer-theorem/

Key findings:
A pilot study of TEG power generation for 3 conditions (static skin, dynamic skin and air flyer top surface) was conducted using load resistances from 10 Ω to 10K Ω. The resistors used were 10, 100, 220, 330, 1k, 2k, 5k and 10k Ω.

- The 10 Ω resistor consistently produced the highest power output under most tested conditions except for series configuration for static body heat condition. It is thus selected as a load for the stage 2 experiments
- Series and hybrid systems generated higher power output, whereas, parallel system produced the least power.
- Series system generally produced higher power output than hybrid and parallel except that static and dynamic body heat conditions?
- Appliance heat generated higher power output than both body heat conditions for series and hybrid configurations. The likely reason is due to its larger temperature difference. Temperature difference for appliance heat is approximately 15C whereas both body heat conditions is 10C.
- All 3 heat source conditions significantly reduced power output from 220 Ω. to 1 kΩ..

Stage 2: Main investigation

To improve experimental design

- Use thermal pads of higher heat transfer efficiency 21 W/mK, use thinner pad to allow faster heat dissipation.
- Use metronome to keep the knee movement speeds consistently at 60 bpm.
- Mark the exact placement for body heat conditions, the same participant, the same leg.

Materials and equipment were streamlined to:

- TEGs (SP1848-27145) x4

- Thermal pad 21 W/mK, 0.5mm - to facilitate heat transfer
- 10 Ω Resistor
- Aluminium foil and ice pack – to dissipate heat
- Breadboard and jumper wires
- Soldering iron + solder – used to solder the wire ends of the TEGs for breadboard connections and connect wiring
- Digital multimeter
- Infrared thermometer - to measure heat source hot and cold side temperatures
- Stop watch
- Metronome – used for dynamic body heat condition
- Exercise band – used for dynamic body heat condition
- Chair – used for dynamic body heat condition

31.05.2026 – 02.06.206

Experiment 1.

- Analyse power output for single TEG configuration for 3 heat source conditions
- Appliance heat may produce higher power output if it creates higher temperature differentials than body heat.

Experiment 2.

- Analyse power output for 3 TEG configuration for 3 heat source conditions
- Find out the best configuration.
- Compare and discuss the effect of 3 heat source conditions

05.06.2026 – 08.06.206

Perform data analysis

- Stage 1
  - The pilot study investigated the effect of load resistance on the power output of parallel, series, and 2×2 hybrid configurations under static body heat, dynamic body heat, and appliance heat conditions.
  - Table + bar chart: mean power output
  - Power vs load resistance line graphs
  - Selection of 10 Ω

- Stage 2
  - Mean voltage ± SD
  - Mean calculated current ± SD
  - Mean ΔT ± SD
  - Mean calculated power ± SD
  - Voltage vs time
  - ΔT vs time
  - Two-way ANOVA
  - Pairwise t-tests

Raw data:

Construct tables and graphs

Table 4. Voltage output (mV) and temperature difference (°C) measured for different electrical configurations under different heat source conditions at a fixed load resistance of 10 Ω.

2×2 Hybrid configuration - Static body heat

Time (s)	**Trial 1**				**Trial 2**				**Trial 3**			
	Hot side Temp (°C)	Cold side Temp (°C)	Temp Diff (°C)	Voltage (mV)	Hot side Temp (°C)	Cold side Temp (°C)	Temp Diff (°C)	Voltage (mV)	Hot side Temp (°C)	Cold side Temp (°C)	Temp Diff (°C)	Voltage (mV)
0	28.3	7.8	20.5	410.0	26.9	5.0	21.9	226.0	25.9	4.7	21.2	200.0
30	28.0	7.8	20.2	378.0	26.7	7.3	19.4	232.0	22.8	6.8	16.0	195.0
60	26.0	3.2	22.8	390.0	26.2	8.8	17.4	230.0	22.4	10.0	12.4	166.0
90	27.7	10.2	17.5	316.0	26.0	8.8	17.2	205.0	21.7	4.1	17.6	239.0
120	27.2	8.0	19.2	307.0	25.5	8.9	16.6	235.0	21.8	5.0	16.8	263.0
150	27.2	12.2	15.0	286.0	24.3	7.6	16.7	228.0	21.8	6.2	15.6	205.0
180	28.2	12.2	16.0	264.0	24.8	8.5	16.3	222.0	22.0	0.2	21.8	216.0
Mean	27.5	5.1	18.7	335.9	25.8	7.8	17.9	225.4	22.6	5.3	17.3	212.0
SD	0.80	3.14	2.7	56.4	1.0	1.4	2.0	9.9	1.5	3.0	3.3	31.5

2×2 Hybrid configuration - Dynamic body heat

Time (s)	**Trial 1**				**Trial 2**				**Trial 3**			
	Hot side Temp (°C)	Cold side Temp (°C)	Temp Diff (°C)	Voltage (mV)	Hot side Temp (°C)	Cold side Temp (°C)	Temp Diff (°C)	Voltage (mV)	Hot side Temp (°C)	Cold side Temp (°C)	Temp Diff (°C)	Voltage (mV)
0	23.0	2.3	20.7	323.0	23.4	3.5	19.9	226.0	22.9	3.6	19.3	194.0
30	23.1	5.7	17.4	256.0	23.4	3.1	20.3	211.0	22.9	1.9	21.0	172.0
60	23.4	6.3	17.1	261.0	23.8	4.3	19.5	201.0	22.9	3.1	19.8	179.0
90	23.8	3.1	20.7	277.0	23.0	3.7	19.3	201.0	23.1	3.0	20.1	166.0
120	23.8	5.7	18.1	238.0	22.9	2.7	20.2	210.0	22.9	3.1	19.8	203.0
150	*23.0*	*6.3*	16.7	*225.0*	*22.9*	*2.5*	20.4	200.0	22.9	6.3	16.6	186.0
180	23.0	5.1	17.9	187.0	22.9	3.1	19.8	198.0	22.9	3.0	19.9	189.0
Mean	23.3	5.1	18.4	252.4	23.2	3.3	19.9	206.7	22.9	3.4	19.5	184.1
SD	0.37	1.59	1.7	42.65	0.4	0.6	0.4	9.9	0.1	1.4	1.4	12.8

2×2 Hybrid configuration - Appliance heat

Time (s)	**Trial 1**				**Trial 2**				**Trial 3**			
	Hot side Temp (°C)	Cold side Temp (°C)	Temp Diff (°C)	Voltage (mV)	Hot side Temp (°C)	Cold side Temp (°C)	Temp Diff (°C)	Voltage (mV)	Hot side Temp (°C)	Cold side Temp (°C)	Temp Diff (°C)	Voltage (mV)
0	42.8	7.3	35.5	153.0	44.4	6.4	38.0	144.5	35.2	7.2	28.0	145.4
30	41.7	6.6	35.1	140.2	42.9	10.7	32.2	136.4	38.9	7.3	31.6	134.4
60	42.1	7.4	34.7	144.8	39.9	5.2	34.7	137.8	37.8	6.6	31.2	140.2
90	37.3	6.7	30.6	138.7	44.3	10.1	34.2	128.8	41.1	9.7	31.4	137.4
120	41.8	9.5	32.3	136.9	32.1	4.8	27.3	127.9	39.8	11.2	28.6	142.5
150	43.5	11.7	31.8	136.1	38.5	8.9	29.6	148.8	45.2	7.0	38.2	139.2
180	43.6	6.9	36.7	132.1	41.1	12.4	28.7	139.6	43.7	6.6	37.1	138.3
Mean	41.8	5.1	33.8	140.3	40.5	8.4	32.1	137.7	40.2	7.9	32.3	139.6
SD	2.14	1.90	2.2	6.8	4.3	2.9	7.6	3.4	3.4	1.8	3.6	3.6

Series configuration - Static body heat

Time (s)	**Trial 1**				**Trial 2**				**Trial 3**			
	Hot side Temp (°C)	Cold side Temp (°C)	Temp Diff (°C)	Voltage (mV)	Hot side Temp (°C)	Cold side Temp (°C)	Temp Diff (°C)	Voltage (mV)	Hot side Temp (°C)	Cold side Temp (°C)	Temp Diff (°C)	Voltage (mV)
0	27.9	6.3	21.6	251.0	24.5	11.6	12.9	232.0	25.1	5.0	20.1	228.0
30	26.0	11.4	14.6	241.0	25.4	10.7	14.7	248.0	24.8	6.7	18.1	213.0
60	24.5	12.7	11.8	198.0	24.2	9.8	14.4	265.0	24.4	5.7	18.7	173.0

90	26.1	11.4	14.7	238.0	24.6	10.3	14.3	257.0	24.2	4.5	19.7	232.0
120	24.4	13.1	11.3	228.0	25.6	6.3	19.3	270.0	24.4	4.5	19.9	207.0
150	24.8	11.9	12.9	256.0	25.4	6.9	18.5	198.0	26.6	4.6	22.0	217.0
180	25.7	10.6	15.1	298.0	24.5	2.8	21.7	228.0	27.2	7.2	20.0	221.0
Mean	25.6	5.1	14.6	244.3	24.9	8.3	16.5	242.6	25.2	5.5	19.8	213.0
SD	1.22	2.3	3.4	30.3	0.6	3.1	3.3	25.2	1.2	1.1	1.2	19.6

Series configuration - Dynamic body heat

Time (s)	**Trial 1**				**Trial 2**				**Trial 3**			
	Hot side Temp (°C)	Cold side Temp (°C)	Temp Diff (°C)	Voltage (mV)	Hot side Temp (°C)	Cold side Temp (°C)	Temp Diff (°C)	Voltage (mV)	Hot side Temp (°C)	Cold side Temp (°C)	Temp Diff (°C)	Voltage (mV)
0	23.3	4.8	18.5	144.0	24	6.9	17.1	198.0	23.6	7.6	16.0	153.0
30	24.2	11.8	12.4	169.0	24	5.6	18.4	201.0	22.8	3.6	19.2	150.0
60	23.4	9.4	14.0	148.0	24	6.2	17.8	210.0	23.2	2.6	20.6	170.0
90	23.9	4.1	19.8	185.0	23	4.2	18.8	196.0	22.4	6.2	16.2	158.0
120	22.9	10.9	12.0	175.0	22.6	6.2	16.4	196.0	23.0	6.8	16.2	201.0
150	22.9	4.9	18.0	203.0	23	5.6	17.4	199.0	23.2	6.2	17.0	198.0
180	23.8	3	20.8	139.0	24.6	4.2	20.4	149.0	22.9	4.4	18.5	144.0
Mean	23.5	7.0	16.5	166.1	23.6	5.6	18.0	192.7	23.0	5.3	17.7	167.7
SD	0.50	3.60	3.6	23.65	0.73	1.03	1.3	19.86	0.38	1.83	1.8	23.16

Series configuration - Appliance heat

Time (s)	**Trial 1**				**Trial 2**				**Trial 3**			
	Hot side Temp (°C)	Cold side Temp (°C)	Temp Diff (°C)	Voltage (mV)	Hot side Temp (°C)	Cold side Temp (°C)	Temp Diff (°C)	Voltage (mV)	Hot side Temp (°C)	Cold side Temp (°C)	Temp Diff (°C)	Voltage (mV)
0	23.3	4.8	18.5	144.0	24	6.9	17.1	198.0	23.6	7.6	16.0	153.0
30	24.2	11.8	12.4	169.0	24	5.6	18.4	201.0	22.8	3.6	19.2	150.0
60	23.4	9.4	14.0	148.0	24	6.2	17.8	210.0	23.2	2.6	20.6	170.0
90	23.9	4.1	19.8	185.0	23	4.2	18.8	196.0	22.4	6.2	16.2	158.0
120	22.9	10.9	12.0	175.0	22.6	6.2	16.4	196.0	23.0	6.8	16.2	201.0
150	22.9	4.9	18.0	203.0	23	5.6	17.4	199.0	23.2	6.2	17.0	198.0
180	23.8	3	20.8	139.0	24.6	4.2	20.4	149.0	22.9	4.4	18.5	144.0
Mean	23.5	7.0	16.5	166.1	23.6	5.6	18.0	192.7	23.0	5.3	17.7	167.7
SD	0.50	3.60	3.6	23.65	0.73	1.03	1.3	19.86	0.38	1.83	1.8	23.16

Parallel configuration - Static body heat

Time (s)	**Trial 1**				**Trial 2**				**Trial 3**			
	Hot side Temp (°C	Cold side Temp (°C)	Temp Diff (°C)	Voltage (mV)	Hot side Temp (°C)	Cold side Temp (°C)	Temp Diff (°C)	Voltage (mV)	Hot side Temp (°C)	Cold side Temp (°C)	Temp Diff (°C)	Voltage (mV)
0	22.5	13.1	9.4	171.0	22.6	2	20.8	132.8	22.1	0.3	21.8	144.5
30	22.4	2.2	20.2	143.9	22.6	0.7	21.9	107.8	22.1	1.8	20.3	77.1
60	22.7	1.3	21.4	148.0	22.7	0.2	22.5	76.2	22.2	0.2	22.0	98.2
90	22.2	0.3	21.9	150.5	22.4	1.1	21.3	117.5	22.2	1.2	21.0	114.8
120	22.9	0.9	22.0	162.9	22.4	1.6	20.8	104.8	22.3	0.1	22.2	106.9
150	22.3	0.4	21.9	126.6	22.5	0.5	22.0	61.8	22.3	1.9	20.4	101.5
180	22.4	0.4	22.0	134.3	22.5	0.9	21.6	100.2	22.4	4.0	18.4	94.7
Mean	22.5	2.7	19.8	148.2	22.5	1.0	21.6	100.2	22.2	1.4	20.9	105.4
SD	0.24	4.7	4.6	15.4	0.1	0.6	0.6	24.1	0.1	1.4	1.3	20.8

Parallel configuration - Dynamic body heat

Time (s)	**Trial 1**				**Trial 2**				**Trial 3**			
	Hot side	Cold side	Temp Diff (°C)	Voltage (mV)	Hot side	Cold side	Temp Diff (°C)	Voltage (mV)	Hot side	Cold side	Temp Diff (°C)	Voltage (mV)

	Temp (°C)	Temp (°C)			Temp (°C)	Temp (°C)			Temp (°C)	Temp (°C)		
0	22.5	5.8	16.7	153.0	23.9	2.9	21.0	134.8	23.2	3.3	19.9	110.5
30	25.5	3.7	21.8	126.8	23.5	10.9	12.6	98.6	23.2	4.5	18.7	107.8
60	25.5	5.7	19.8	122.2	23.5	1.8	21.7	114.8	23.3	4.0	19.3	94.7
90	25.1	6.3	18.8	106.6	23.6	2.4	21.2	99.7	23.7	9.9	13.8	95.8
120	25.5	4.9	20.6	117.2	23.5	7.7	15.8	101.8	23.7	2.0	21.7	103.3
150	25.1	7.5	17.6	121.8	23.3	3.1	20.2	95.6	22.9	6.0	16.9	102.6
180	25.2	4.4	20.8	130.0	23.3	3.1	20.2	118.1	23.7	2.1	21.6	101.8
Mean	24.9	5.1	19.4	125.4	23.8	4.6	19.0	109.1	23.9	4.5	18.8	102.4
SD	1.08	1.3	1.8	14.3	0.2	3.4	3.4	14.2	0.3	2.7	2.8	5.8

Parallel configuration - Appliance heat

Time (s)	**Trial 1**				**Trial 2**				**Trial 3**			
	Hot side Temp (°C	Cold side Temp (°C)	Temp Diff (°C)	Voltage (mV)	Hot side Temp (°C)	Cold side Temp (°C)	Temp Diff (°C)	Voltage (mV)	Hot side Temp (°C)	Cold side Temp (°C)	Temp Diff (°C)	Voltage (mV)
0	34.1	16.5	17.6	111.5	33.1	2	31.1	83.8	43.6	7.0	36.6	101.6
30	34.5	12.4	22.1	67.3	36.3	3.1	33.2	90.9	38.8	7.1	31.7	104.5
60	35.3	19.3	16.0	89.8	32.7	13.6	19.1	93.3	34.8	1.3	33.5	97.4
90	29.2	18.3	10.9	63.8	33.6	1.0	32.6	89.1	40.8	8.6	32.2	113.2
120	46.0	10.1	35.9	119.2	37.3	9.6	27.7	90.9	42.4	6.0	36.4	97.6
50	36.9	9.7	27.2	112.8	41.3	1.7	39.6	95.9	31.4	11.0	20.4	107.9
180	41.7	3.3	38.4	111.8	40.3	7.8	32.5	129.9	35.7	11.3	24.4	97.2
Mean	36.8	5.1	24.0	96.6	36.4	5.5	30.8	96.3	38.2	7.5	30.7	102.8
SD	5.50	5.68	10.3	23.1	3.5	4.8	6.3	15.3	4.4	3.4	6.1	6.1

Single TEG - Static body heat

Time (s)	**Trial 1**				**Trial 2**				**Trial 3**			
	Hot side Temp (°C)	Cold side Temp (°C)	Temp Diff (°C)	Voltage (mV)	Hot side Temp (°C)	Cold side Temp (°C)	Temp Diff (°C)	Voltage (mV)	Hot side Temp (°C)	Cold side Temp (°C)	Temp Diff (°C)	Voltage (mV)
0	26.3	12.1	14.2	149.4	26.4	8.4	18.0	159.4	25.0	9.4	15.6	91.8
30	27.7	13.9	13.8	145.8	25.1	10.3	14.8	144.5	24.1	6.1	18.0	96.5
60	26.3	14.3	12.0	160.4	26.1	13.7	12.4	136.5	25.1	5.5	19.6	118.6
90	24.6	14.9	9.7	167.8	25.2	8.5	16.7	126.7	21.2	9.8	11.4	114.8
120	25.9	13.0	12.9	170.9	25.2	11.1	14.1	124.8	25.1	14.9	10.2	109.9
150	24.6	9.8	14.8	178.2	25.1	14.2	10.9	106.9	24.2	0.2	24.0	100.4
180	25.9	7.1	18.8	164.8	24.8	7.4	17.4	105.8	25.0	6.6	18.4	94.8
Mean	25.9	12.2	13.7	162.5	25.4	10.5	14.9	129.2	24.2	7.5	16.7	103.8
SD	1.1	2.8	2.8	11.6	0.6	2.7	2.65	19.5	1.41	4.54	4.79	10.54

Single TEG - Dynamic body heat

Time (s)	**Trial 1**				**Trial 2**				**Trial 3**			
	Hot side Temp (°C)	Cold side Temp (°C)	Temp Diff (°C)	Voltage (mV)	Hot side Temp (°C)	Cold side Temp (°C)	Temp Diff (°C)	Voltage (mV)	Hot side Temp (°C)	Cold side Temp (°C)	Temp Diff (°C)	Voltage (mV)
0	24.3	6.6	17.7	119.2	22.2	2.8	19.4	104.9	21.9	1.0	20.9	126.9
30	24.4	4.7	19.7	94.7	21.0	6.0	15.0	109.8	20.2	4.0	16.2	106.6
60	24.0	12.4	11.6	91.2	22.3	2.1	20.2	116.9	22.7	2.1	20.6	96.6
90	22.6	10.7	11.9	105.8	22.3	5.5	16.8	103.5	21.0	1.0	20.0	99.6
120	20.5	7.4	13.1	89.8	21.0	6.9	14.1	111.8	20.3	3.0	17.3	97.5
150	23.6	6.0	17.6	81.8	20.6	1.5	19.1	106.3	21.6	1.0	20.6	96.8
180	20.1	6.8	13.3	92.4	20.2	7.5	12.7	107.9	22.5	1.2	21.3	90.8
Mean	22.8	7.8	15.0	96.4	21.4	4.6	16.8	108.7	21.5	1.9	19.6	102.1
SD	1.8	2.7	3.3	12.3	0.9	2.4	2.9	4.6	1.0	1.2	2.0	11.9

Single TEG - Appliance heat

Time (s)	Trial 1				Trial 2				Trial 3			
	Hot side Temp (°C)	Cold side Temp (°C)	Temp Diff (°C)	Voltage (mV)	Hot side Temp (°C)	Cold side Temp (°C)	Temp Diff (°C)	Voltage (mV)	Hot side Temp (°C)	Cold side Temp (°C)	Temp Diff (°C)	Voltage (mV)
0	28.0	6.6	21.4	77.5	28.4	14.5	13.9	82.2	25.8	11.1	14.7	79.9
30	25.3	12.8	12.5	82.8	25.3	12.8	12.5	84.5	24.5	10.2	14.3	82.3
60	33.2	5.5	27.7	86.4	25.8	9.2	16.6	95.8	23.7	9.4	14.3	79.7
90	25.8	4.2	21.6	76.8	24.9	9.2	15.7	80.7	25.1	13.0	12.1	81.2
120	24.6	12.7	11.9	78.8	31.8	7.8	24.0	79.0	24.8	9.1	15.7	74.8
150	26.2	12.6	13.6	76.0	24.7	7.8	16.9	82.4	33.6	9.2	24.4	83.8
180	24.3	11.4	12.9	83.3	23.9	9.6	14.3	73.4	28.4	5.1	23.3	79.9
Mean	26.8	9.4	17.4	80.2	26.4	10.1	16.3	82.6	26.6	9.6	17.0	80.2
SD	3.1	3.8	6.2	3.9	2.8	2.6	3.7	6.8	3.4	2.4	4.8	2.8

Notes:

Data analysis – planning:

Summary statistics:
Mean Voltage
Mean Current
Mean Power

Graphs:
Voltage vs Time
Temperature difference vs Time

Inferential statistics:
Two-Way ANOVA With Replication
Response variable: Mean Power for each trial
To find out:

- *Main effect of Configuration*
- *Main effect of Heat Source*
- *Interaction effect (Configuration × Heat Source)*

Notes:

Lay out the results:

Tables
A. Mean voltage ± SD
B. Mean current
C. Mean temperature difference (ΔT)
± SD
D. Mean power output

Bar charts
A. Mean voltage ± SD
B. Mean current
C. Mean temperature difference (ΔT) ± SD
D. Mean power output

Line Charts
Voltage vs time for three trials
Temperature difference (ΔT) vs time for three trials

3 trials of 7 measurements were used to find out
A. Mean voltage ± SD
C. Mean temperature difference (ΔT) ± SD
B. Mean current
D. Mean power output

Voltage versus time for three trials
Evaluate trends: Initial high output, decline over time, fluctuations, consistency between trials.

Notes:

Creating graphs using excel

Ref:
https://www.mrexcel.com/board/threads/scatter-plot-with-continuous-y-and-categorical-x-variables.252814/
https://help.tableau.com/current/pro/desktop/en-us/multiple_measures.htm
https://support.microsoft.com/en-us/office/change-axis-labels-in-a-chart-1c32436b-fb12-450b-aefa-cc7e4584456a

Que: How to use excel to calculate statistical difference for 2 independent variables (3 configurations and 3 conditions)?

Use ANOVA test- if data meets normal distribution criteria.
- *Single Factor: to test one variable across 3 conditions. - if different people or items were used in each condition.*
- *Two-Factor With/Without Replication: to evaluate how two different independent variables interact simultaneously.*

Interpret the Results:
Que: How to interpret P-values?

Read P-Value thresholds:
- *P-values < 0.05: The conditions caused a significant difference for that specific variable.*
- *P-value ≥ 0.05: The conditions did not cause any meaningful difference for that specific variable.*

If P-value > 0.05, there is no statistically significant difference between conditions.
If P-value < 0.05, there is a statistically significant difference between at least two of the conditions.

Note: If the ANOVA returns a significant difference, perform a Post-Hoc Test (such as Tukey's HSD) to identify exactly which conditions differ from one another.

Two Sample t Test: unequal variances – to find significant difference for each pair

Ref:
https://www.youtube.com/watch?v=QwHPphoJizg
https://www.youtube.com/watch?v=wFPIDa7xncU
https://real-statistics.com/students-t-distribution/two-independent-samples-t-test/two-sample-t-test-uequal-variances/

13.06.2026 – 14.06.206

Stage 3… coming soon

Plan: To use hybrid TEG system to power up a LED. – running out of time!

Notes:

To be specific, for 2 independent variables (3 configurations and 3 conditions), each variable has a set of 21 time series observations of voltage (obtained from 7 values x 3 trials), how to run ANOVA test to calculate statistical difference?

2 independent variables:
- *3 TEG configurations:*

Parallel
Series
Hybrid
- *Against 3 conditions:*

Static body heat - at rest
Dynamic body heat – with movement
Appliance heat

Dependent Variable:
- *Voltage*

For each Configuration × Condition combination, you have:
3 trials
7 voltage measurements during each trial (time-series observations every 30 seconds)

To compare 3 TEG configurations against 3 heat source conditions:
combination (e.g., 7 points for Parallel under Body Heat at Rest x 3 trials)
Ie. One dependent variable (Voltage) being measured under the combination of two categorical independent variables: 3 trials, TEG Configuration (3 levels) and Condition (3 levels).

2 options:

ANOVA: Two-Factor With/Without Replication: Used when evaluating how two different independent variables interact

Anova: Two-Factor Without Replication – For same groups (repeated measures): Used when the same configuration were tested across all three conditions. - But does not interaction between configurations and heat source.

To compare the effect of heat sources:
Run this test three separate times (once for each configuration).

To compare the effect of electrical configuration:
Run this test three separate times (once for each heat source).

B. Anova: Two-Factor With Replication – used to evaluate the main effect of the configurations, the main effect of the conditions, and whether they interact with each other. Used in this study
.
Main Effect of Configuration
"Does voltage differ between Parallel, Series, and Hybrid?"

Main Effect of Condition
"Does voltage differ between Static Body Heat, Dynamic Body Heat, and Appliance Heat?"

Interaction Effect
"Does the effect of configuration depend on the heat source?"

Ref:
https://support.microsoft.com/en-US/Excel/calculate-multiple-results-by-using-a-data-table
https://stattrek.com/anova/repeated-measures/excel
https://www.youtube.com/watch?v=wFPIDa7xncU

15.06.2026 – 27.06.206

Results computed.
Data analysis.
Comparing results of Stage 1 and Stage 2.

Discussions:

Que. How effectively does each configuration scale when more TEG modules are added?

For scalability, power output will be analysed for energy harvesting performance.
Note: Voltage shows how much electrical potential is generated. A system can produce a high voltage but very little usable energy if the current is low (e.g. open circuit voltage, when subject to very high load resistance as shown in power-resistance graphs). Power incorporates both voltage and current.

Que. What can thermoelectric theory predict?

Voltage is proportional to temperature difference (Seebeck effect)
Power depends on both thermal and electrical conditions.
Power depends on:
- voltage
- internal resistance
- load matching

Simply adding modules does not guarantee proportional increases in power. Adding more modules changes the system. When four TEGs are added, several things can happen simultaneously.

1. Electrical effects
   - Series:
     - voltage increases
     - internal resistance increases
   - Parallel:
     - current capacity increases
     - internal resistance decreases
   - Hybrid:
     - intermediate behaviour
2. Thermal effects
   - The modules must share the available heat.
   - If heat input is limited (as in body heat harvesting):
     - each module may receive less heat,
     - ΔT across each module may decrease,
     - power may increase less than expected.

Que. Since 4-module TEG system was used to generate power, would a perfectly efficient scaling theoretically produce about 4× the power of a single module under identical thermal conditions?

To assess how effectively additional TEG modules increased power generation, the power output of each four-module configuration was expressed relative to the output of a single TEG module.

Ideal engineering expectation based on assumption:

- all modules have identical properties
- all modules experience the same ΔT
- there is no thermal interaction between modules
- load matching is optimal
- heat supply is unlimited

A theoretical expectation is:
Under ideal conditions, if each module experiences a similar temperature difference and thermal and electrical losses are negligible, each module contributed equally to power generation, total power should increase approximately in proportion to the number of modules, a four-module system would be expected to produce approximately four times the power of a single module. However, this relationship was not observed for all configurations.

Results of Stage 2:

Table 5. Power scaling of 4-module TEG system

Configuration	Scaling
Parallel	0.8–1.5×
Series	2.1–3.0×
2×2 Hybrid	3.0–4.4×

This result supports that electrical configuration was a major determinant of scalability.
The 2×2 hybrid produced about 3–4.4 times the power of a single TEG, approaching the theoretical four-fold increase. – best scaling in Stage 2.
The 2×2 hybrid produced approximately:

3.9× more power than a single TEG under static body heat
4.5× more power under dynamic body heat
3.0× more power under appliance heat

The series configuration produced about 2.1–3.0 times the power.
The parallel configuration produced only 0.8–1.5 times the power.

The results suggest:
Hybrid configuration approached proportional scaling.
This implies:
- ΔT was largely maintained,
- electrical losses were relatively small,
- the configuration utilised the available thermal energy efficiently.

Series configuration showed moderate scaling.
This implies
- some electrical or thermal losses,
- less effective utilisation of additional modules.

Parallel configuration showed poor scaling.
This implies
- voltage became limiting,
- thermal energy was not converted efficiently under the 10 Ω load (load matching issue)

Discussion:
- Scaling was not linear. Adding more TEG modules did not automatically produce a proportional increase in power generation.
- Hybrid configuration achieved the best utilisation efficiency of the added modules.
- Instead, the effectiveness of scaling depended strongly on the electrical configuration and how efficiently the available temperature gradient was converted into electrical energy.
- The near-4× performance of the 2×2 hybrid configuration suggests that it utilised the additional modules more effectively than the series or parallel configurations under the tested conditions.
- In contrast, the relatively poor scaling observed in the parallel configuration indicates that adding modules alone was insufficient to maximise power output if the electrical configuration and the thermal conditions did not effectively utilise the available thermal energy.
- Therefore, the results suggest that optimising electrical configuration and thermal management in maintaining an effective temperature gradient could be more important strategy than increasing the number of thermoelectric modules when designing efficient low-grade energy-harvesting systems.
- Parallel configuration produced only 0.8× the power of a single TEG under static body heat – This reflected that adding four modules in parallel was less effective than using a single module, indicating system design is more critical than module quantity.

Conclusion: Power scaling was highly configuration-dependent, demonstrating that the performance of a multi-module TEG system cannot be predicted from module quantity alone.

Que. What does thermoelectric research inform?

Thermoelectric research has shown that power scaling is often non-linear because performance is influenced by electrical configuration, thermal coupling, temperature distribution, and load matching.

- Power does not necessarily scale linearly with module quantity.
  Chen et al. (2012): Although adding modules in series increased output power, the performance could not be predicted linearly due to module non-uniformity and thermoelectric effects within the TE system.

- Electrical configuration strongly affects scalability
  Roshan et al. (2026): Comparing series, parallel and hybrid TEG configurations, hybrid arrangements achieved the highest overall performance and efficiency, while performance varied substantially with electrical configuration and load resistance. Hybrid > Series > Parallel

- Load matching
  Maximum power depends on both electrical impedance matching and thermal impedance matching.

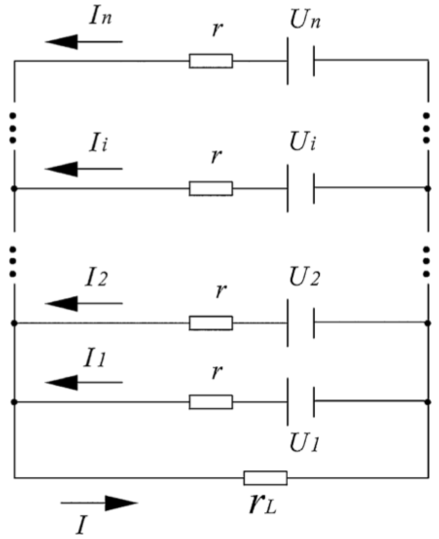

Figure 3 (a). Simple parallel circuit diagram (Liang et al., 2011).

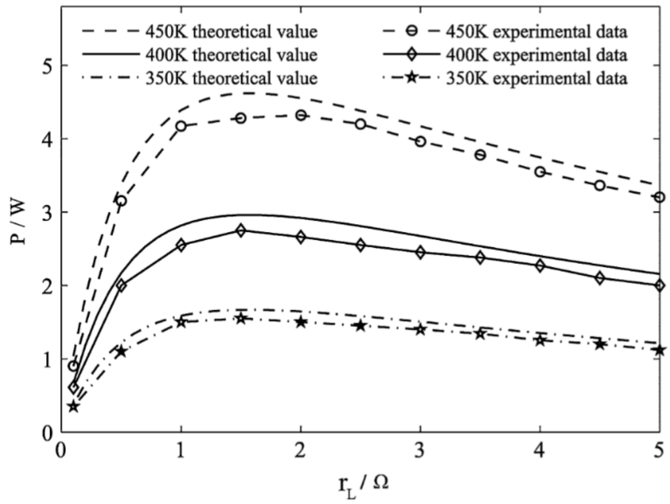

Figure 3 (b). Output power P as a function of load rL under different heat source temperature. The maximum power point for this specific TEG is 1.5 Ohm. (Liang et al., 2011).

Notes: Research 1

Analytical model of parallel thermoelectric generator. (Liang et al.; 2011)

Findings:

- *Only all TE modules in the parallel TEG have the same inherent parameters and work in the same condition, the parallel properties of the parallel TEG are the same as the parallel properties of common DC power.*
- *Contact effect will reduce the output power of parallel TEG. The existence of contact resistance is just like the increase of the TE module's internal resistance, which leads to the deceases of output power. The thermal contact resistance reduces the output power by reducing the temperature difference between the two sides of thermocouples.*
- *In the practical application, as the parameters of TE module are fixed, the main method of reducing the influence of contact effect is reducing the thermal contact resistance between the TE module and the heat source or heat sink.*

Ref:

Liang, G, Zhou, J & Huang, X 2011, 'Analytical model of parallel thermoelectric generator', Applied Energy, vol. 88, no. 12, pp. 5193–5199, viewed June 2026, <https://doi.org/10.1016/j.apenergy.2011.07.041>.

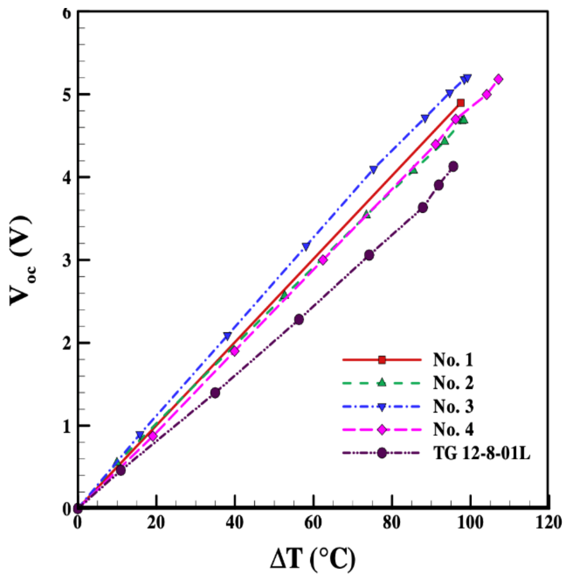

Figure 4(a). Distributions of open circuit voltage of 4 thermoelectric modules and a thermoelectric generator (Chen et al., 2012).

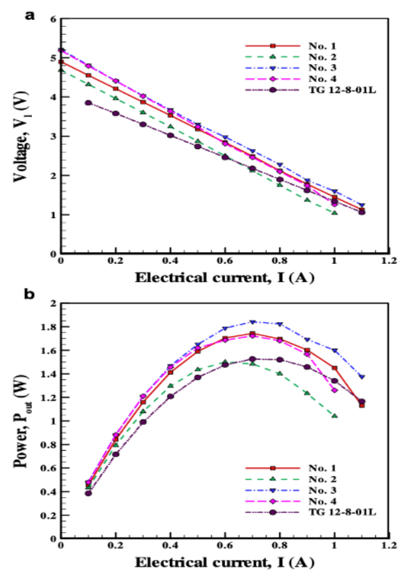

Figure 4(b). Distributions of (a) output voltage and (b) power of 4 thermoelectric modules and a thermoelectric generator (Chen et al., 2012).

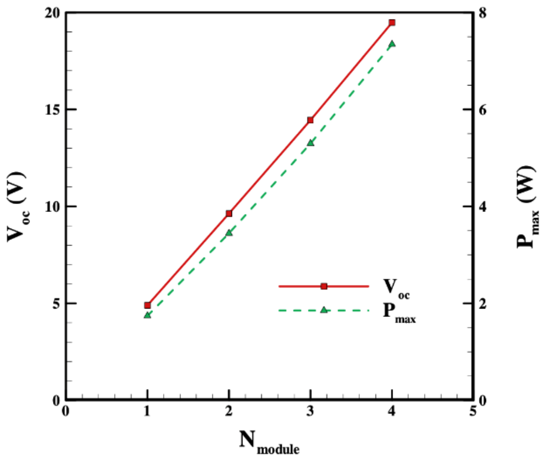

Figure 4(c). Distributions of open circuit voltage and the maximum output power with number of TE modules in series (n = 1-4) (Chen et al., 2012).

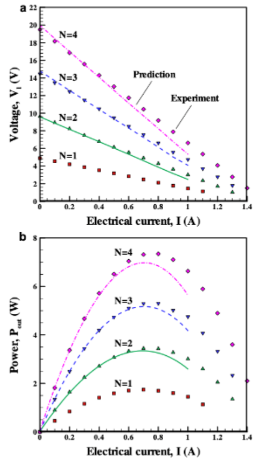

Figure 4(d). Distributions of (a) output voltage and (b) power of thermoelectric modules in series versus electrical current (n = 1- 4). (Chen et al., 2012).

Note: Research 2

Experimental study on thermoelectric modules for power generation at various operating conditions (Chen et al., 2012)

T = 100C

Findings:

- *At a fixed water flow rate, increasing heating temperature leads to the better performance of the module. This reflects that power generation from the TEM depends strongly on the heat source. However, the temperature of heat source is subject to the allowed maximum operating temperature of TEM.*
- *Under appropriate operating conditions, the open circuit voltage, maximum power are linearly proportional to the number of modules in series (n = 1 - 4).*
- *Nevertheless, due to the Peltier effect and inherent non-uniformity among the TEMs, the performances of TEMs in series cannot be simply predicted by adding the data of each module together when electrical current is increased.*
- *The TEMs are suitable for power generation by recovering waste heat when the temperature of the system is lower than 150C.*

Ref:

Chen, W-H, Liao, C-Y, Hung, C-I & Huang, W-L 2012, 'Experimental study on thermoelectric modules for power generation at various operating conditions', Energy, vol. 45, no. 1, pp. 874–881, viewed June 2026, <https://doi.org/10.1016/j.energy.2012.06.076>.

25.06.2026

Comparing my data with the most recent study in April 2026. Experimental results for a single module.

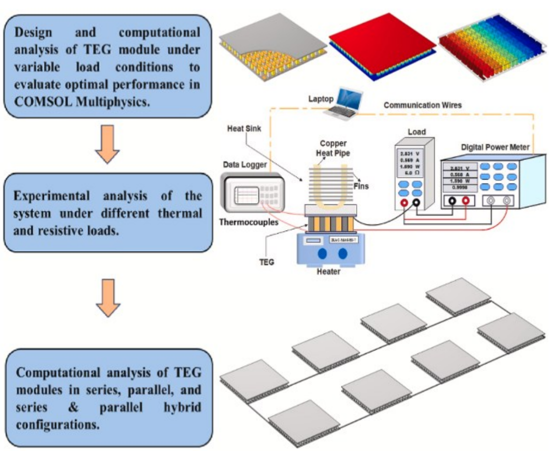

Figure 5(a). Experiment setup (Manghwar et al., 2026).

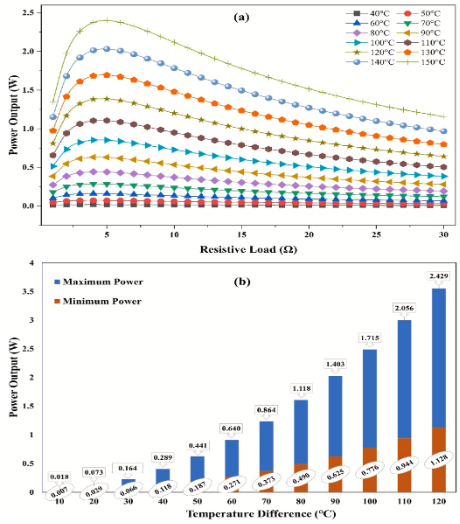

Figure 5(b). Power output for a single TEG module (a) under variable resistive load and hot side temperatures (b) Minimum and maximum power achieved at various temperature differences (Manghwar et al., 2026).

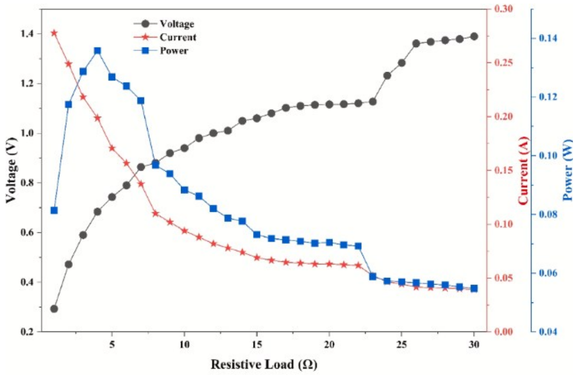

Figure 5(c). Variation in voltage, current and power at different resistive loads (Manghwar et al., 2026).

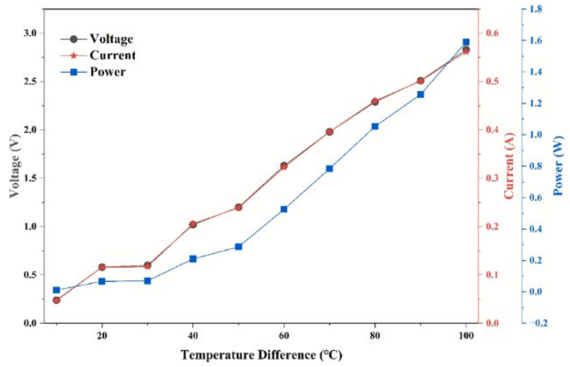

Figure 5(d). Variation in voltage, current and power at various temperature differences (Manghwar et al., 2026).

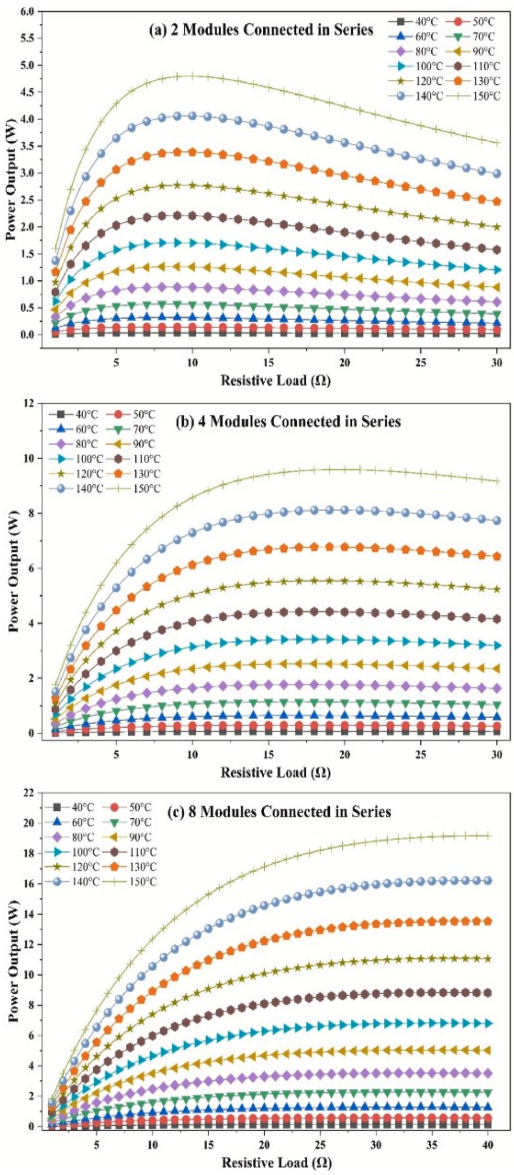

Figure 5(e). Power output for TEG modules under variable resistive load and hot side temperatures (a) 2 modules, (b) 4 modules, (c) 8 modules connected in series (Manghwar et al., 2026).

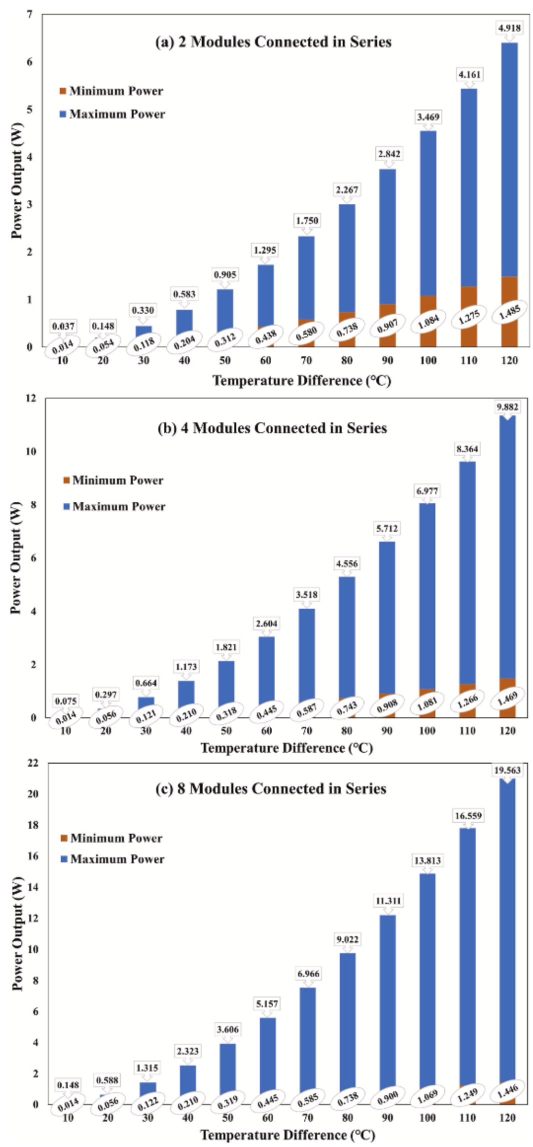

Figure 5(f). Minimum and maximum power achievable at various temperature differences (a) 2 modules, (b) 4 modules, (c) 8 modules in series. The hot side temperature was varied from 40 ◦C to 150 ◦C, whereas the cold side was maintained at 30 ◦C (Manghwar et al., 2026).

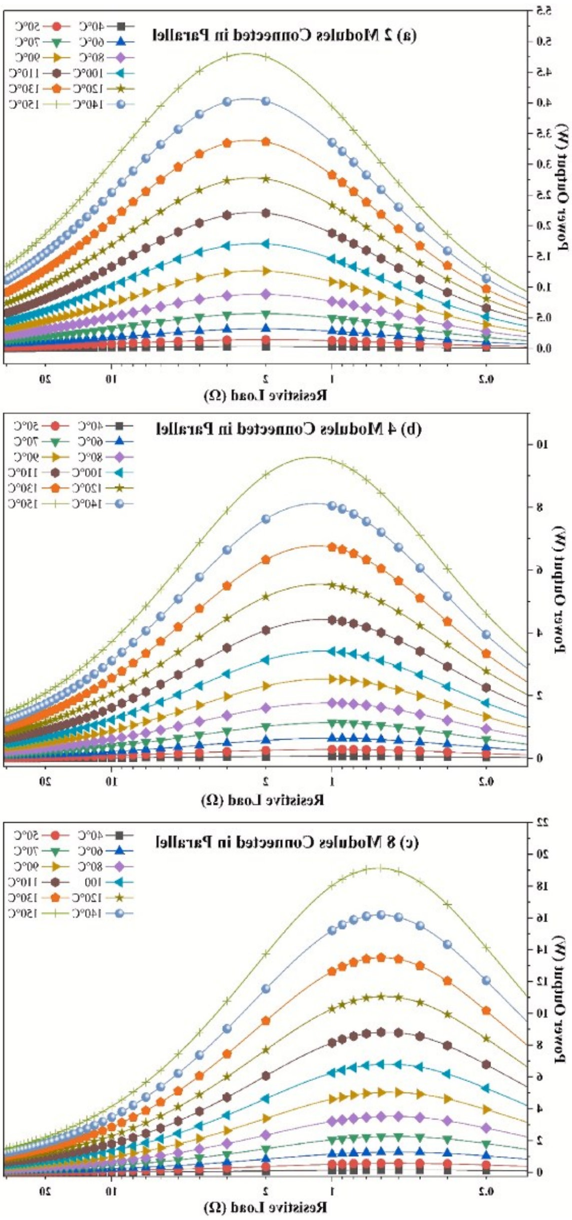

Figure 5(g). Power output for TEG modules under variable resistive load and hot side temperatures (a) 2 modules, (b) 4 modules, (c) 8 modules connected in Parallel (Manghwar et al., 2026).

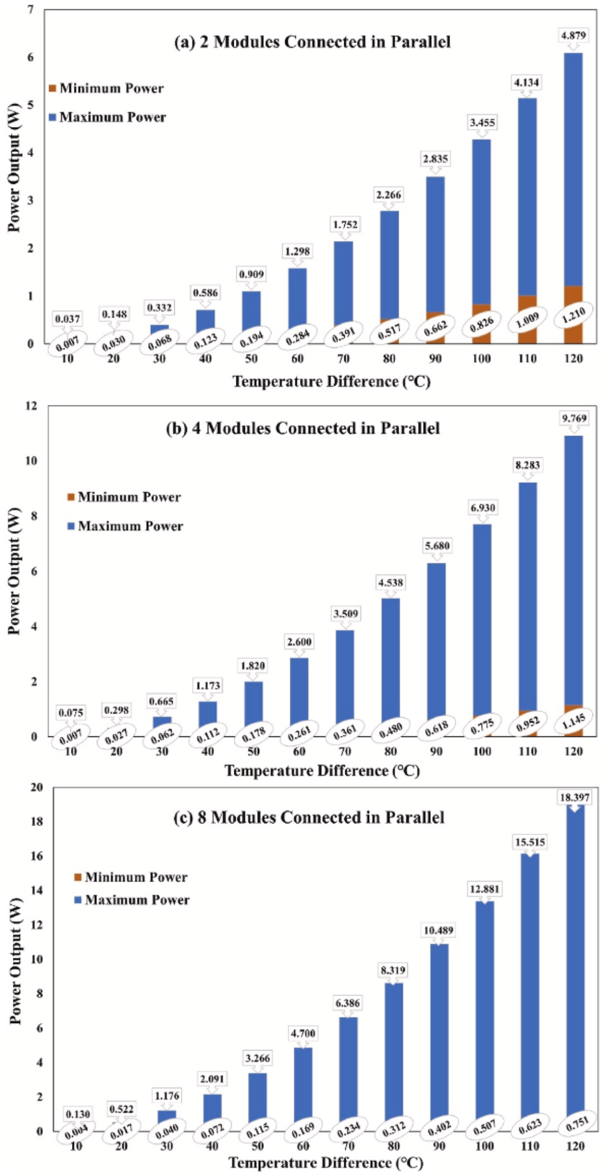

Figure 5(f). Minimum and maximum power achievable at various temperature differences (a) 2 modules, (b) 4 modules, (c) 8 modules in parallel. The hot side temperature was varied from 40 ◦C to 150 ◦C, whereas the cold side was maintained at 30 ◦C (Manghwar et al., 2026).

Table 6. Material properties of the thermoelectric module SP1848-12745 (Manghwar et al., 2026)

Property	Material			
	Alumina (Ceramic Substrate)	Copper (Electrode Contacts)	Bi_2Te_3 (P-type Leg)	Bi_2Te_3 (N-type Leg)
Heat Capacity at Constant Pressure (C_p) [J/kg*K]	900	385	154	154
Density (ρ) [kg/m^3]	3900	8960	7700	7700
Seebeck Coefficient (S) [V/K]	-	-	$S_P(T)$	$S_N(T)$
Electrical Conductivity (σ) [S/m]	-	5.998*10^7	$\sigma_P(T)$	$\sigma_N(T)$
Thermal Conductivity (k) [W/m*K]	-	400	$k_P(T)$	$k_N(T)$

Note: Research 3

Computational and experimental investigation of thermoelectric generators in series-parallel configurations under variable resistive loads and temperature gradients. (Manghwar et al., 2026)

TEG module SP1848-12745
254 thermoelectric legs coupled electrically in series and thermally in parallel.
The internal resistance of the single TEG module is around 4Ω as specified in the manufacturer

- *The experimental setup includes the TEG module, heat source, heat sink, programmable D.C load, thermal paste, K-type thermocouple, data logger, and digital power meter.*
- *Experimental results were obtained within laboratory conditions where ambient temperature was maintained around 30 ◦C.*
- *Investigated performance evaluation of thermoelectric generators under varying temperature gradients and resistive loads between 1Ω and 30Ω and extended up to 40Ω for eight modules in series.*
- *Evaluated thermoelectric performance of two, four, and eight modules in both series and parallel arrangements.*
- *Represented low grade waste heat recovery potential from coal fired power plants and oil and gas sector.*

Findings:
- *The optimum resistive load for maximum power generation depends on both temperature and configuration. For series connections, the optimum load ranged from 8Ω to 10Ω for two modules and 31Ω–39Ω for eight modules. In contrast, parallel configurations achieved optimal power within 1Ω–3Ω across all conditions. The maximum power generated from a single thermoelectric module is 1.69W at 5Ω resistive load at a temperature difference of 100 °C - surpasses the experimental value by 6.29%.*
- *The maximum power output for eight modules configured in series, parallel, and hybrid arrangement was measured as 13.53W, 12.60W, and 13.55W, respectively. The average power output was also found out to be higher in case of hybrid configuration.*
- *The highest efficiency of 3.84% for hybrid configuration, whereas series and parallel configuration achieved the efficiency of 3.79% and 3.77% under the matched resistive load condition.*
- *These findings confirm that series*-parallel hybrid configuration provide relatively stable performance across varying load and temperature conditions.

Ref:
Manghwar, R, Selvaraj, J, Khoharo, H, Kumar, L & Ahmad, MS 2026, 'Computational and experimental investigation of thermoelectric generators in series-parallel configurations under variable resistive loads and temperature gradients', Case Studies in Thermal Engineering, vol. 80, Elsevier BV, p. 107913, viewed June 2026, <https://doi.org/10.1016/j.csite.2026.107913>.

Note: Research 4

Optimal working conditions for thermoelectric generators with realistic thermal coupling. (Apertet et al., 2011)

Both electrical and thermal conditions of the TEG must be considered
As for all real systems, when thermal dissipative couplings exist, the thermal conditions would be different.

Findings:
- *TEG requires electrical and thermal impedance matching to maximise the output power.*
- *Thermal impedance depends on the thermal conductivity at zero electrical current and TEG figure of merit.*

Ref:
Apertet, Y, Ouerdane, H, Glavatskaya, O, Goupil, C & Lecoeur, P 2012, 'Optimal working conditions for thermoelectric generators with realistic thermal coupling', Europhysics Letters, vol. 97, no. 2, p. 28001, viewed June 2026, <https://doi.org/10.1209/0295-5075/97/28001>.

Note: Research notes

Number of modules does not necessarily increase the output power.
- *Optimal number of modules depends on geometry, material properties, thermal and electrical contacts. Therefore, it is essential to consider effective design of system to minimize the thermal and electrical resistance consisting of multiple TEG modules.*
- *In practical waste heat recovery applications such as automotive exhaust systems and industrial processes, both thermal conditions and electrical load vary simultaneously, making the identification of matched load conditions essential for optimal power generation.*
- *Need to identify matched resistive loads for different configurations, providing practical insight for optimal power generation and system design of TEG-based waste heat recovery systems.*

The practical performance of commercial TEGs is governed by temperature difference, internal electrical resistance, thermal contact resistance and module configurations.
- *TEG performance is highly dependent on the load resistance, which plays a crucial role in optimizing the TEG's power output. Therefore, it is essential to calculate the matched resistive load, which compensates for the rise in internal resistance, to ensure stable and optimal TEG electrical power under specific temperature difference.*
- *TEG practical deployment is often constrained by variations in internal resistance and load matching conditions.*

Internal electrical resistance:

A. Montecucco, J. Siviter, A.R. Knox, The effect of temperature mismatch on thermoelectric generators electrically connected in series and parallel, Appl. Energy 123 (2014) 47–54.

- *Performance analysis for TEGs connected in series and parallel electrical connection under mismatched temperature conditions was performed.*
- *Series configurations yield more power with feasible control; however, the magnitude of the mismatched temperature increases in the series connection.*

Z. Gu, et al., Hundred-Watt implantable TEG module for large-scale exhaust gas waste heat recovery, Energies 17 (3) (2024).

- *Proposed the series connection of modules for WHR out of three other configurations*
- *The optimal power output was subject to losses if variations in thermal and electrical characteristics were taken into account.*

S. Harish, et al., Performance of bismuth telluride modules under thermal cycling in an automotive exhaust thermoelectric generator, Energy Convers. Manag. 232 (2021) 113900.

- *Increased internal resistance accounts for reduced TEG performance; this increase is due to the Peltier effect, current flow and thermoelectric legs temperature rise.*

R. Merienne, et al., Thermal cycling of thermoelectric generators: the effect of heating rate, Appl. Energy 237 (2019) 671–681.

- *TEG modules under varying heating rates and thermal cycling were examined, where an increase in internal resistance was observed for slow to faster thermal cycling rates.*

Complete Scientific Report …

Acknowledgements

- I acknowledge that informed consent was obtained from the participant involved in the body heat investigations.
- I am grateful to my mother for her advice and constructive feedback, which assisted in improving the experimental design and methodology.
- I sincerely thank my parents for their support in purchasing the materials and equipment required to complete this investigation.

OSA RISK ASSESSMENT FORM

for all entries in (✓) ☐ Models & Inventions and ☑ Scientific Inquiry

This must be included with your report, log book or entry. One form per entry.

NAME: Chloe Yaan Yuit Yew ID: 0749-006

SCHOOL: University Senior College

Activity: Give a brief outline of what you are planning to do.

I am planning to investigates how electrical configurations (parallel, series, and 2×2 hybrid) and heat sources (static body heat, dynamic body heat and appliance heat) affect the voltage, current, and power output of a thermoelectric generator (TEG) system composed of four SP1848-27145 modules. Stage 1 of the investigation is a pilot study in which power output is measured across a range of load resistances to identify a suitable load resistor for the main experiment. In Stage 2, the selected load resistance is used to evaluate the electrical performance of a single TEG module (baseline) and three four-module TEG configurations under three heat source conditions. Voltage, current, and power output are measured and analysed to determine how configuration and heat source influence energy harvesting performance.

Are there possible risks? Consider the following:

- **Chemical risks: Are you using chemicals? If so, check with your teacher that any chemicals to be used are on the approved list for schools. Check the safety requirements for their use, such as eye protection and eyewash facilities, availability of running water, use of gloves, a well-ventilated area or fume cupboard.**
- **Thermal risks: Are you heating things? Could you be burnt?**
- **Biological risks: Are you working with micro-organisms such as mould and bacteria?**
- **Sharps risks: Are you cutting things, and is there a risk of injury from sharp objects?**
- **Electrical risks: Are you using mains (240 volt) electricity? How will you make sure that this is safe? Could you use a battery instead?**

Risks	How I will control/manage the risk
Thermal hazards (burns from soldering iron and air fryer)	Personal protective equipment, including a lab coat and heat-resistant gloves will be worn when handling hot equipment. Hot surfaces will be allowed to cool before contact where possible, and care is taken to avoid direct skin contact.
Fume inhalation hazards (soldering fumes)	Safety glasses and a surgical mask will be worn during soldering to minimise fume exposure. All soldering will be conducted in a well-ventilated area to prevent the accumulation of airborne contaminants.
Electrical hazards (electric shock, short circuits, equipment damage)	All electrical equipment (air fryer, multimeter, soldering station) will be operated according to manufacturer instructions. Electrical components and connections will be inspected before use. Care will be taken to keep all electrical equipment away from moisture, melted ice, and condensation from the ice pack.
Sharp object hazards (cuts and punctures from wire cutters, scissors, and exposed wire ends)	Sharp tools will be handled carefully and stored safely when not in use. Safety glasses will be worn during wire cutting to protect against flying wire fragments and exposed wire ends will be managed to minimize injury risk.

Risk Assessment indicates that this activity can be safely carried out.

RISK ASSESSMENT COMPLETED BY (student name(s)): Chloe Yaan Yuit Yew

SIGNATURE(S): *Chloe Yew*

☑ By ticking this box, I/we state that my/our project adheres to the listed criteria for this Category.

TEACHER'S NAME: Valerie Bradshaw

SIGNATURE: *Valerie Bradshaw* DATE: 20/05/2026